SOUTH CAROLINA ELECTRIC & GAS COMPANY
POST OFFICE 764
COLUMBIA, SOUTH CAROLINA 29218

O. W. DIXON, JR.
VICE PRESIDENT
NUCLEAR OPERATIONS

June 22, 1983

Mr. Harold R. Denton, Director
Office of Nuclear Reactor Regulation
U.S. Nuclear Regulatory Commission
Washington, D.C. 20555

Subject: Virgil C. Summer Nuclear Station
Docket No. 50/395
Operating License No. NPF-12
Seismic Confirmatory Program

Dear Mr. Denton:

On September 1, 1982, representatives of the South Carolina Electric and Gas Company (SCE&G) presented to members of the NRC Staff, a proposed Seismic Confirmatory Program to satisfy License Condition 2.C(25) of the Virgil C. Summer Nuclear Station Operating License. After incorporation of Staff comments on the Program, SCE&G formally submitted its Seismic Confirmatory Program on September 24, 1982.

Report I, concerning the experimental phase of the Program, was filed on February 1, 1983. Additionally, an Addendum was filed to the Report on March 9, 1983, and a meeting was held with the Staff on March 10, 1983, to review the Report. NRC questions were transmitted informally and draft responses were presented to the NRC at a meeting on April 28, 1983. In a letter dated May 4, 1983, SCE&G received formal questions from the Staff concerning the program.

Additional Staff comments and questions were documented to SCE&G in a meeting summary dated June 10, 1983.

This letter serves to transmit formally ten copies of the responses to Staff questions discussed on April 28, 1983, and the further questions contained in the meeting summary. The initial questions are numbered 1-6 as in the Staff's letter. The questions labeled 1 and 2 in the NRC's meeting summary are herein labeled 3A and 2A respectively.

As discussed in the summary section of our Report, the experimental results demonstrate a reduction in the "Monticello enveloping response spectrum." Taking into account this reduction, the equipment margin analysis to be performed for

B001
1/10

the "Monticello enveloping response spectrum" will be encompassed in the equipment margin analysis to be conducted for the "ACRS response spectrum" (M_L=4.5 spectrum, anchored at .22g, as discussed at our ACRS hearings in February and March 1981). Equipment margin analysis for safe shutdown equipment for the "ACRS response spectrum" is scheduled for completion prior to startup after the first refueling outage.

It is our understanding, based on conversations with the NRC Staff, that these questions address the primary areas of Staff concern and no further questions are anticipated. SCE&G considers the attached responses, together with the previously filed reports, sufficient information for completion of Staff review of our program thus far.

We request an expeditious completion of your review and concurrence in our schedule for program completion.

Yours very truly,

O. W. Dixon, Jr.

NEC:OWD/fjc
cc: V. C. Summer
T. C. Nichols, Jr./O. W. Dixon, Jr.
E. H. Crews, Jr.
E. C. Roberts
H. N. Cyrus
J. P. O'Reilly
Group/General Managers
O. S. Bradham
R. B. Clary
C. A. Price
A. R. Koon
C. L. Ligon (NSRC)
G. J. Braddick
J. C. Miller
J. L. Skolds
C. Chen
S. S. Alexander
R. R. Mahan
J. A. Blume
M. R. Sommerville
J. B. Knotts, Jr.
NPCF
File (Lic./Eng.)

Question 1. Considering (a) propagation path, (b) soil amplification, (c) soil-structure interaction and (d) scattering, what biases in the relative responses of the foundation and free-field sites could be introduced by the shallowness of the explosion sources, compared to the average depth of reservoir-induced earthquakes? (Refer to Joyner's letter). Justify or modify the estimated reduction factors in light of your answer.

Referring to the April 8, 1983 letter from Dr. W.B. Joyner to Dr. J.L. King, the question as to the effect of source depth on the relative responses of the foundation and free-field sites is stated on page 1 of that letter as follows:

> "If we accept the description of the dominant portion of the seismograms as a combination of S-waves and higher mode surface waves, we have to presume that the relative excitation of the various components of this combination is sensitive to the depth of the source, and further, that the relative response of foundation and free-field sites is sensitive to the relative excitation of the components."

While the first presumption in this statement is valid, it does not follow that "the relative response of foundation and free-field sites is sensitive to the relative excitation of the components" of the S and higher-mode group. The composition of the S and higher-mode group differs for Test 1, 3, and 4 records because of different epicentral distances, propagation path effects, and excitation at the shotpoints; yet Auxiliary Building/free-field spectral modulus ratios are similar for the three tests. The excitation of higher mode surface waves relative to that of body waves was significantly greater for Test 3 than for Test 4, as is apparent in comparing the records shown in Figures IV.A.1 - 3 and IV.A.4 - 6 of Appendix B.

There are several lines of evidence relevant to this issue which are addressed below: (A) explosion tests with distinctly different signatures, (B) waveforms of RIS events of differing focal depths, and (C) comparison of explosion and RIS records. In Section D below, these are summarized and conclusions are drawn for each potential influence separately.

A. EXPLOSION TEST 5 RESULTS

Distinct differences in Test 5 signals generated by shallow shots in saprolite and deeper shots in rock provide an opportunity to compare for these two cases the relative response of foundation and free-field sites. Differences in excitation and partitioning of energy at the saprolite/bedrock interface, rather than differences in shot depth per se, are primarily responsible for the dissimilarity of the records for shots in saprolite and rock.

Three of the Test 5 shot holes were drilled to depths 50 ft below the bedrock surface of Charlotte Belt Gneiss, while a fourth (hole #5A) was drilled to 100 ft below bedrock. The subsurface depths at which the initial set of shots was fired were 108, 116, 157 and 210 ft (see Table III.A.2, Appendix B, p.15). Subsequent charges emplaced on rubble at shallower depths included three shots (3, 7, and 8) in saprolite.

The Test 5 shots were recorded at a radial array of sites including the foundation of the Fairfield Pumped Storage Facility (hydroplant) at a distance of 1930 ft and a small aperture array on the dam abutment centered at a distance of 3180 ft (see Figure III.A.5). Records obtained in the Auxiliary Building foundation at a distance of 7500 ft are unusable because of poor signal/noise ratio. For the present purposes the hydroplant serves as a good example of a massive embedded structure. The foundation of the hydroplant is 80 ft below grade. In the following comparisons of shallow and deep shots recorded in the hydroplant and on the dam abutment free-field array, the signal amplitudes are not scaled to account for the closer distance of the hydroplant. The sole purpose of the comparison is to investigate the effect of the two different explosion source types on the relative response of foundation and free-field sites.

The differences between the signals generated by shots in saprolite and rock are illustrated in Figures 1.1 - 12. Hydroplant signals and spectra for shots 6 and 8 are shown in Figures 1.1 - 3. Shot 8 was at a depth of 50 ft in saprolite and 16 feet above bedrock, while shot 6 was 100 feet below the

saprolite-bedrock interface at a depth of 210 ft, quite close to the computed focal depth and hypocenter of the October 16, 1979 earthquake. There are readily apparent differences in the signatures and the spectra, with the shallow source producing relatively stronger high-frequency content than the deep shot. Differences of the same kind are observed for recordings on saprolite at the dam abutment (Figures 1.4 - 6).

Signals from all Test 5 shots form two distinct groups, depending on emplacement of the source in saprolite or bedrock. Signatures of the saprolite shots are very similar to each other (Figures 1.7, 1.8, and 1.9), as are those for the shots in rock (Figures 1.10, 1.11, and 1.12). Within each group, the effects of differences in shot depth and distance from the saprolite/rock interface are relatively insignificant. The differences between the two groups are attributable to partitioning of energy into different body wave phases or surface wave modes, and to differences in coupling. The difference in coupling is evidenced by the similarity of signal amplitudes despite a considerable difference in charge weight (13.5 lb for the saprolite shots versus 121 - 122 lb for the shots in rock).

Despite the differences in their signatures, the shots in saprolite and rock produced nearly the same relative response of hydroplant foundation and free-field sites. Spectral modulus ratios were computed using the three free-field stations in the dam-abutment array (stations P1, P4, and P5). No adjustment was made for the difference in epicentral distance (1930 ft to the hydroplant versus 3180 ft to the center of the dam abutment array). Spectral modulus ratios for the shots in saprolite (shots 3, 7, and 8) shown in Figures 1.13, 15, and 17 are very similar to those for the shots in rock (shots 4, 5, and 6; Figures 1.14, 16, and 18) for vertical, radial, and transverse components.

In summary, there are strong differences in source excitation and wave character for Test 5 shots in saprolite and in rock, but at most these only weakly affect the computed spectral modulus ratios between foundation and free-field sites. The dissimilarity of the saprolite and rock shot records is

not due primarily to differences in focal depth per se, but rather to differences in excitation and partitioning of energy at the saprolite/bedrock interface.

B. SHALLOW RIS RESULTS

To investigate the effects of focal depth on the composition of the S and higher mode surface wave group, USGS accelerograph recordings at the dam abutment can be compared for nearby RIS events spanning a range of more than 1 km in focal depth. Corrected USGS accelerograph records for thirteen RIS events are given in Applicant's Additional Seismic Testimony, 1981, Volume 2. Velocity records of the RIS events can in turn be compared with the dam abutment records of the Test 5 shots in rock, which were located close to the hypocenter of the October 16, 1979 RIS earthquake, a little less than 1 km northwest of the dam abutment.

Records of a group of three RIS events all located approximately 1 km to the west of the dam abutment, but with different hypocentral depths, are shown in Figures 1.19 - 27. The hypocentral depths of the three events are 0.36 km (05:47 UTC, October 17, 1978), 1.16 km (08:54 UTC, October 7, 1979), and 1.34 km (23:20 UTC, October 8, 1979). There is no apparent tendency for the records to become simpler and shorter in duration with increasing focal depth, as might be expected in the case of simple geologic structure. Comparing these records with the October 16, 1979 records (Figures 1.28 - 30), it is apparent that there are no systematic effects of focal depth on the records at the dam abutment, as all of these seismograms, while complex, have the same basic nature. Finally, consider the records shown in Figures 1.31 - 33 for a relatively deep RIS event at short epicentral distance (depth 1.74 km and epicentral distance 0.35 km). This event at 16:14 UTC on October 25, 1978, occurred almost directly under the dam abutment and yet the records are as complex as any of the others. These results corroborate the inference that the complex nature of the waves recorded in this area arises largely from heterogeneities along the propagation path and from near-receiver effects, and that neither source depth nor angle of incidence appreciably affects the character of the recorded ground motion.

Other data for RIS events at Monticello Reservoir contained in a M.S. thesis by Hutchenson (1982)* further demonstrates that source depth does not cause a systematic change in the character of ground motion recordings. In particular, examination of the large suite of digitally recorded seismograms included in the Appendix of Hutchenson's thesis shows:

1. There is little variation in event waveforms from comparable magnitude events that occur in local clusters regardless of depth; this indicates that depth of focus does not introduce systematic changes in duration or wave character of ground motion. Note that this conclusion is based on hypocentral depths ranging from .05 to 1.87 km, estimated from the entire 10 station network (events denoted by TN in Hutchenson's Table 3), which gives the best depth determination.

2. An obvious control on the event waveforms is magnitude, because relatively more low frequency energy is generated for the larger events as the corner frequency shifts to lower values; this effect is evident in the seismograms presented by Hutchenson. However, this spectral shaping would have no effect on foundation to free-field spectral modulus ratios.

3. There are large variations among signatures for comparable magnitude events located at approximately the same distance from a particular receiver, but at a different azimuth; this provides further corroboration that propagation path is a dominant factor in controlling the duration and character of ground motion for shallow RIS events at Monticello Reservoir.

Therefore, the data presented by Hutchenson further substantiates the fact that propagation path and receiver site effects significantly influence the ground motion observed, while no systematic depth effects can be discerned. Clearly depth of focus does not strongly influence the waveform character of ground motion generated by shallow RIS events at Monticello Reservoir.

---

*Hutchenson, K.D., 1982, Source Studies of Reservoir Induced Earthquakes at Monticello Reservoir, South Carolina, M.S. Thesis, U. of South Carolina, 120 p. and Appendices.

C. COMPARISON OF EXPLOSION AND RIS RESULTS

It is instructive to compare the USGS dam abutment records of RIS with the explosion seismograms produced at the dam abutment during Test 5 (Figures 1.34 - 36). To compare the explosion seismograms with the USGS records, refer to the center (velocity) trace in Figures 1.19-33; note that the time scales are different. Considering that the accelerograms shown in the earlier figures probably all begin with the S-wave group, the durations and character of the dam abutment explosion seismograms in Figures 1.34-36 (the traces labelled P2) are comparable with those for the RIS events. This indicates that the same basic wave groups travel from source to receiver whether the source is an explosion or an earthquake. As pointed out in Appendix B, because these waves have such high group velocities, they must be body and higher-mode surface waves whose energy travels from source to receiver mainly in the bedrock under the saprolite.

D. SUMMARY AND CONCLUSIONS

The foregoing evidence indicates that the focal depth of the seismic source does not affect significantly the foundation/free-field spectral modulus ratios. The evidence and arguments are summarized as follows. Firstly, although the composition of the S and higher-mode surface wave group differs for Test 1, 3, and 4 records because of differences in epicentral distance (hence propagation path and angle of incidence differences) and in excitation at the shot points, the Auxiliary Building/free-field spectral modulus ratios are similar for the three tests. Secondly, distinct seismic source differences observed for Test 5 shots detonated in saprolite and in rock produced little variation in the hydroplant foundation/free-field spectral modulus ratios. Thus, differences in the seismic source have little influence on the reduction factors observed for large foundations. Thirdly, examination of dam abutment recordings of RIS events shows that focal depth is not a significant factor controlling the waveform character of the records. Hutchenson's (1982) data further demonstrate that depth of focus for RIS events does not systematically affect the duration or waveform character of recorded ground motion.

Also, Test 5 recordings for explosions at different depths in the bedrock show no systematic depth dependence.

The influence of specific factors stated in the question, namely (a) propagation path, (b) soil amplification, (c) soil structure interaction, and (d) scattering, are evaluated as follows.

With regard to (a) propagation path, the foregoing comparisons of earthquake and explosion records at the same recording site reveal no significant differences between the signature of explosions in rock and the shallower RIS events on one hand, and the signatures of shallow and deep RIS events on the other. In all cases the records are dominated by body waves and higher mode surface waves whose energy travels from source to receiver mainly in the bedrock. The complexity of both earthquake and explosion signals is attributable mainly to heterogeneities along the entire propagation path and near-receiver effects.

The influence of focal depth on (b) soil amplification effects can be evaluated by comparing dam abutment records of RIS events of different depth. Compare, for example, the records for an event of hypocentral depth 0.36 km and epicentral distance 1.04 km (Figures 1.19 - 21) with those for an event of hypocentral depth 1.74 km and epicentral distance 0.35 km (Figures 1.31 - 33). The waveforms for these events are similar despite the difference in body wave angles of incidence. Differences in soil amplification would be most pronounced on the displacement records, but such are not apparent in the data.

Two sets of evidence indicate that (c) soil-structure interaction and (d) scattering are not sensitive to variations in the composition of seismic signals at the Summer site. Associated with the recordings of Test 1, 3, and 4 shots are differences in body-wave angle of incidence and in the composition of the S and higher-mode surface wave group, due to different distances to the VCSNS structures (14,000; 3,700; and 4,300 ft respectively). In addition, there are differences in seismic excitation produced at the three shot locations. The excitation of higher-mode surface waves relative to that of body waves was significantly greater for Test 3 than for Test 4, as is apparent in

comparing Figures IV.A.-3 and IV.A.4 - 6 of Appendix B. Despite these differences, the Auxiliary Building/free-field spectral modulus ratios are similar for the three tests. The second set of evidence consists of the hydroplant and free-field recordings of the two distinctly different source types produced by Test 5 shots in saprolite and in rock. Despite the differences in their signatures, the shots in saprolite and rock produced nearly the same relative response of hydroplant foundation and free-field sites.

Considering propagation path, soil amplification, soil structure interaction and scattering, it is concluded from analyzing earthquake and explosion records that the shallowness of the explosion sources does not introduce bias in the relative responses of foundation and free-field sites. There is no signficant difference in the spectral modulus ratios observed for different S+ higher mode levels of excitation and different angles of incidence. Therefore, the explosion tests are appropriate for estimating foundation to free-field spectral response for shallow RIS events at Monticello Reservoir.

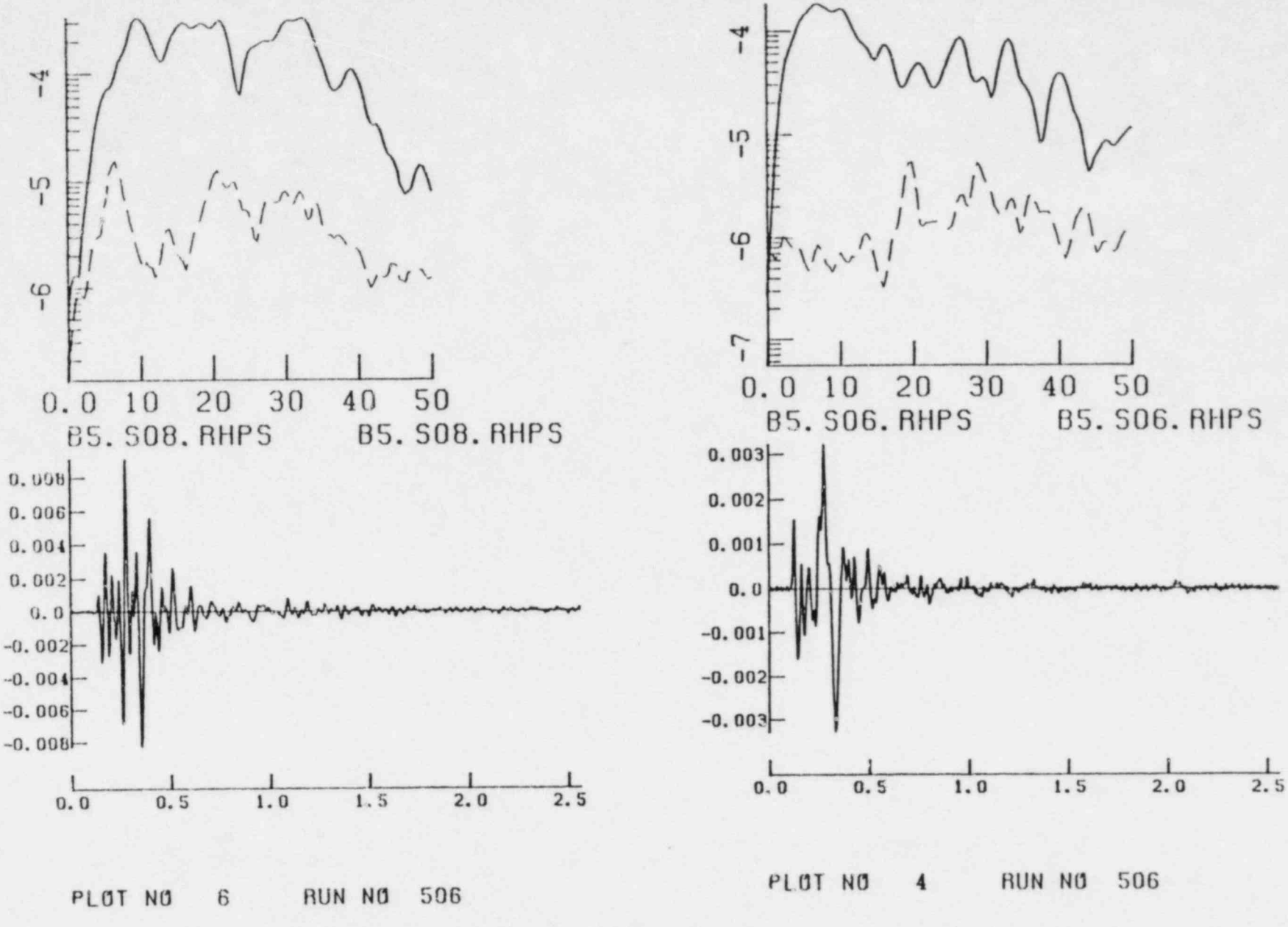

FIGURE 1.1 Vertical component seismograms and Fourier spectra for Test 5, shot 8 (50 ft depth; left) and shot 6 (210 ft depth; right) recorded on the hydroplant foundation (HP).

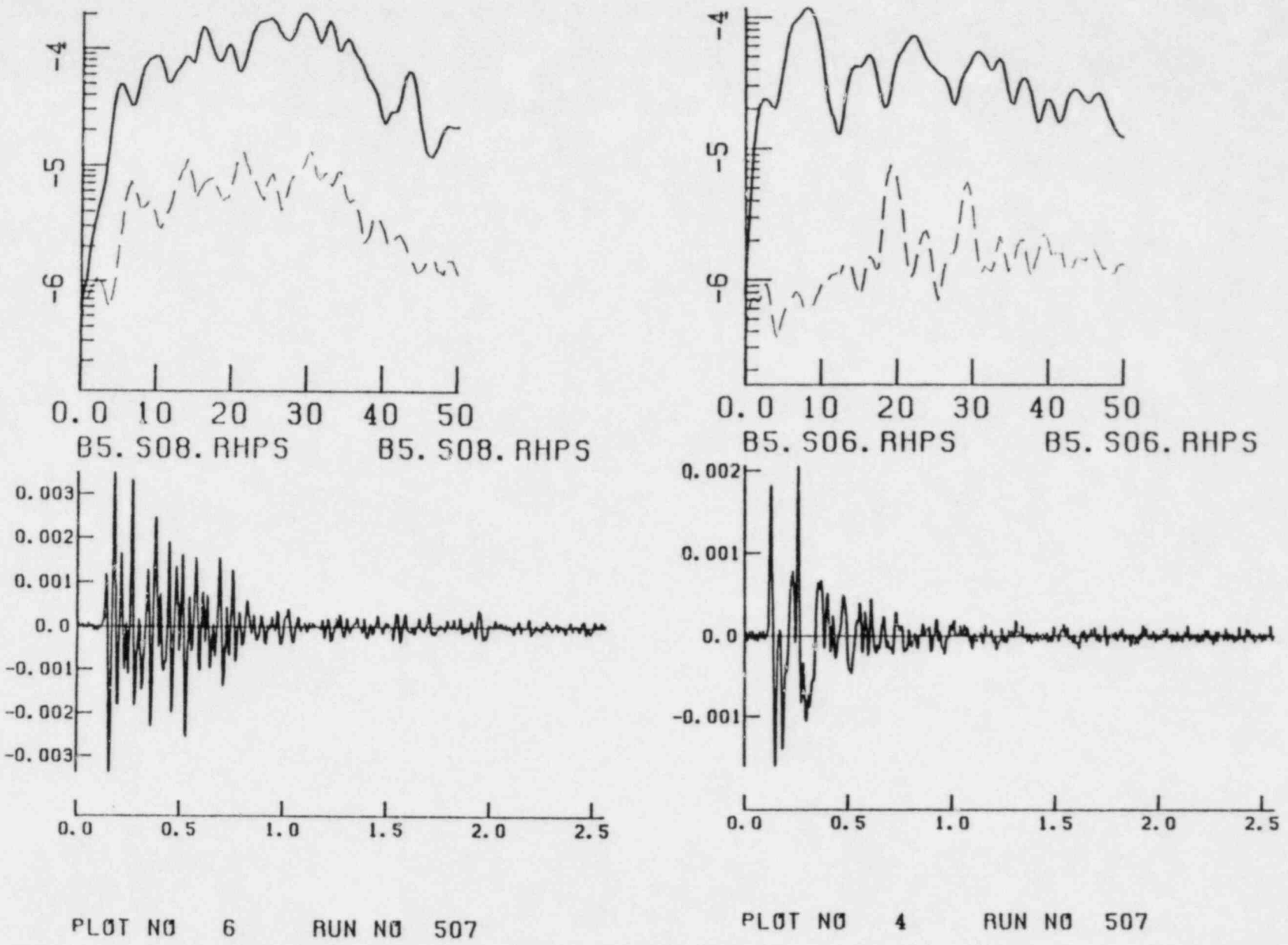

FIGURE 1.2 Radial component seismograms and Fourier spectra for Test 5, shot 8 (50 ft depth; left) and shot 6 (210 ft depth; right) recorded on the hydroplant foundation (HP).

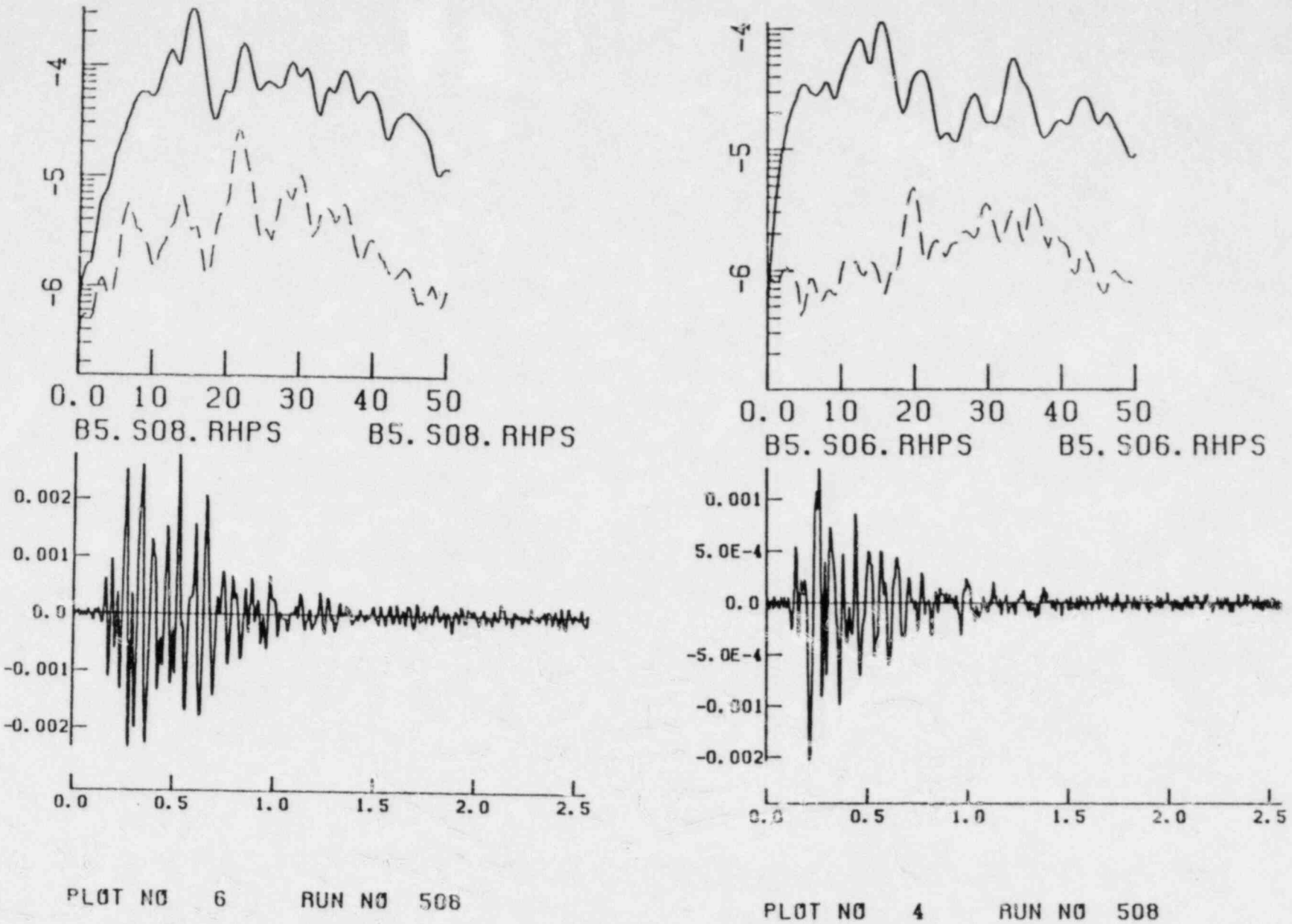

FIGURE 1.3 Transverse component seismograms and Fourier spectra for Test 5, shot 8 (50 ft depth; left) and shot 6 (210 ft depth; right) recorded on the hydroplant foundation (HP).

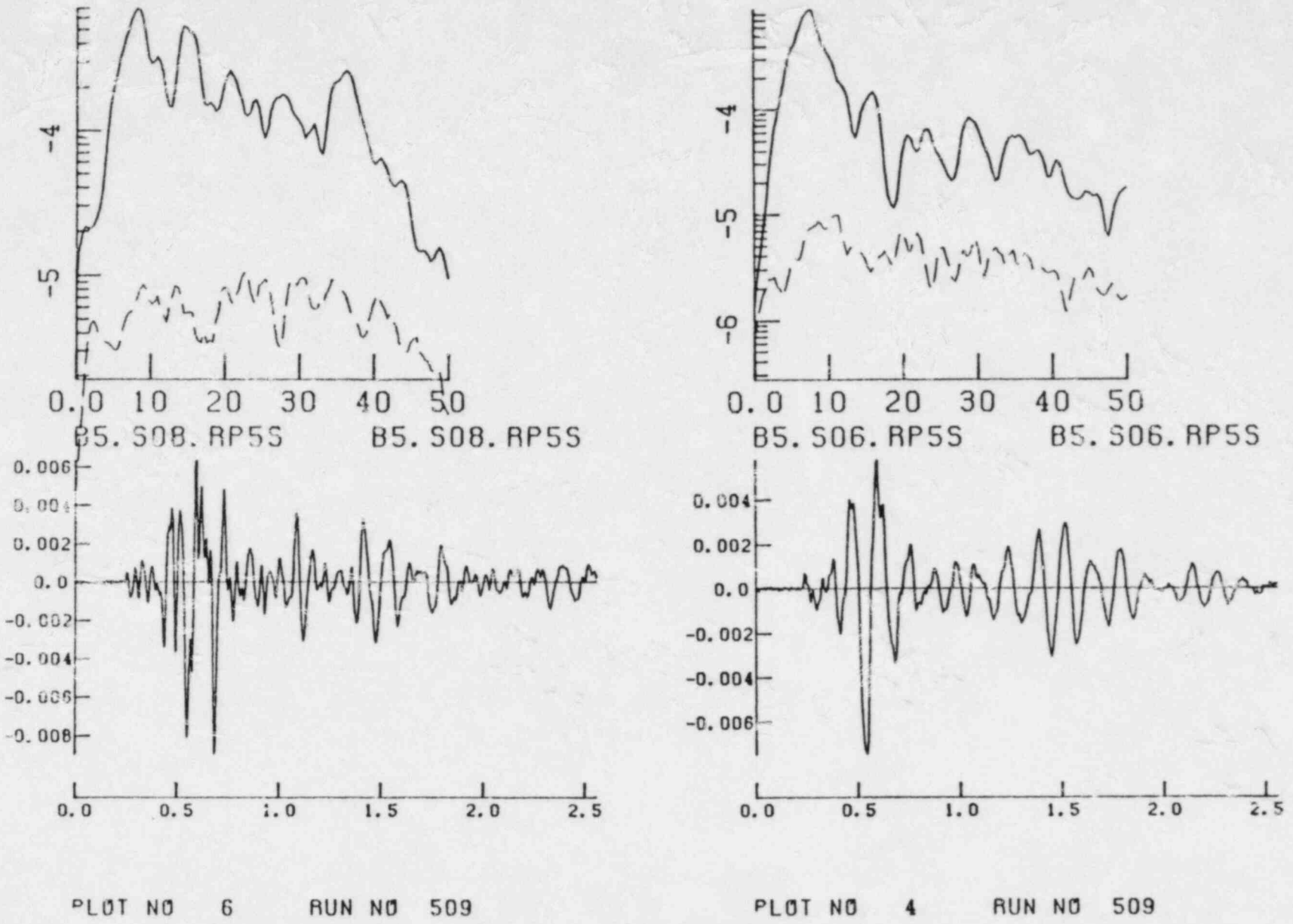

FIGURE 1.4 Vertical component seismograms and Fourier spectra for Test 5, shot 8 (50 ft depth; left) and shot 6 (210 ft depth; right) recorded in the free field on the dam abutment (P5).

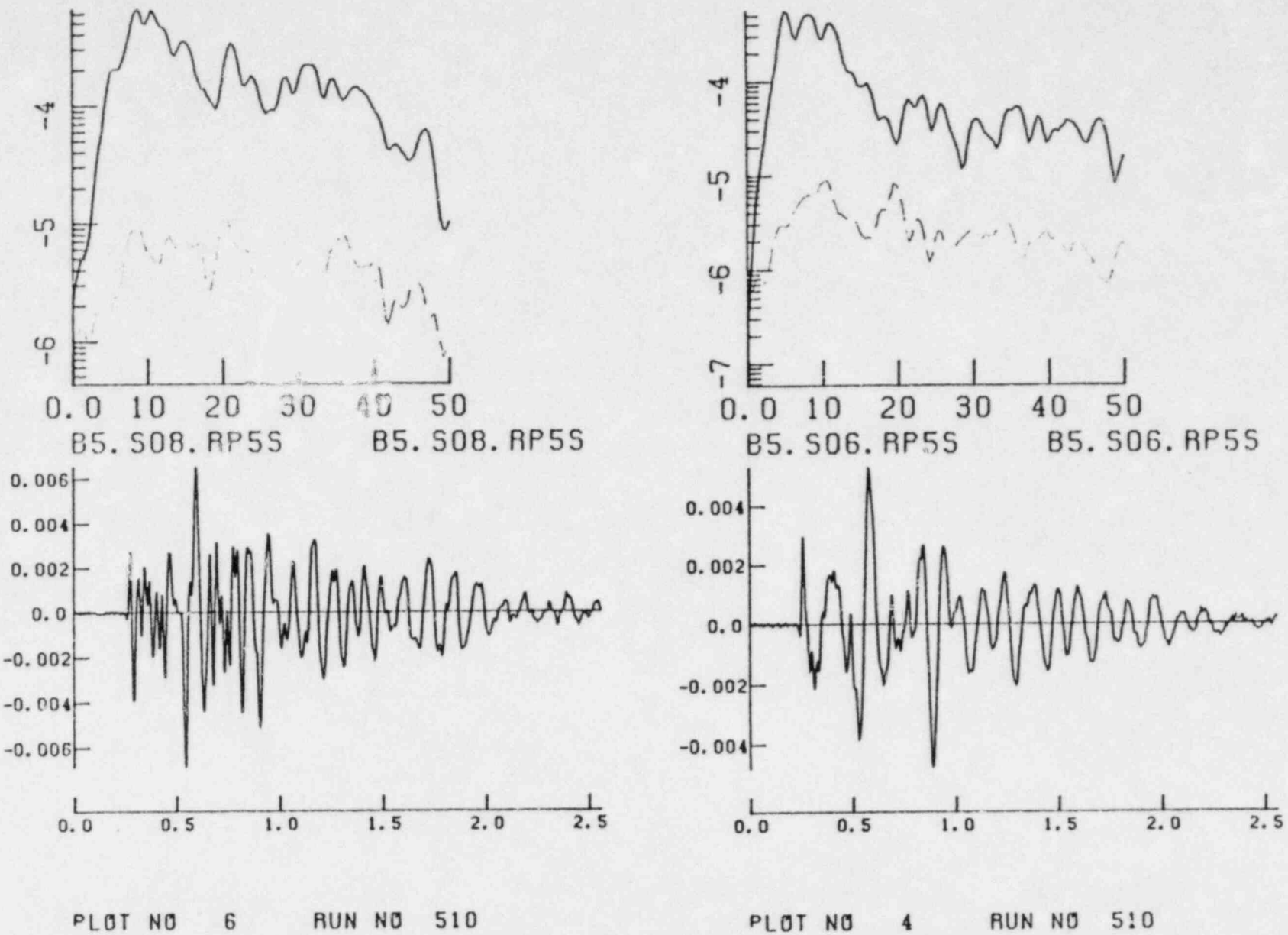

FIGURE 1.5 Radial component seismograms and Fourier spectra for Test 5, shot 8 (50 ft depth; left) and shot 6 (210 ft depth; right) recorded in the free field on the dam abutment (P5).

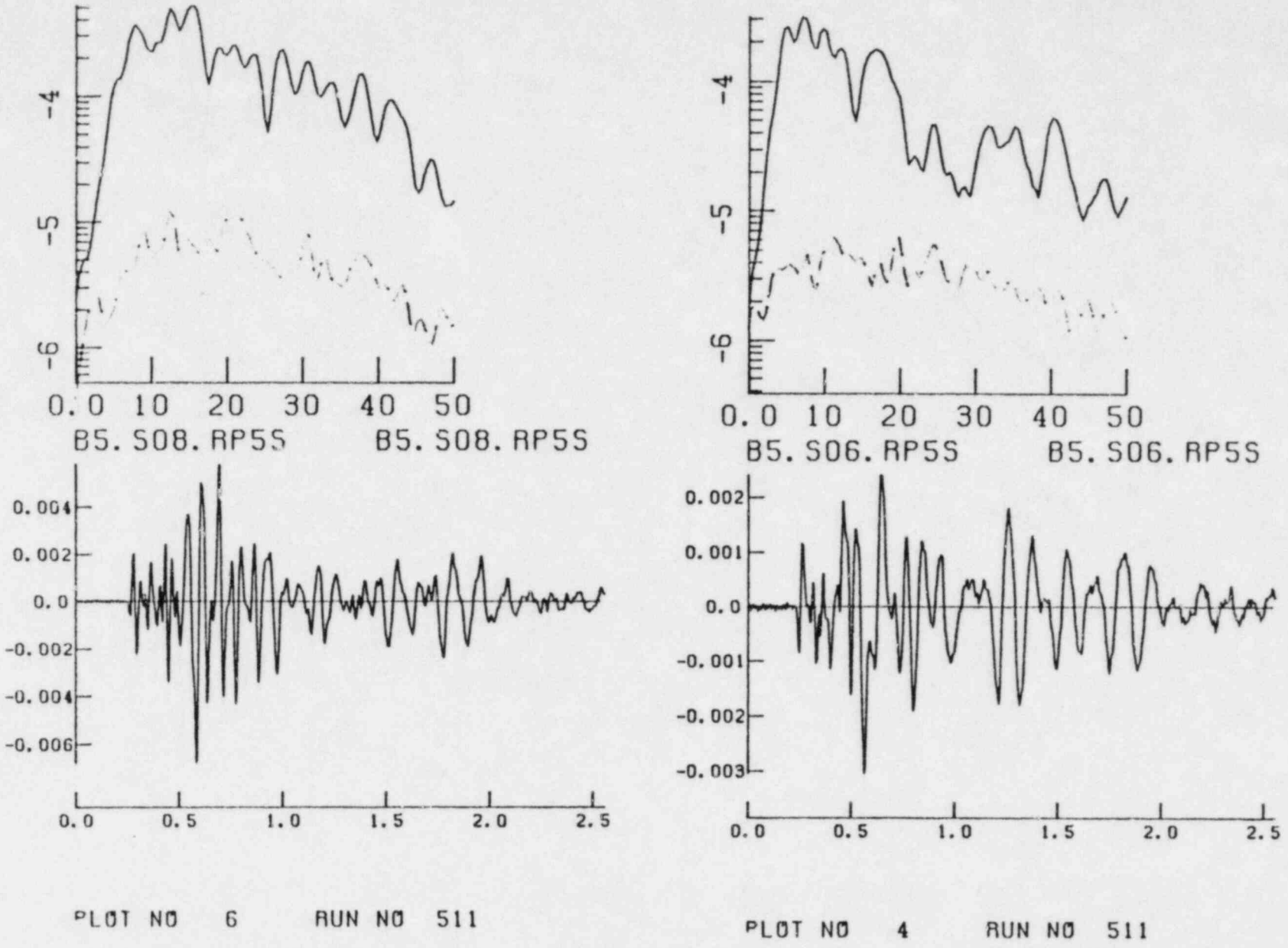

FIGURE 1.6 Transverse component seismograms and Fourier spectra for Test 5, shot 8 (50 ft depth; left) and shot 6 (210 ft depth; right) recorded in the free field on the dam abutment (P5).

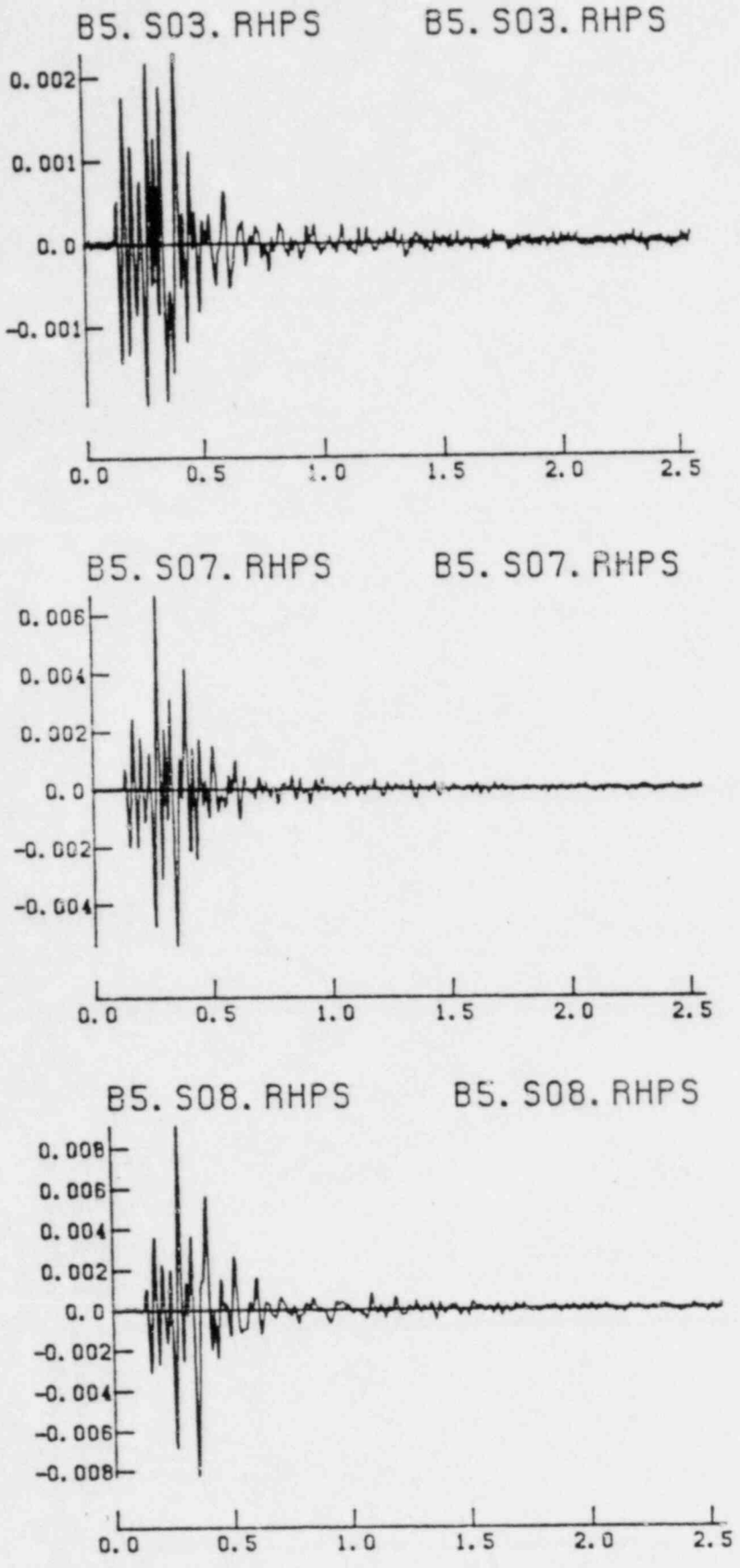

FIGURE 1.7 Vertical component hydroplant foundation records of Test 5 shots in saprolite. The subsurface depths of shots 3, 7, and 8, shown from top to bottom, were 46, 67, and 50 ft.

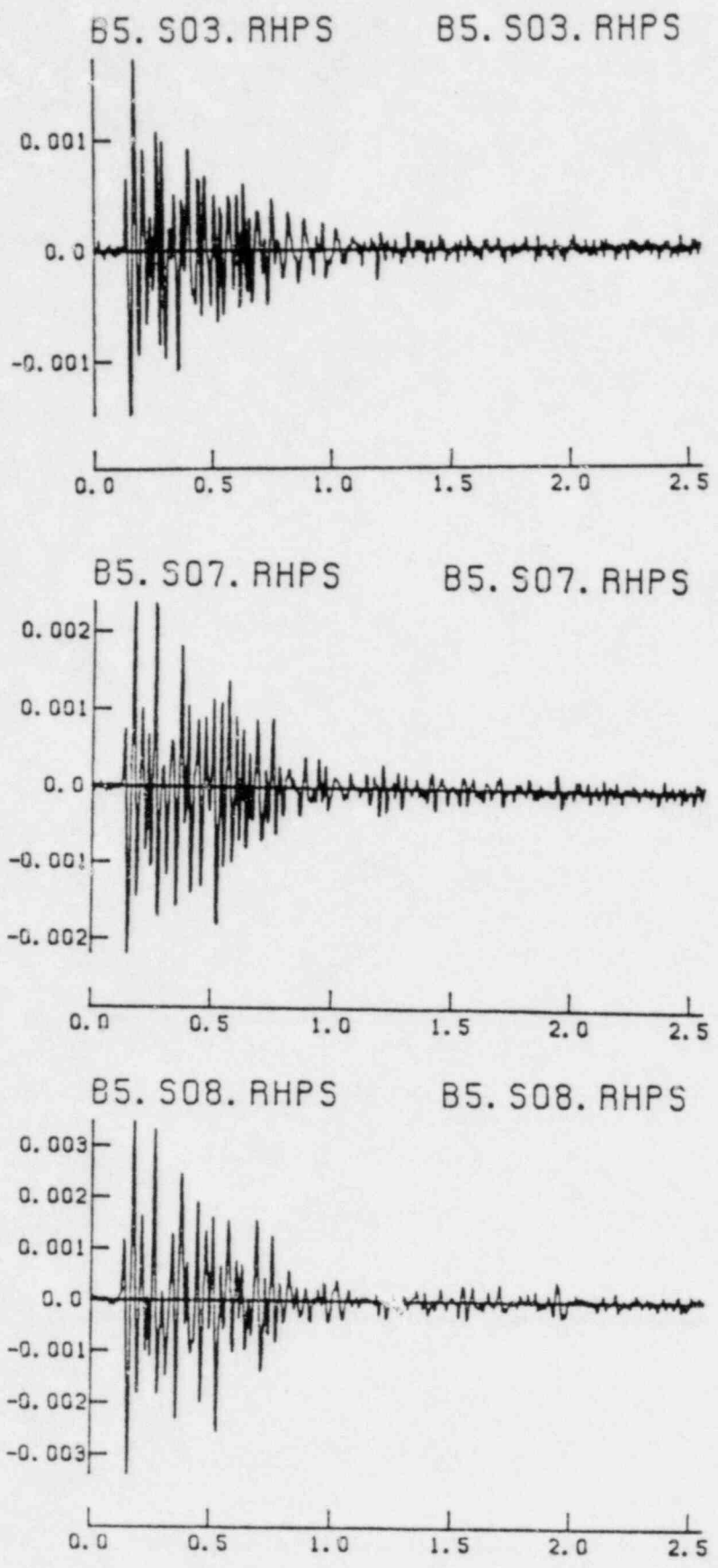

FIGURE 1.8 Radial component hydroplant foundation records of Test 5 shots in saprolite. The subsurface depths of shots 3, 7, and 8, shown from top to bottom, were 46, 67, and 50 ft.

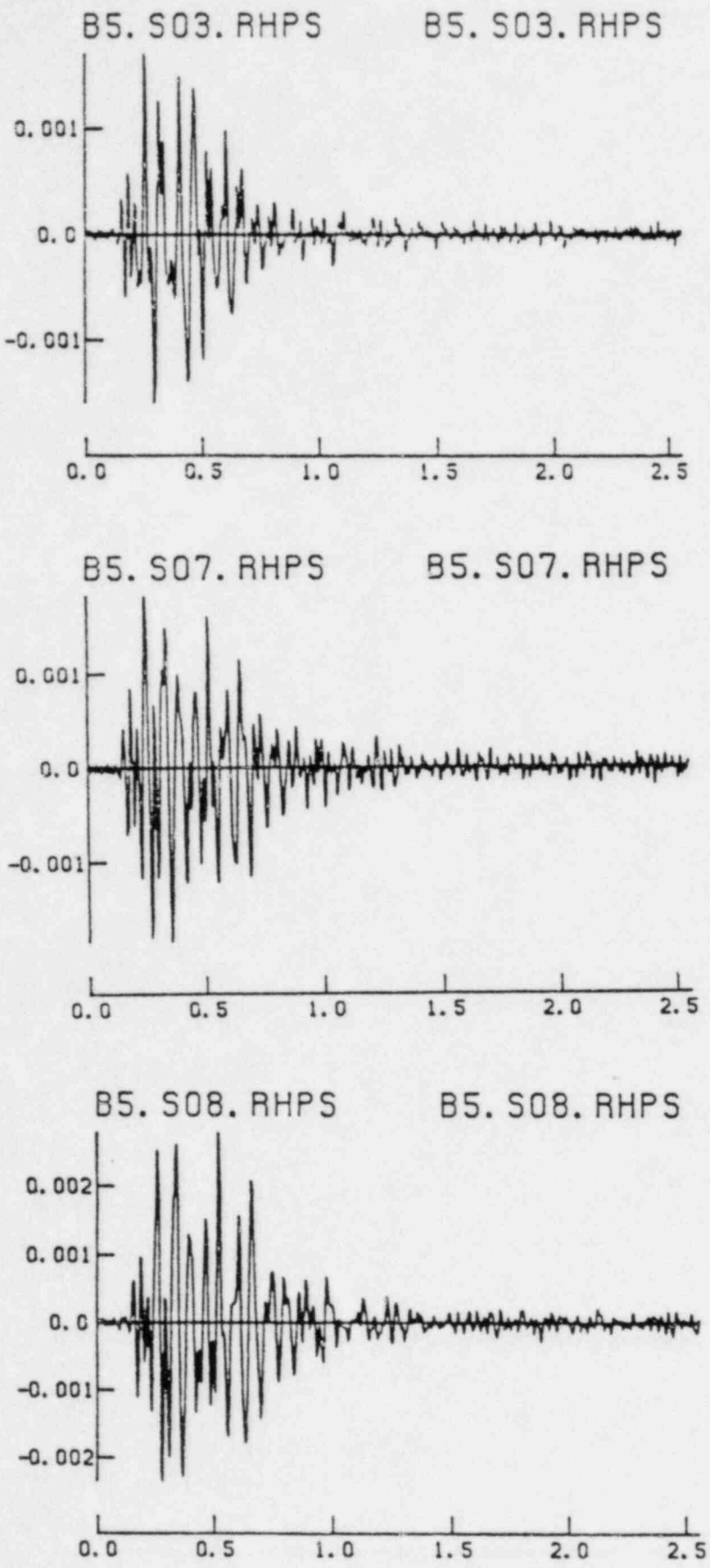

FIGURE 1.9 Transverse component hydroplant foundation records of Test 5 shots in saprolite. The subsurface depths of shots 3, 7, and 8, shown from top to bottom, were 46, 67, and 50 ft.

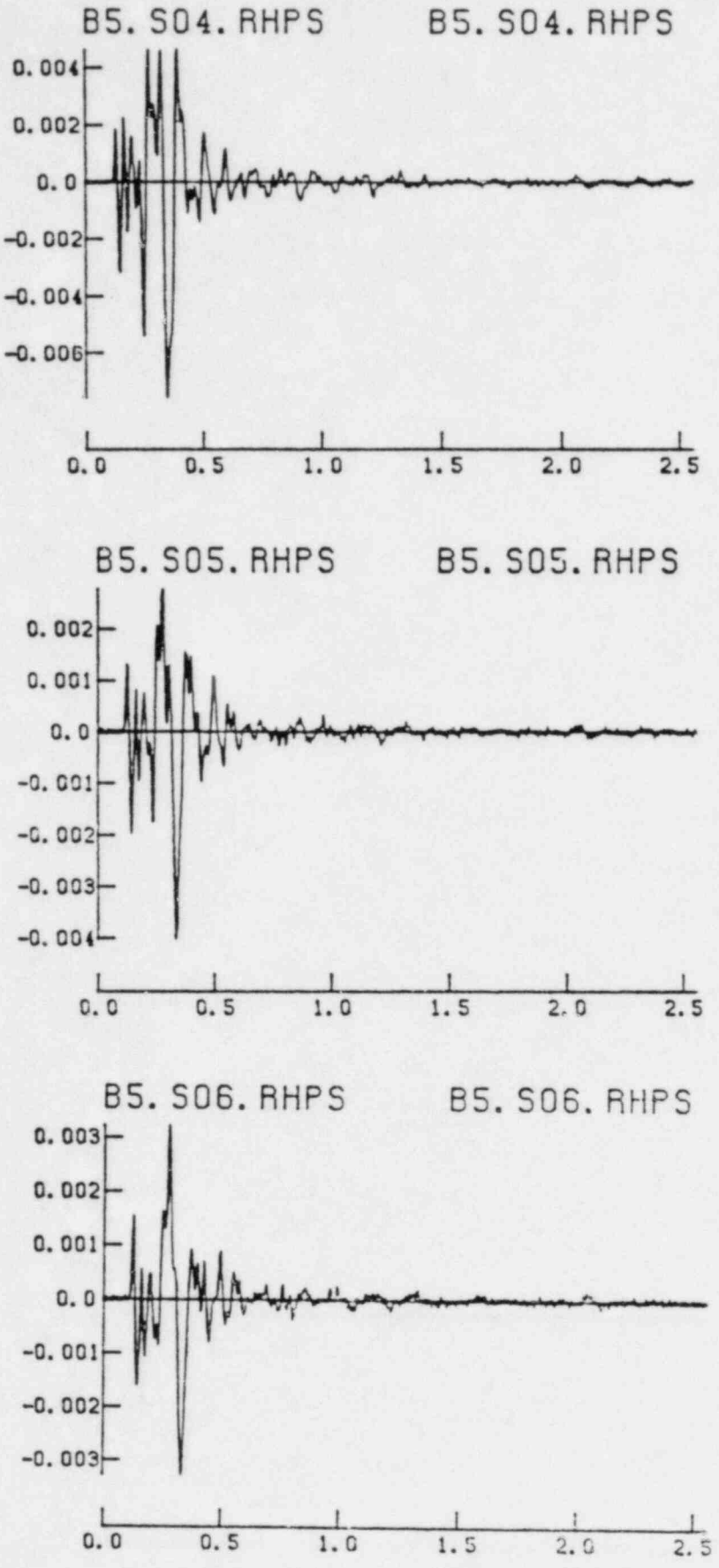

FIGURE 1.10 Vertical component hydroplant foundation records of Test 5 shots in rock. The subsurface depths of shots 4, 5, and 6, shown from top to bottom, were 116, 157, and 219 ft.

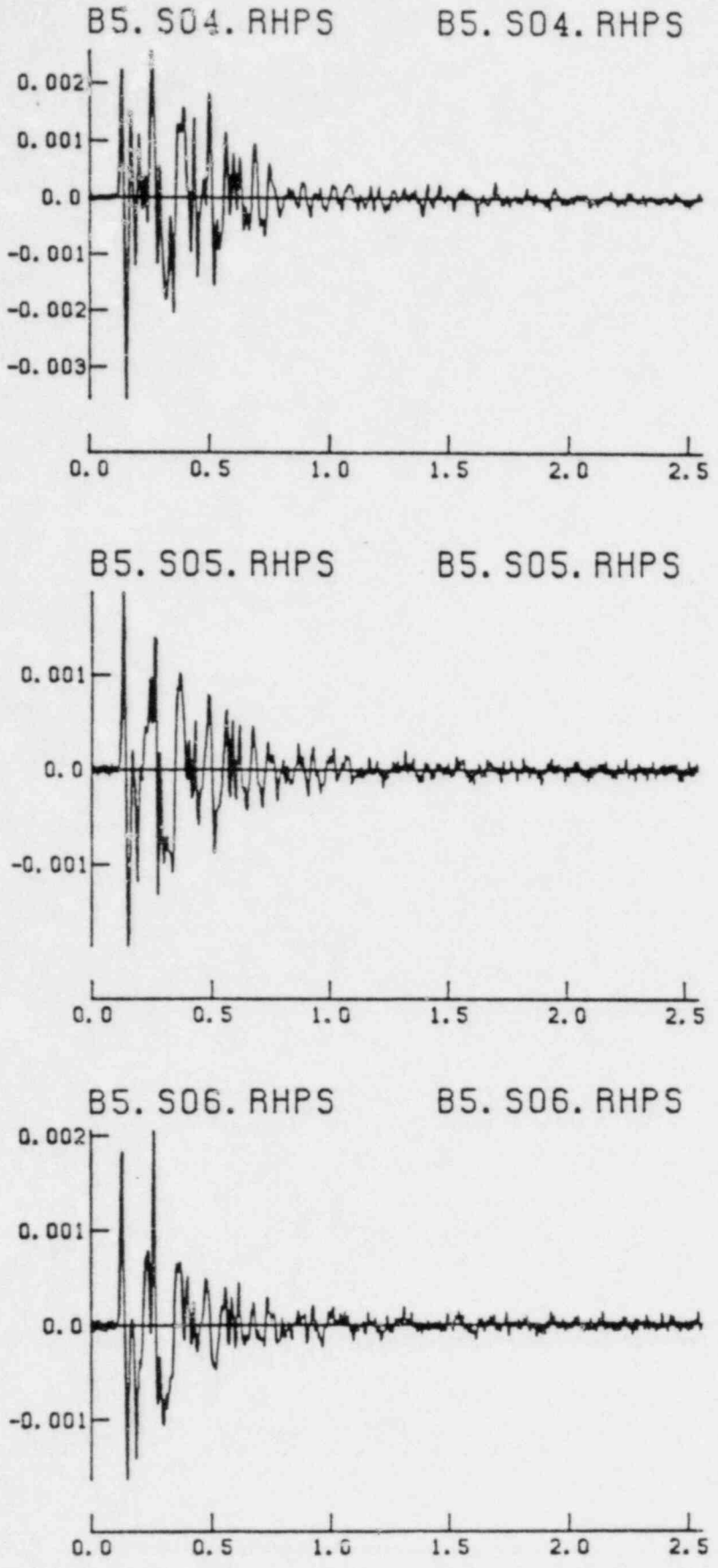

FIGURE 1.11 Radial component hydroplant foundation records of Test 5 shots in rock. The subsurface depths of shots 4, 5, and 6, shown from top to bottom were 116, 157, and 210 ft.

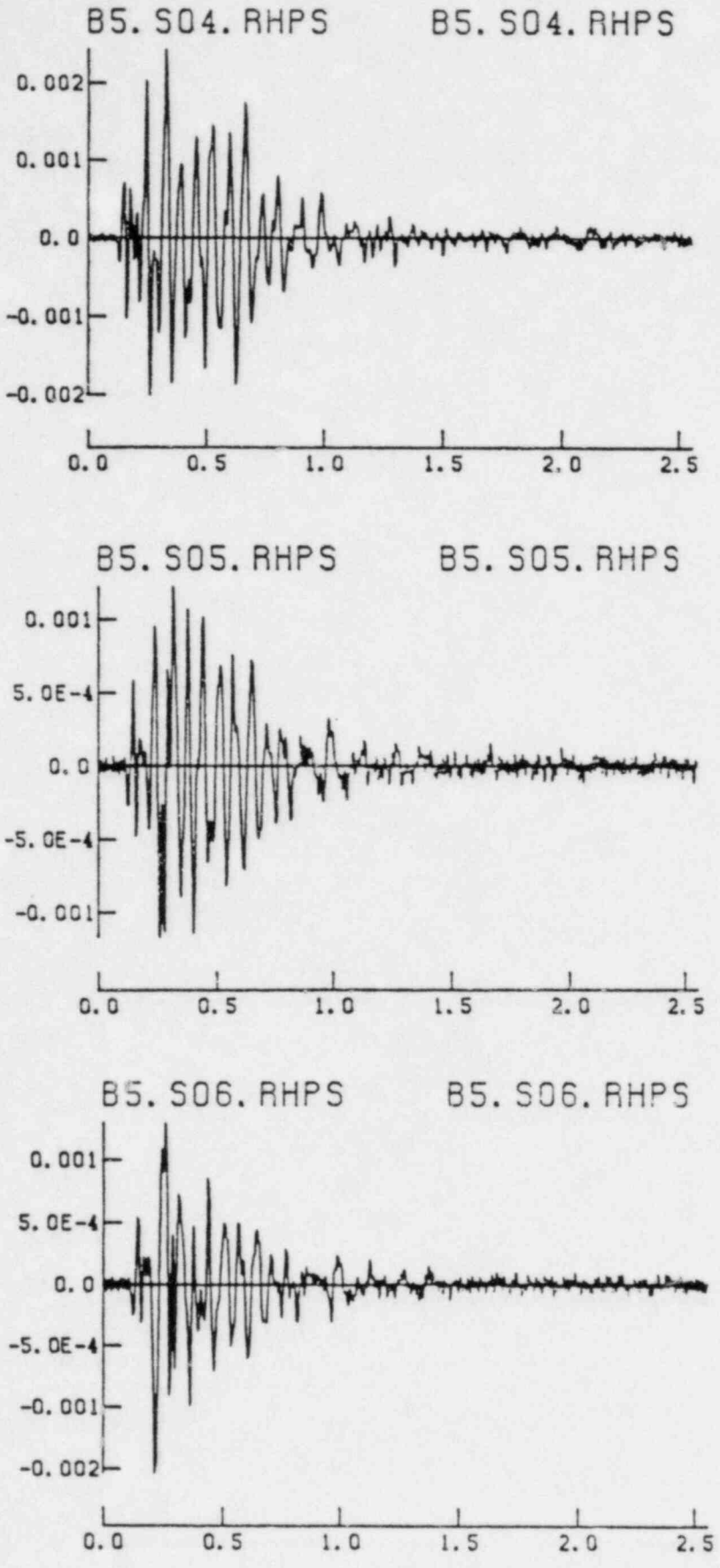

FIGURE 1.12 Transverse component hydroplant foundation records of Test 5 shots in rock. The subsurface depths of shots 4, 5, and 6, shown from top to bottom, were 116, 157, and 210 ft.

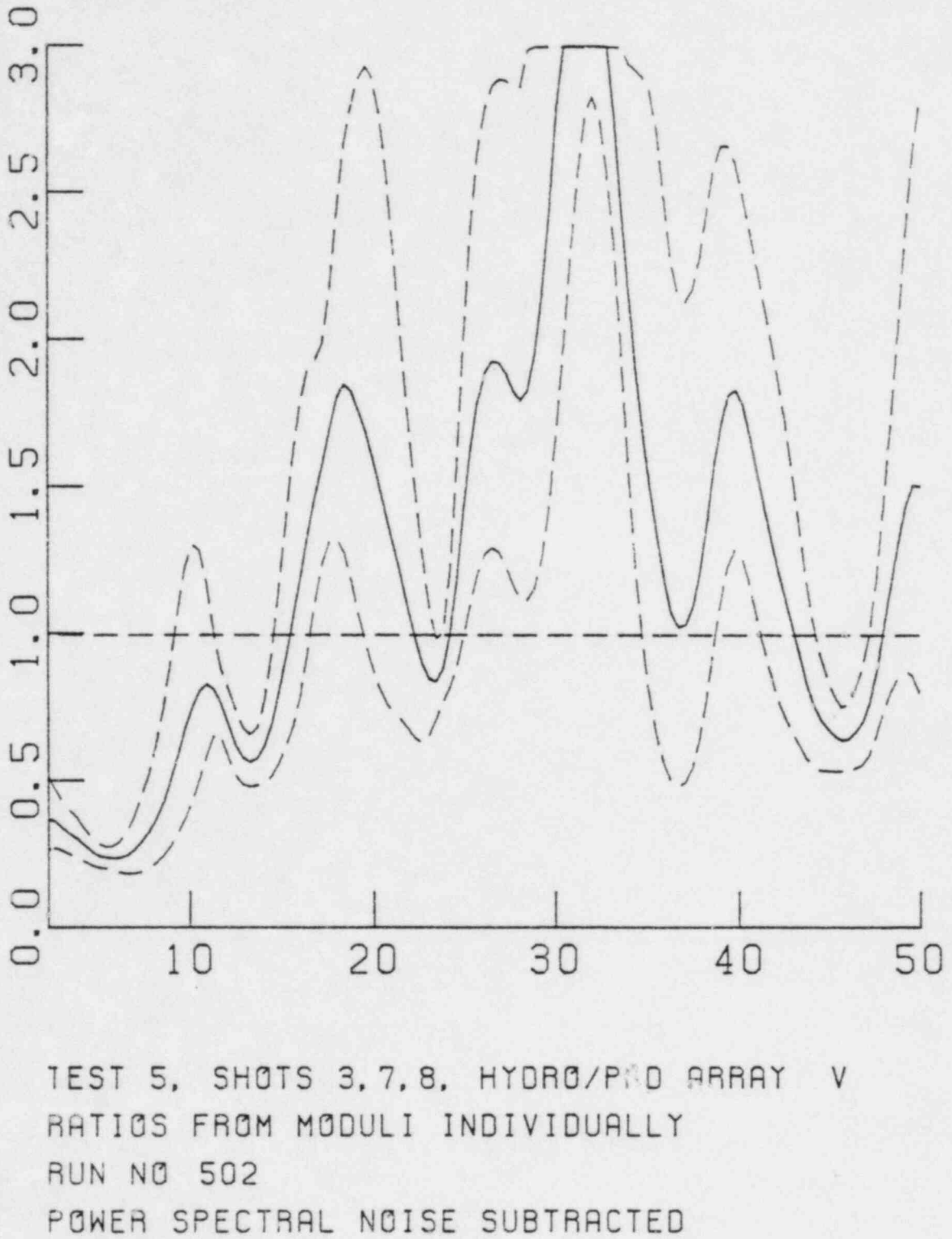

FIGURE 1.13 Vertical component spectral modulus ratio, hydroplant foundation/dam abutment free field, for shallow Test 5 shots (3, 7, 8) in saprolite. Note that the signals have not been scaled for epicentral distance (1930 ft to the hydroplant vs. 3180 ft to the center of the dam abutment array).

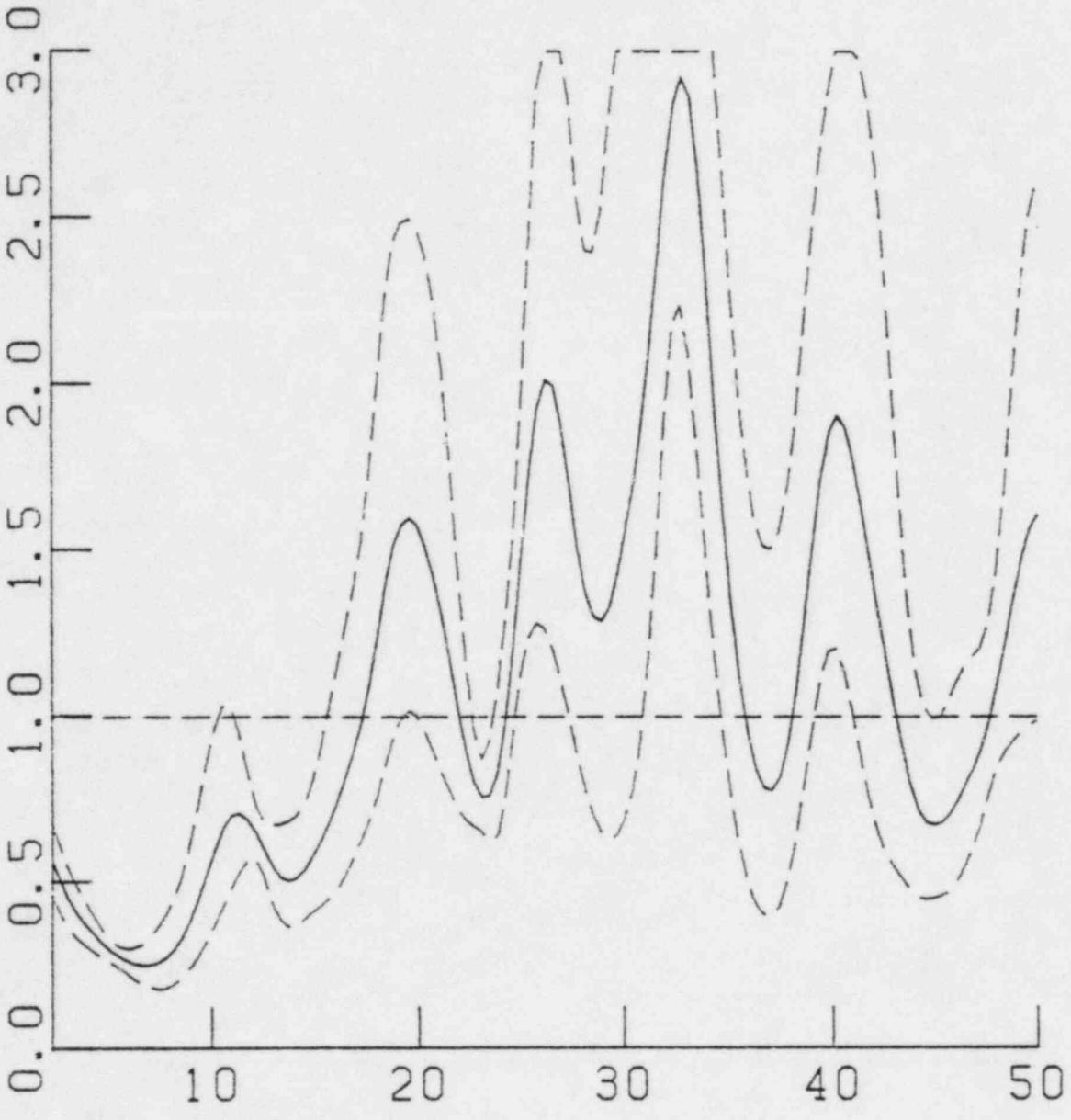

FIGURE 1.14 Vertical component spectral modulus ratio, hydroplant foundation/dam abutment free field, for deep Test 5 shots (4, 5, 6) in gneiss. Note that the signals have not been scaled for epicentral distance (1930 ft to the hydroplant vs. 3180 ft to the center of the dam abutment array).

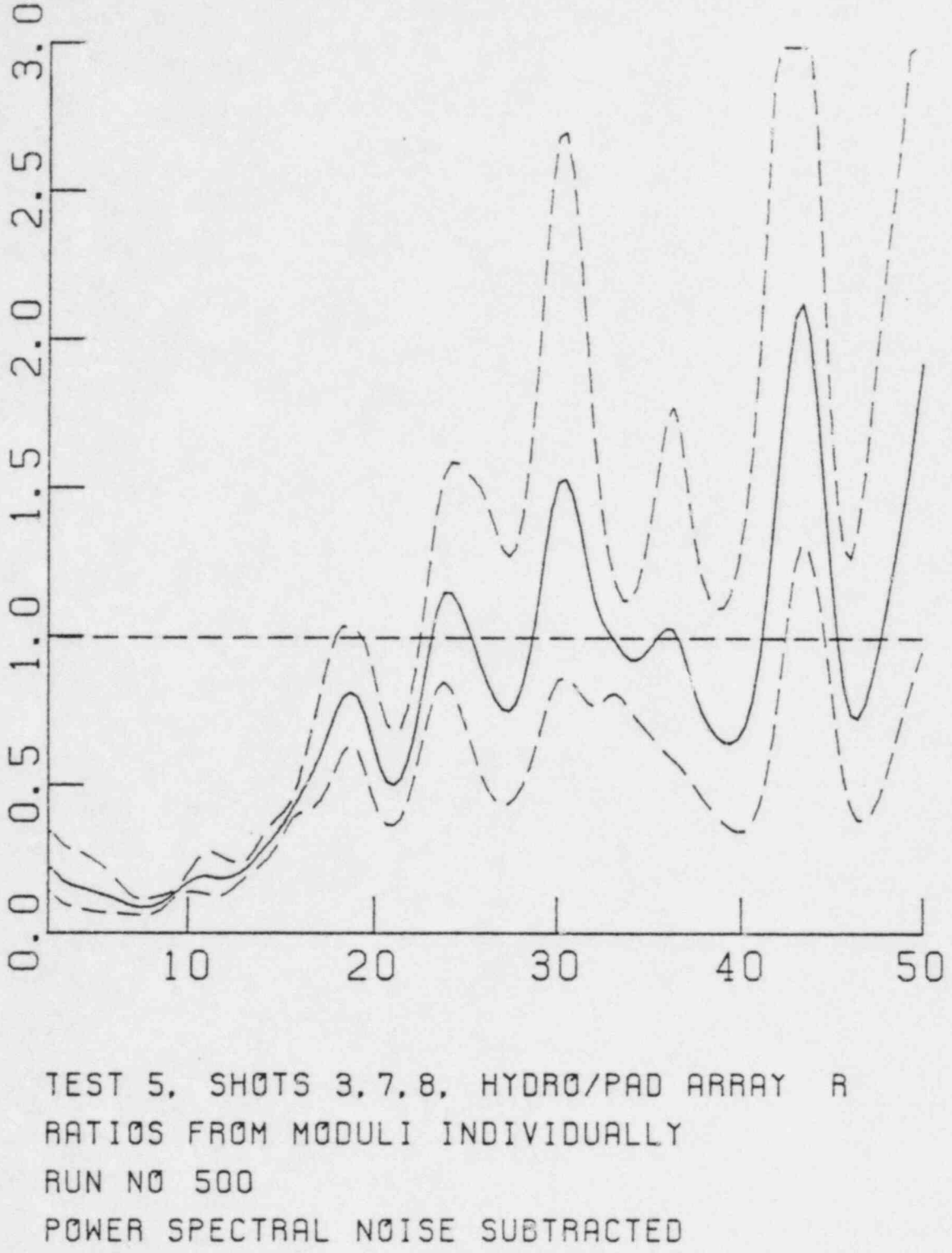

FIGURE 1.15 Radial component spectral modulus ratio, hydroplant foundation/dam abutment free field, for shallow Test 5 shots (3, 7, 8) in saprolite. Note that the signals have not been scaled for epicentral distance (1930 ft to the hydroplant vs. 3180 ft to the center of the dam abutment array).

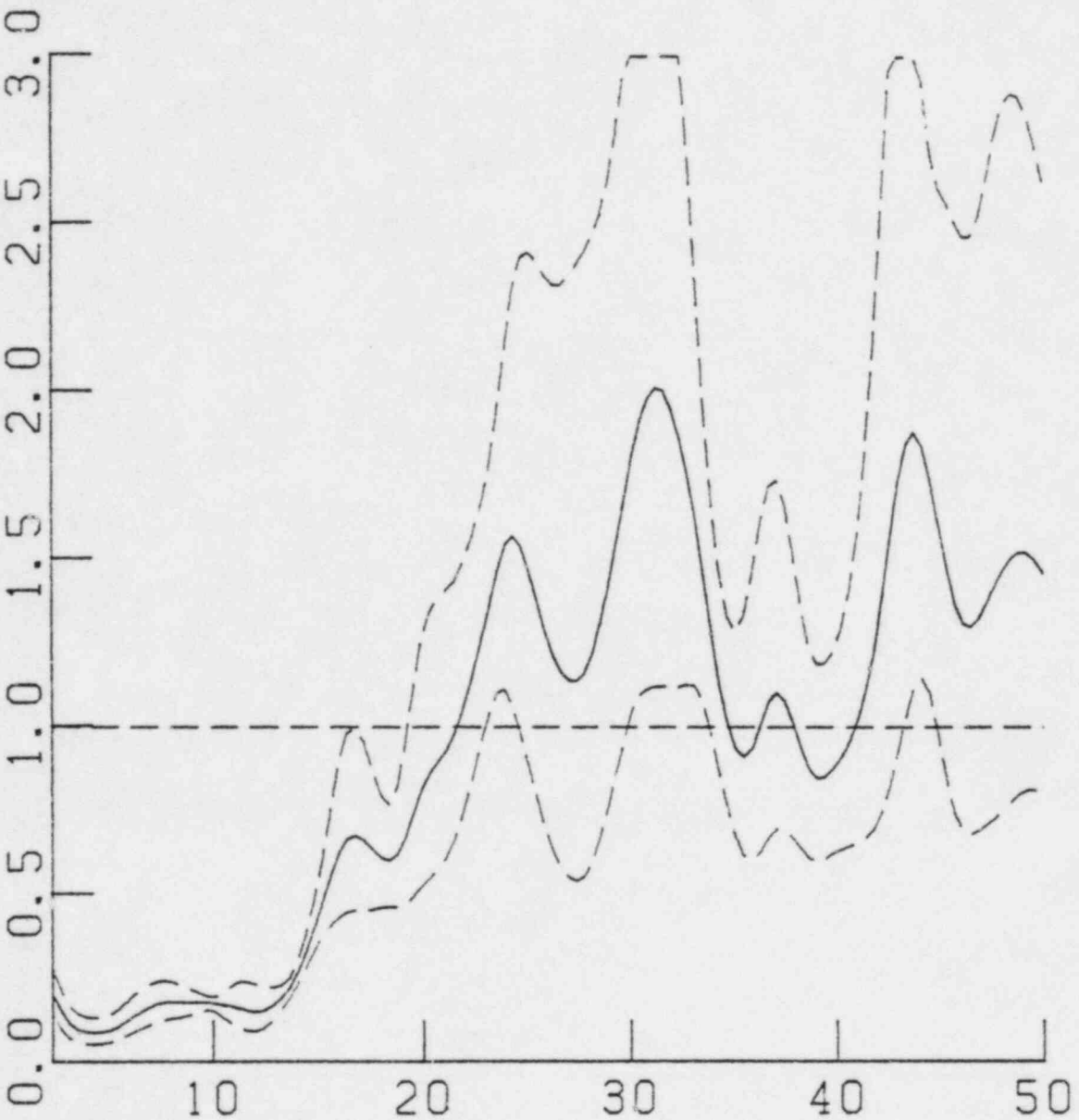

FIGURE 1.16 Radial component spectral modulus ratio, hydroplant foundation/dam abutment free field, for deep Test 5 shots (4, 5, 6) in gneiss. Note that the signals have not been scaled for epicentral distance (1930 ft to the hydroplant vs. 3180 ft to the center of the dam abutment array).

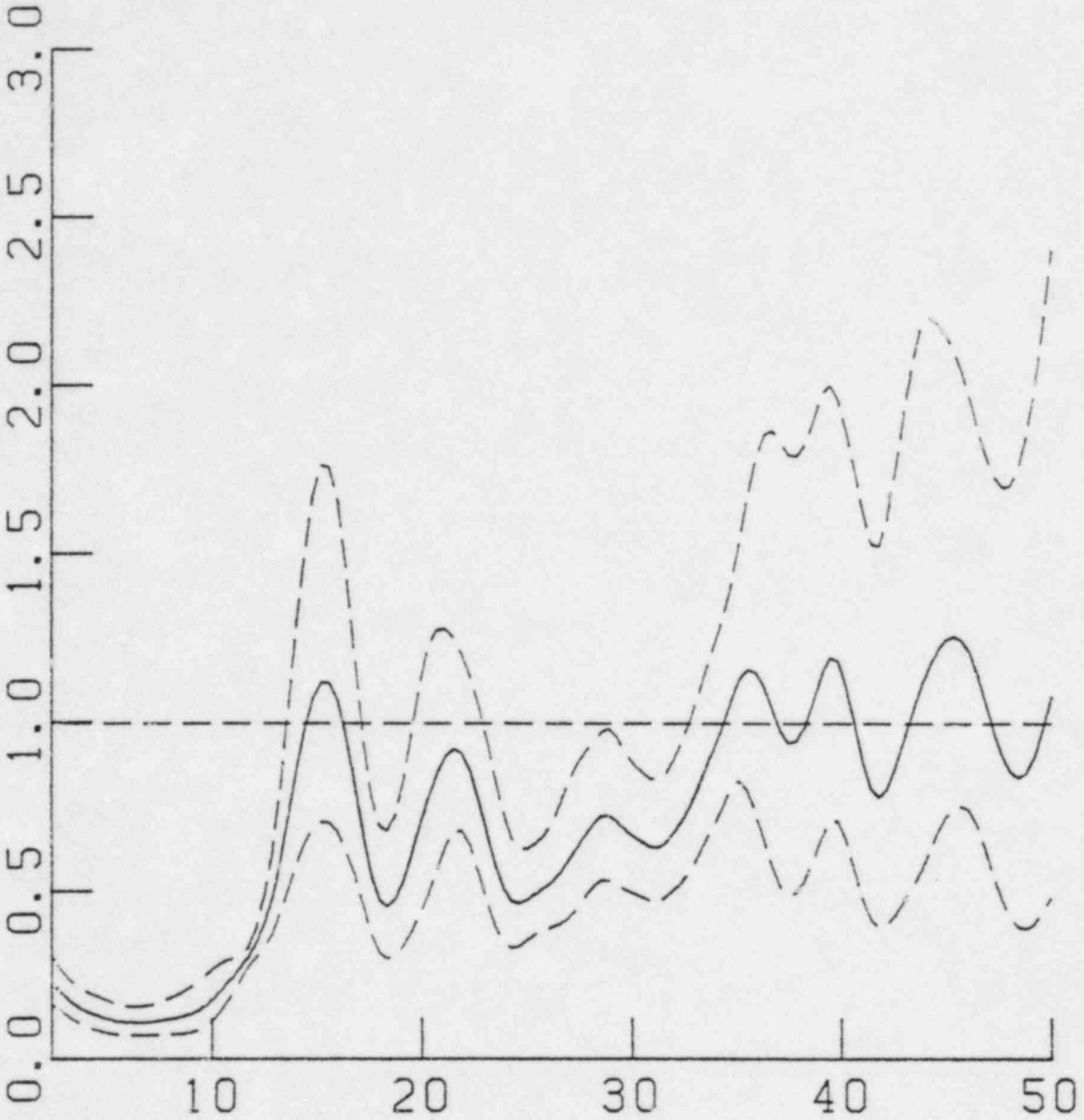

FIGURE 1.17 Transverse component spectral modulus ratio, hydroplant foundation/dam abutment free field, for shallow Test 5 shots (3, 7, 8) in saprolite. Note that the signals have not been scaled for epicentral distance (1930 ft to the hydroplant vs. 3180 ft to the center of the dam abutment array).

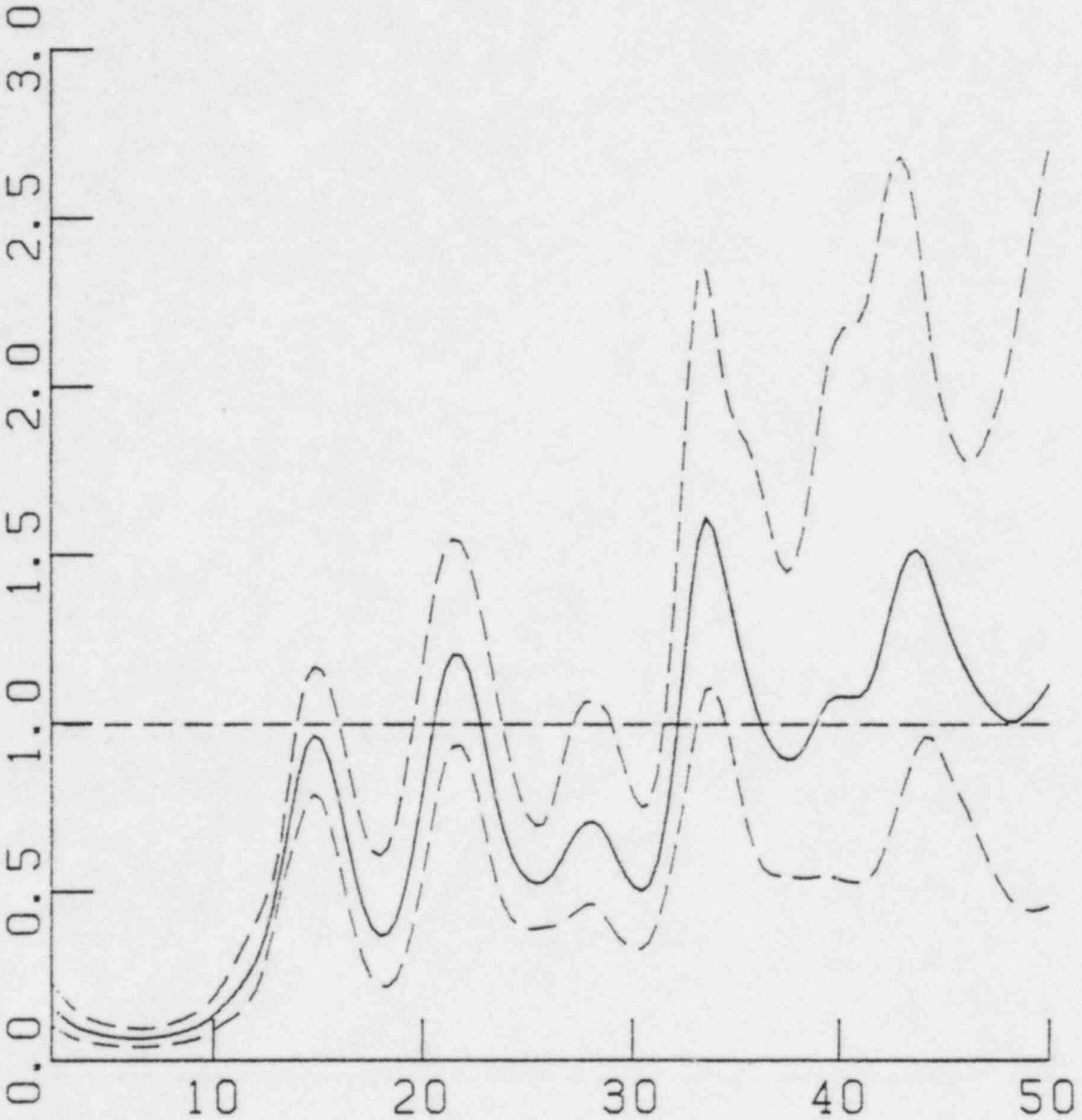

FIGURE 1.18 Transverse component spectral modulus ratio, hydroplant foundation/dam abutment free field, for deep Test 5 shots (4, 5, 6) in gneiss. Note that the signals have not been scaled for epicentral distance (1930 ft to the hydroplant vs. 3180 ft to the center of the dam abutment array).

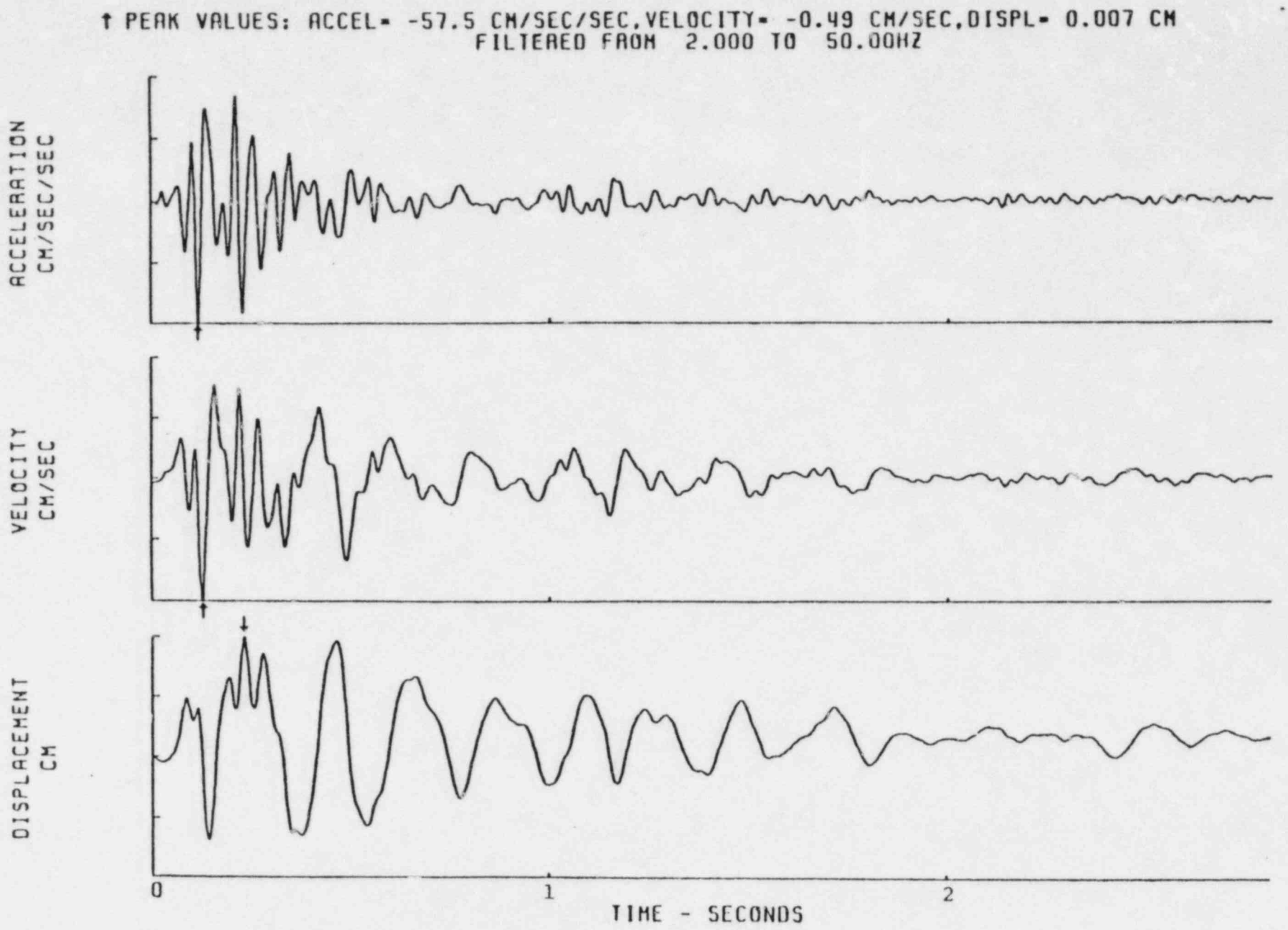

FIGURE 1.19 South component corrected USGS dam abutment record of the M_L 2.2 RIS event of 05:47 UTC, 10/17/78, with hypocentral depth 0.36 km and epicentral distance 1.04 km.

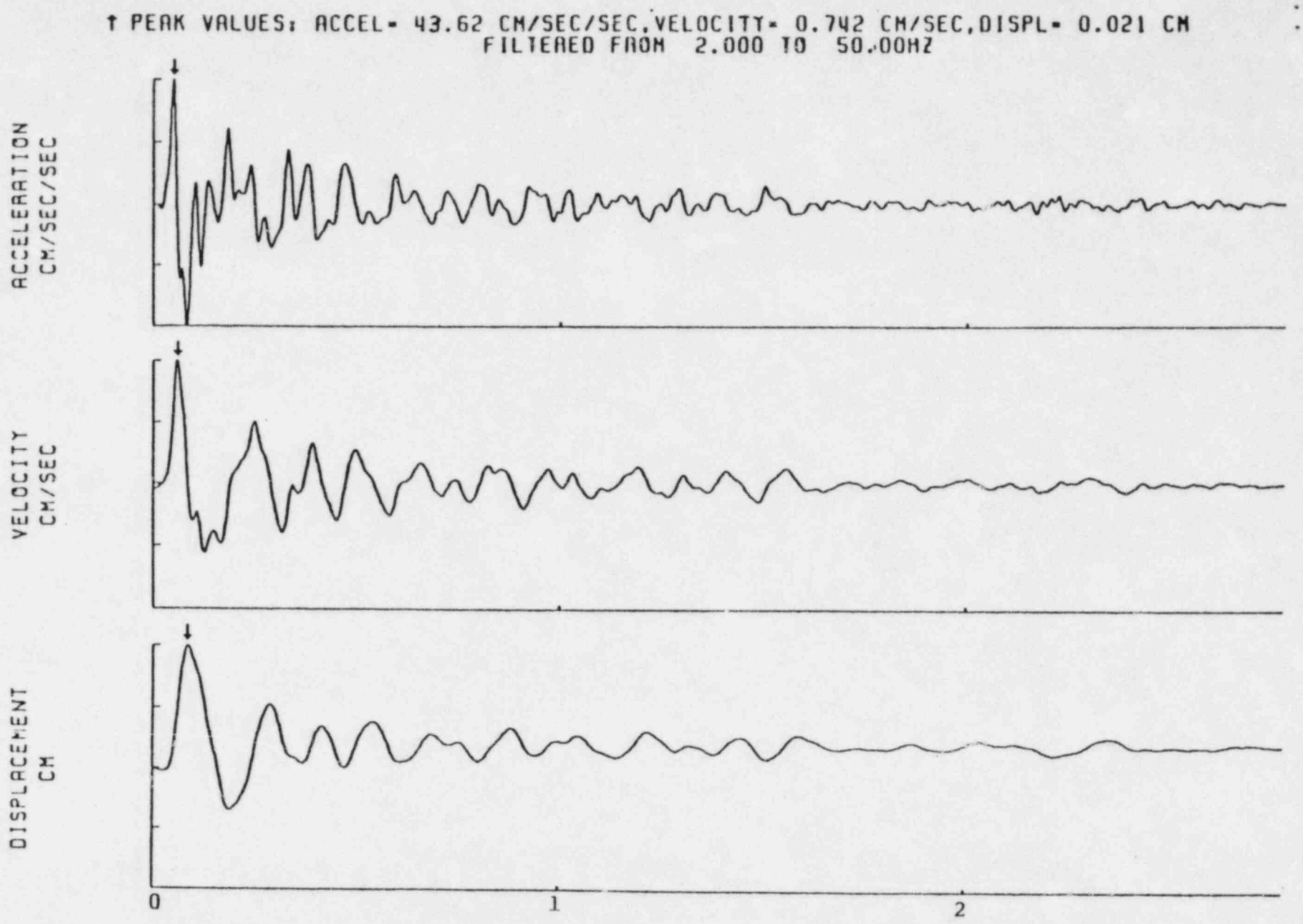

FIGURE 1.20 Vertical component corrected USGS dam abutment record of the M_L 2.2 RIS event of 05:47 UTC, 10/17/78, with hypocentral depth 0.36 km and epicentral distance 1.04 km.

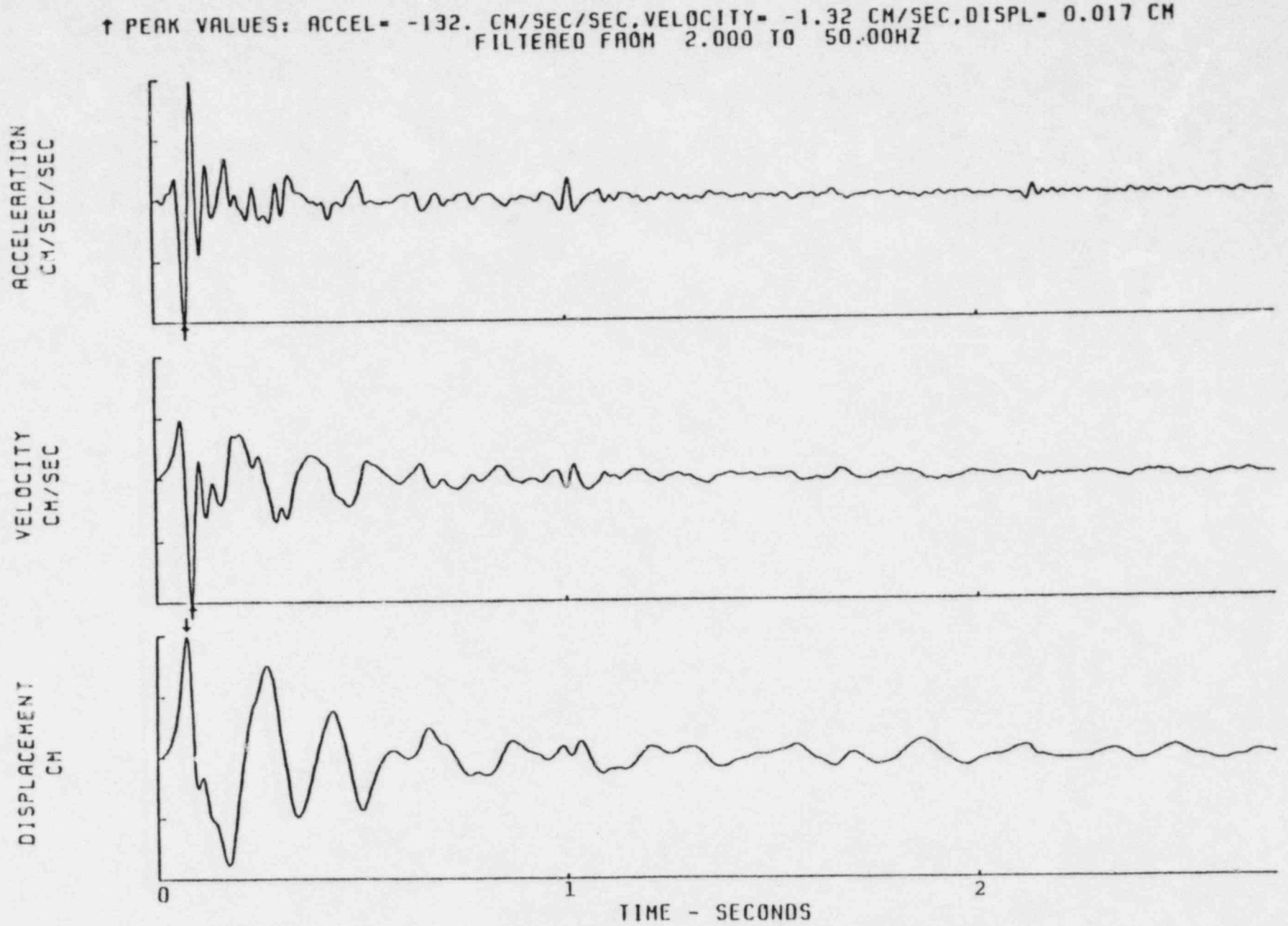

FIGURE 1.21 East component corrected USGS dam abutment record of the M_L 2.2 RIS event of 05:47 UTC, 10/17/78, with hypocentral depth 0.36 km and epicentral distance 1.04 km.

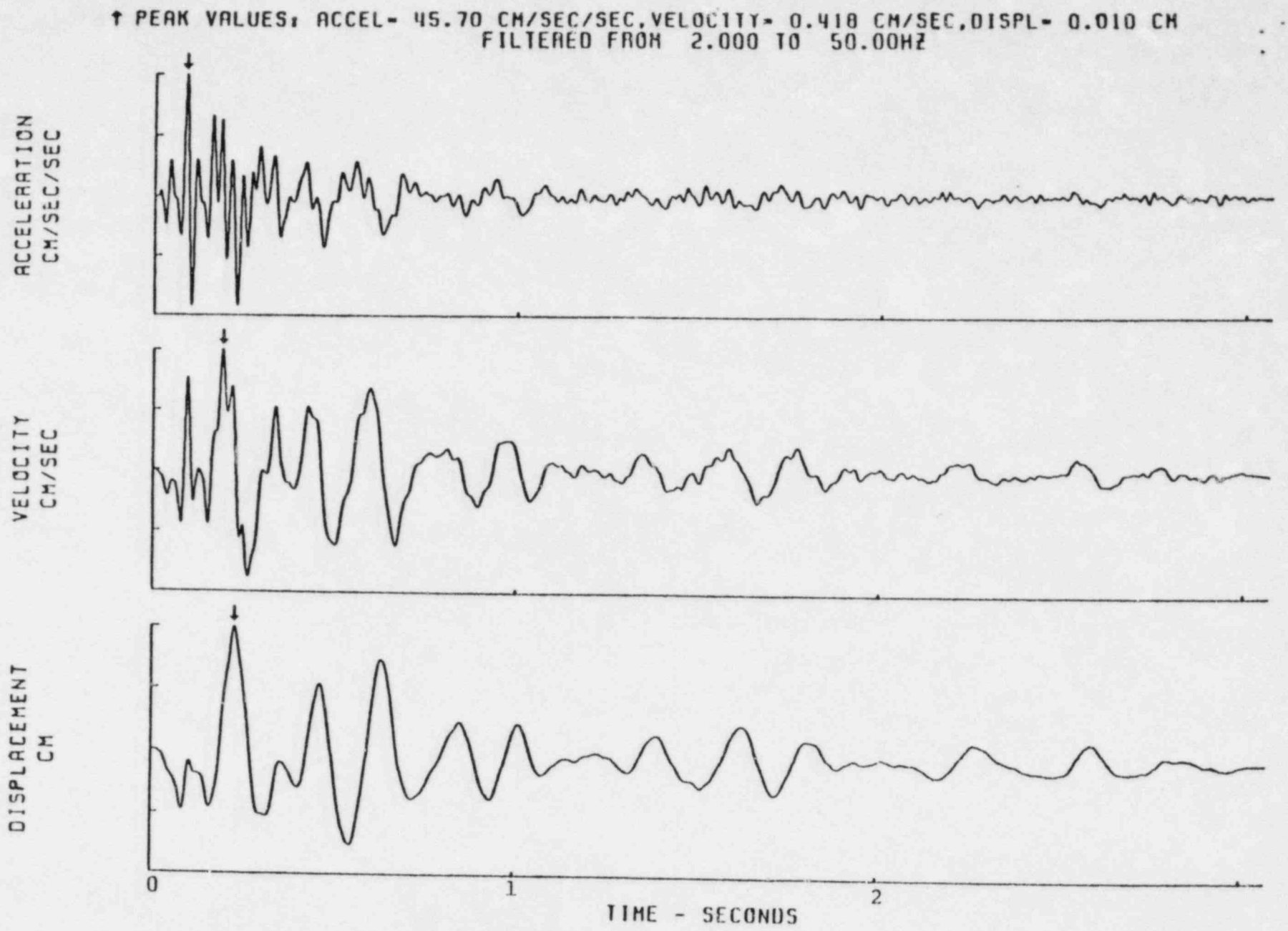

FIGURE 1.22 South component corrected USGS dam abutment record of the M_L 2.6 RIS event of 23:20 UTC, 10/08/79, with hypocentral depth 1.34 km and epicentral distance 1.05 km.

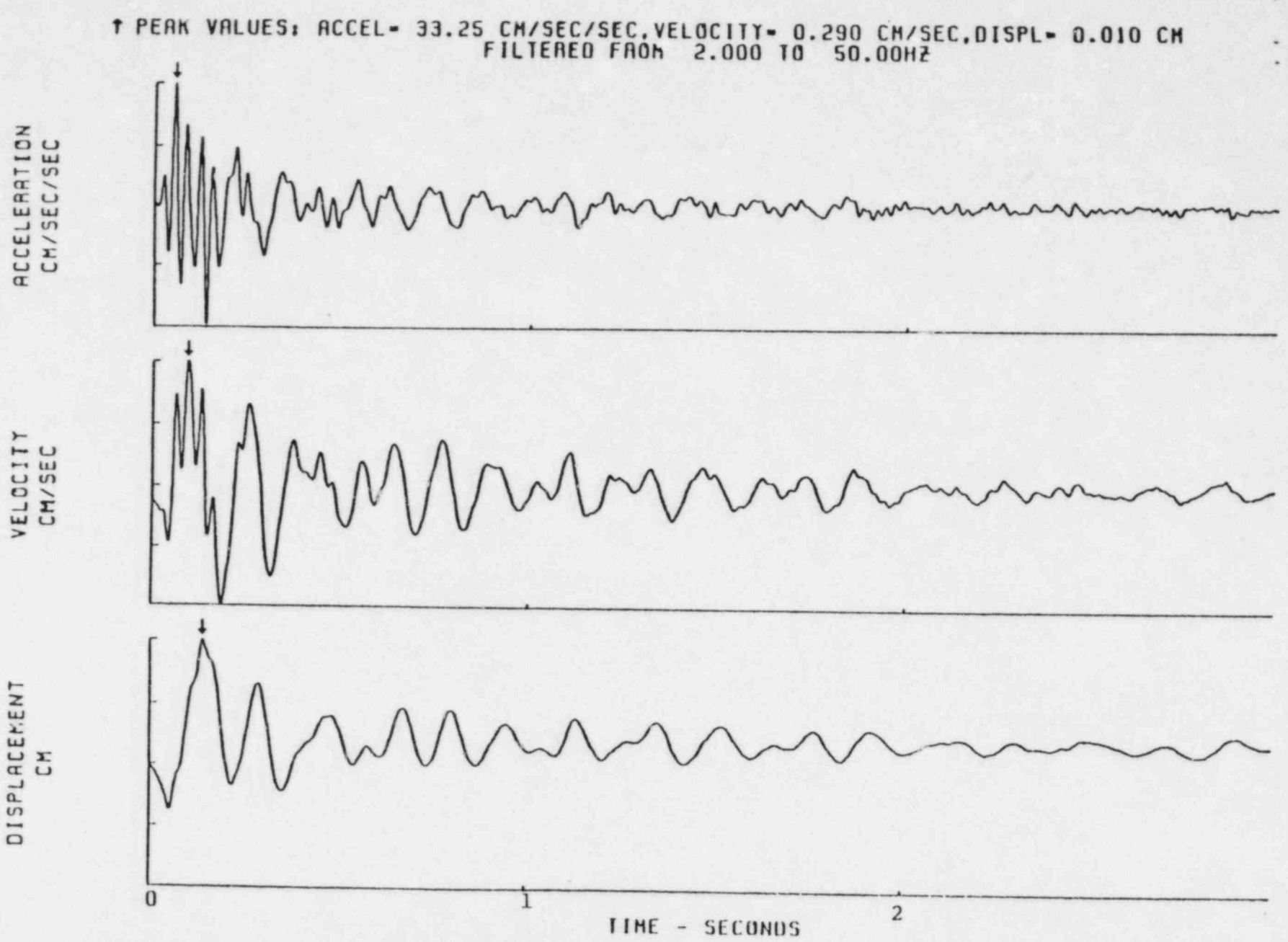

FIGURE 1.23 Vertical component corrected USGS dam abutment record of the M_L 2.6 RIS event of 23:20 UTC, 10/08/79, with hypocentral depth 1.34 km and epicentral distance 1.05 km.

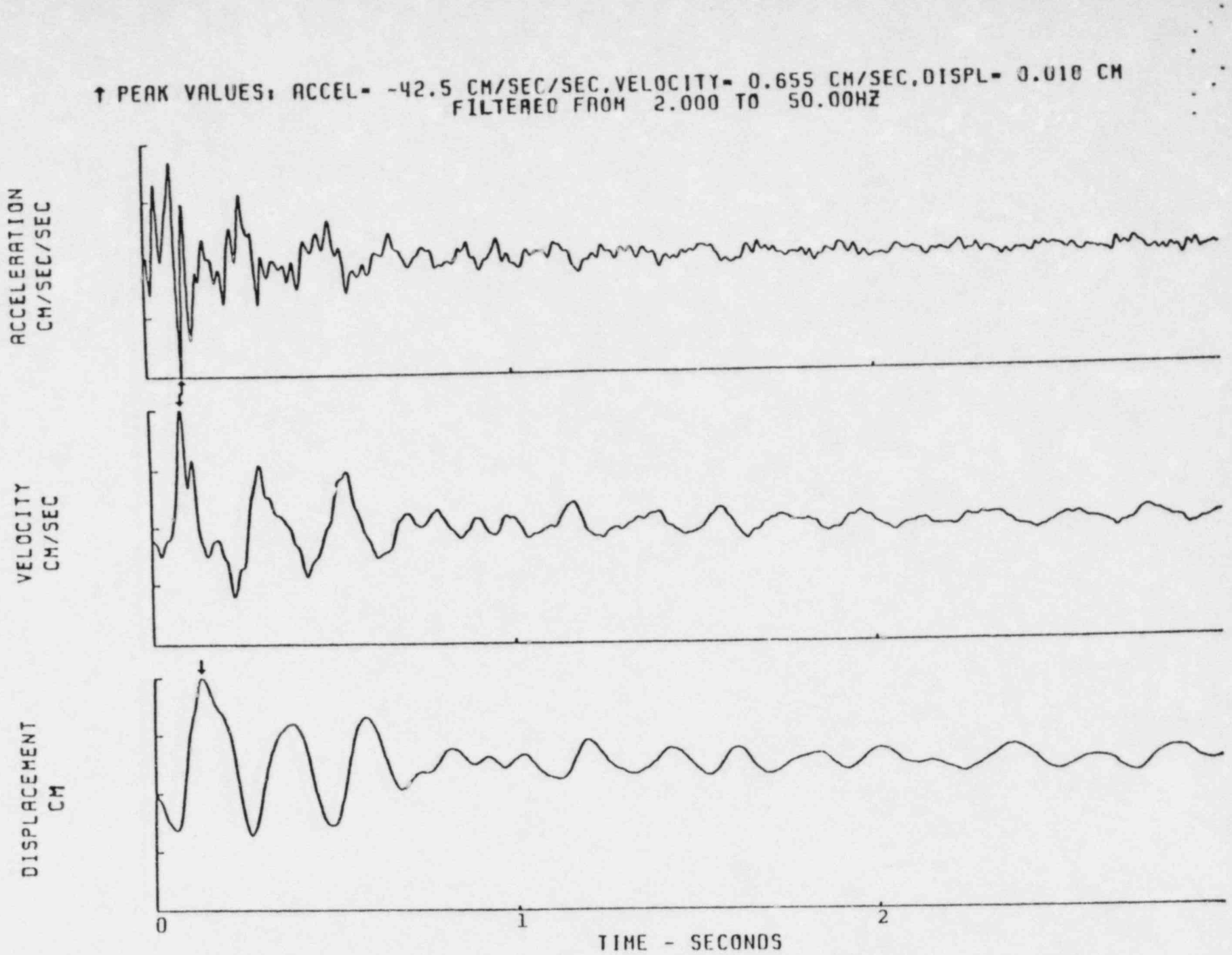

FIGURE 1.24 East component corrected USGS dam abutment record of the M_L 2.6 RIS event of 23:20 UTC, 10/08/79, with hypocentral depth 1.34 km and epicentral distance 1.05 km.

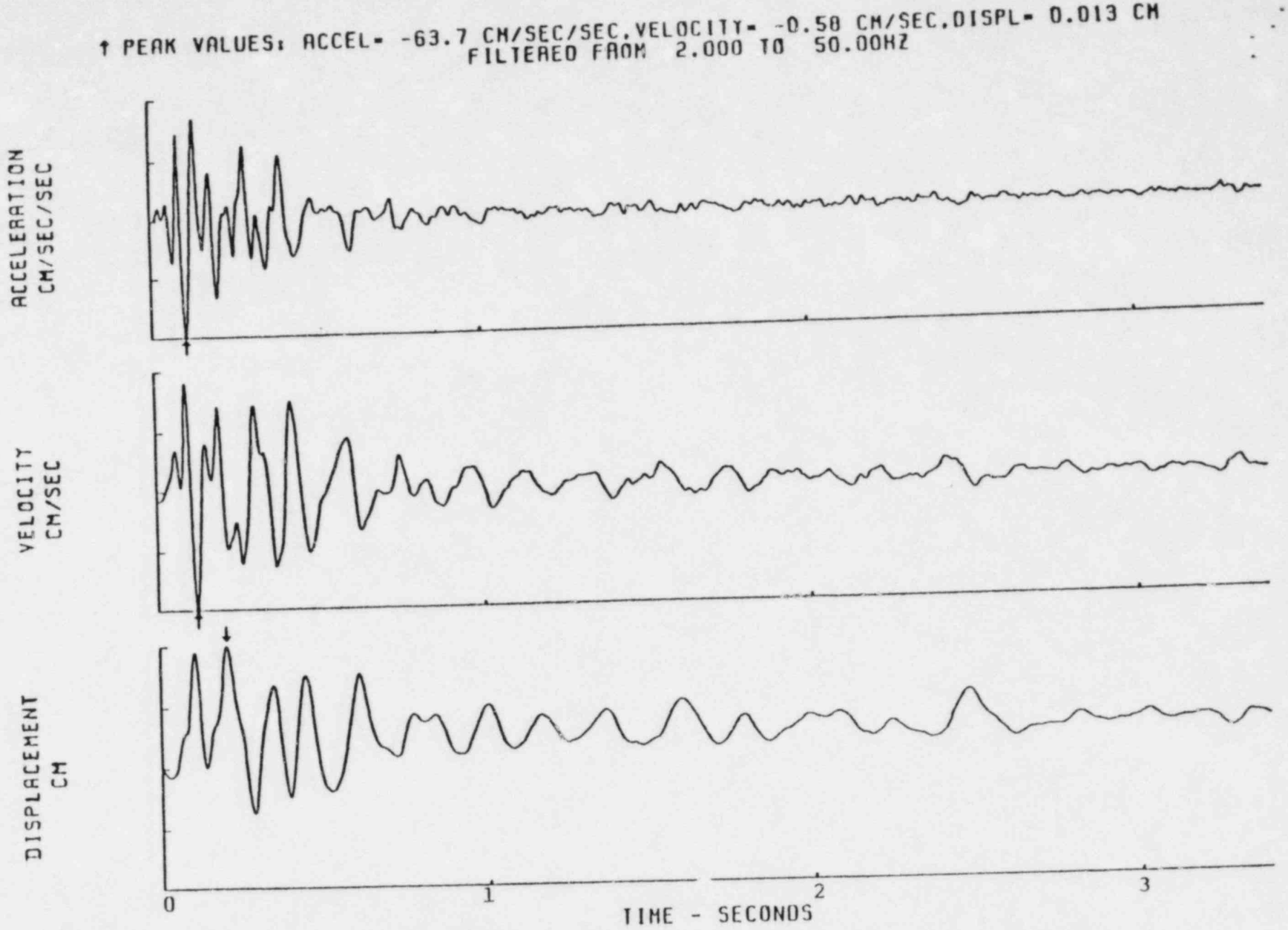

FIGURE 1.25 South component corrected USGS dam abutment record of the M_L 2.8 RIS event of 08:54 UTC, 10/07/79, with hypocentral depth 1.16 km and epicentral distance 1.40 km.

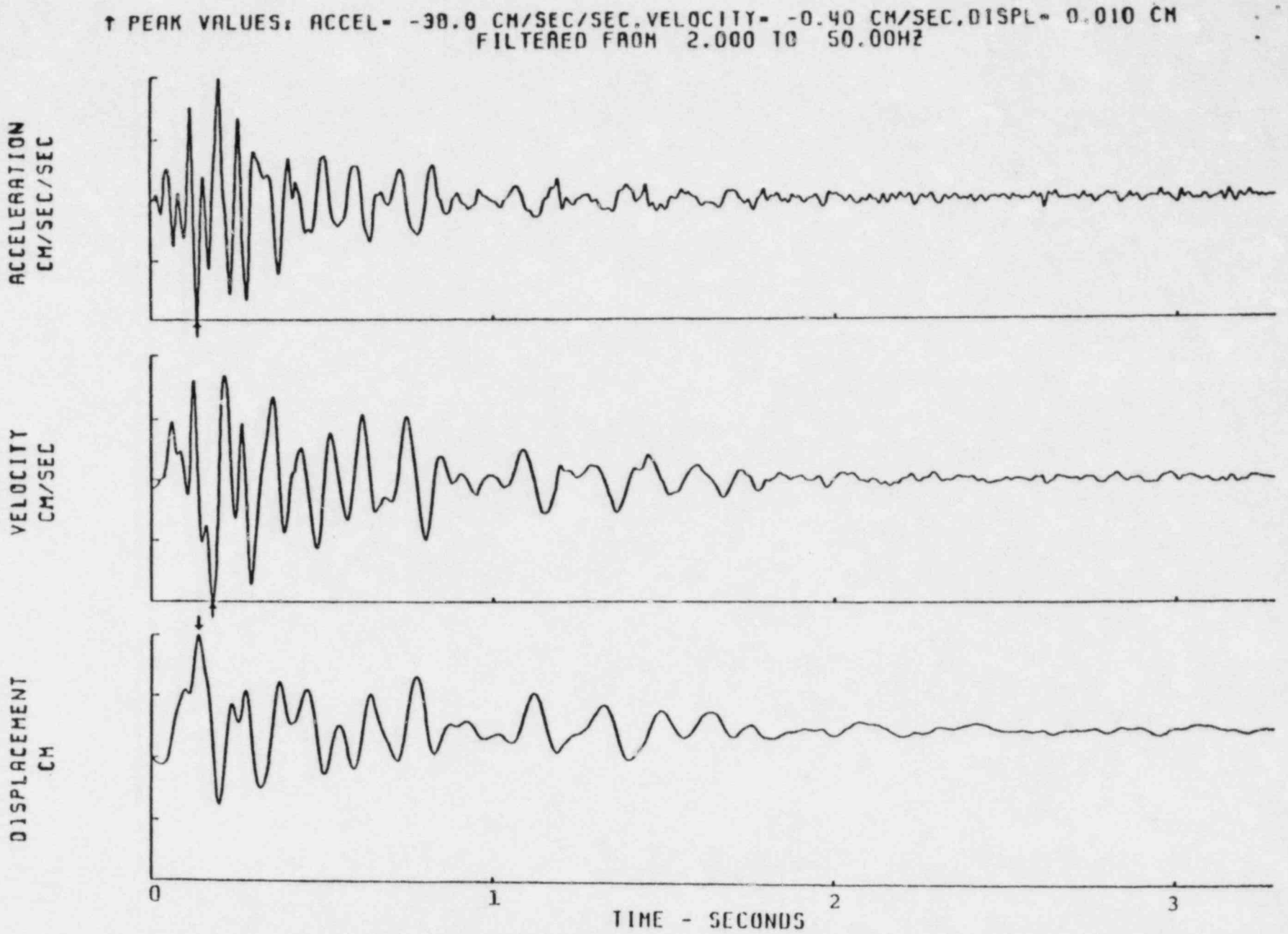

FIGURE 1.26 Vertical component corrected USGS dam abutment record of the M_L 2.8 RIS event of 08:54 UTC, 10/07/79, with hypocentral depth 1.16 km and epicentral distance 1.40 km.

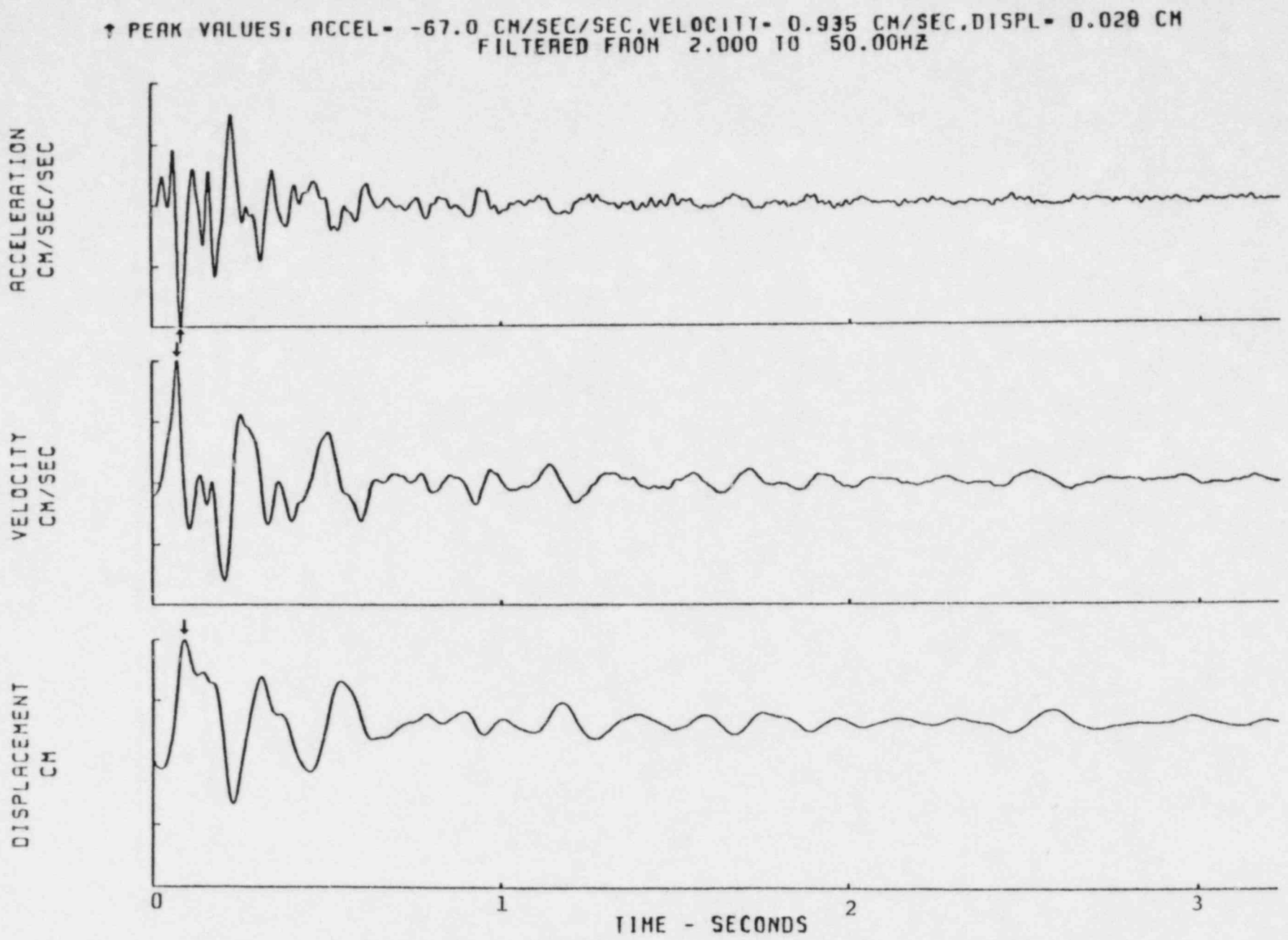

FIGURE 1.27 East component corrected USGS dam abutment record of the M_L 2.8 RIS event of 08:54 UTC, 10/07/79, with hypocentral depth 1.16 km and epicentral distance 1.05 km.

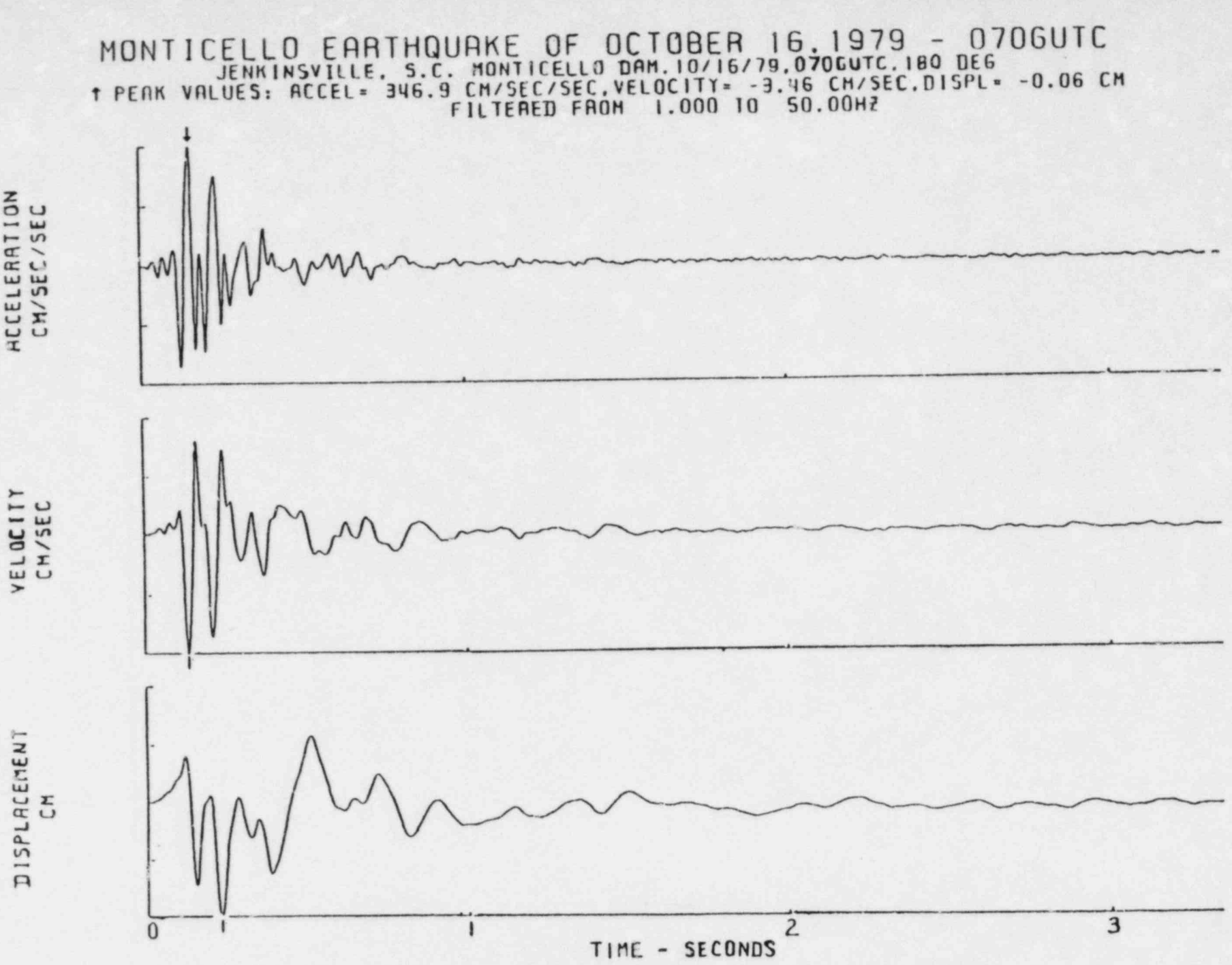

FIGURE 1.28 South component corrected USGS dam abutment record of the M_L 2.8 RIS event of the 07:06 UTC, 10/16/79, with hypocentral depth 0.07 km and epicentral distance 0.78 km.

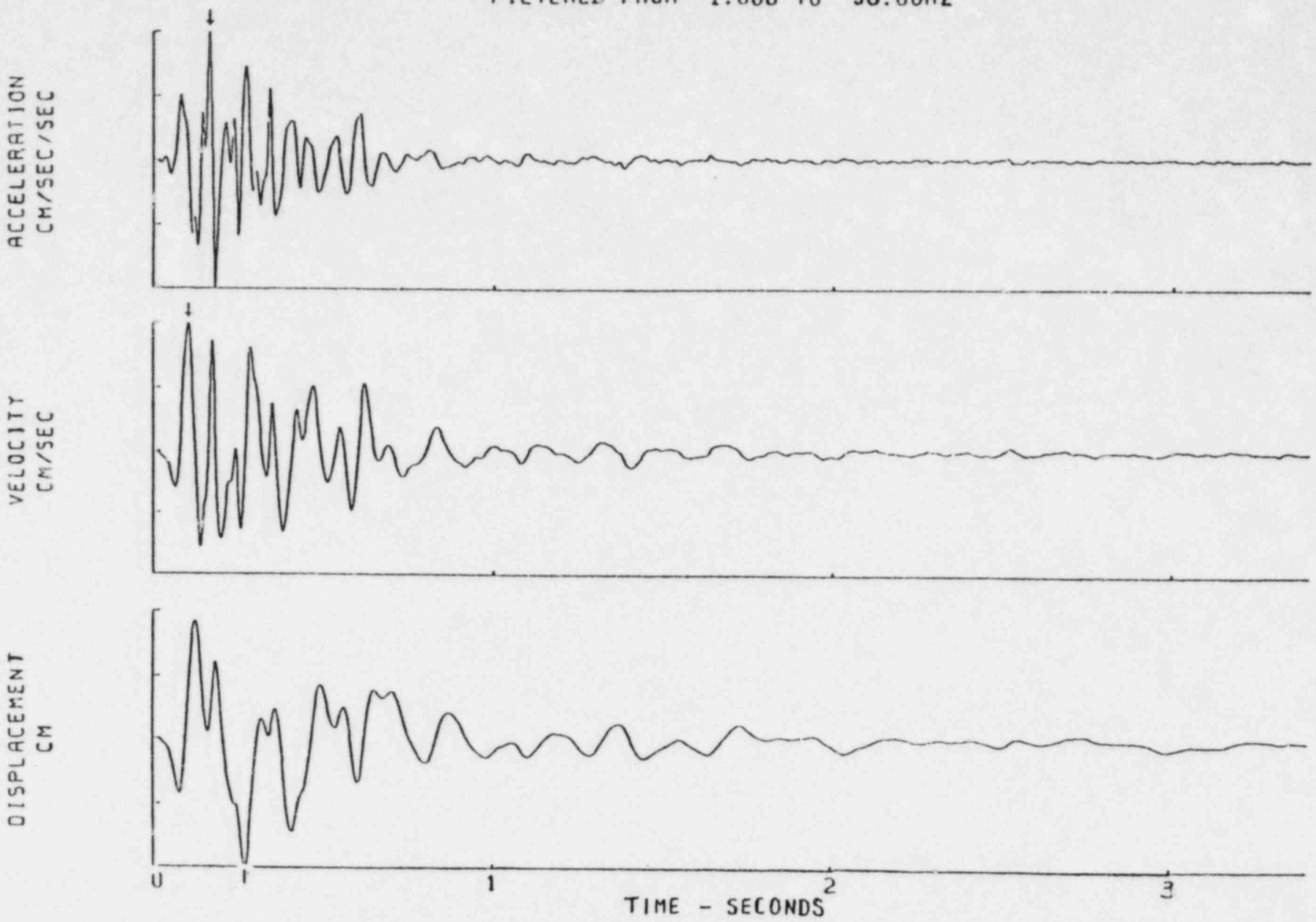

FIGURE 1.29 Vertical component corrected USGS dam abutment record of the M_L 2.8 RIS event of the 07:06 UTC, 10/16/79, with hypocentral depth 0.07 km and epicentral distance 0.78 km.

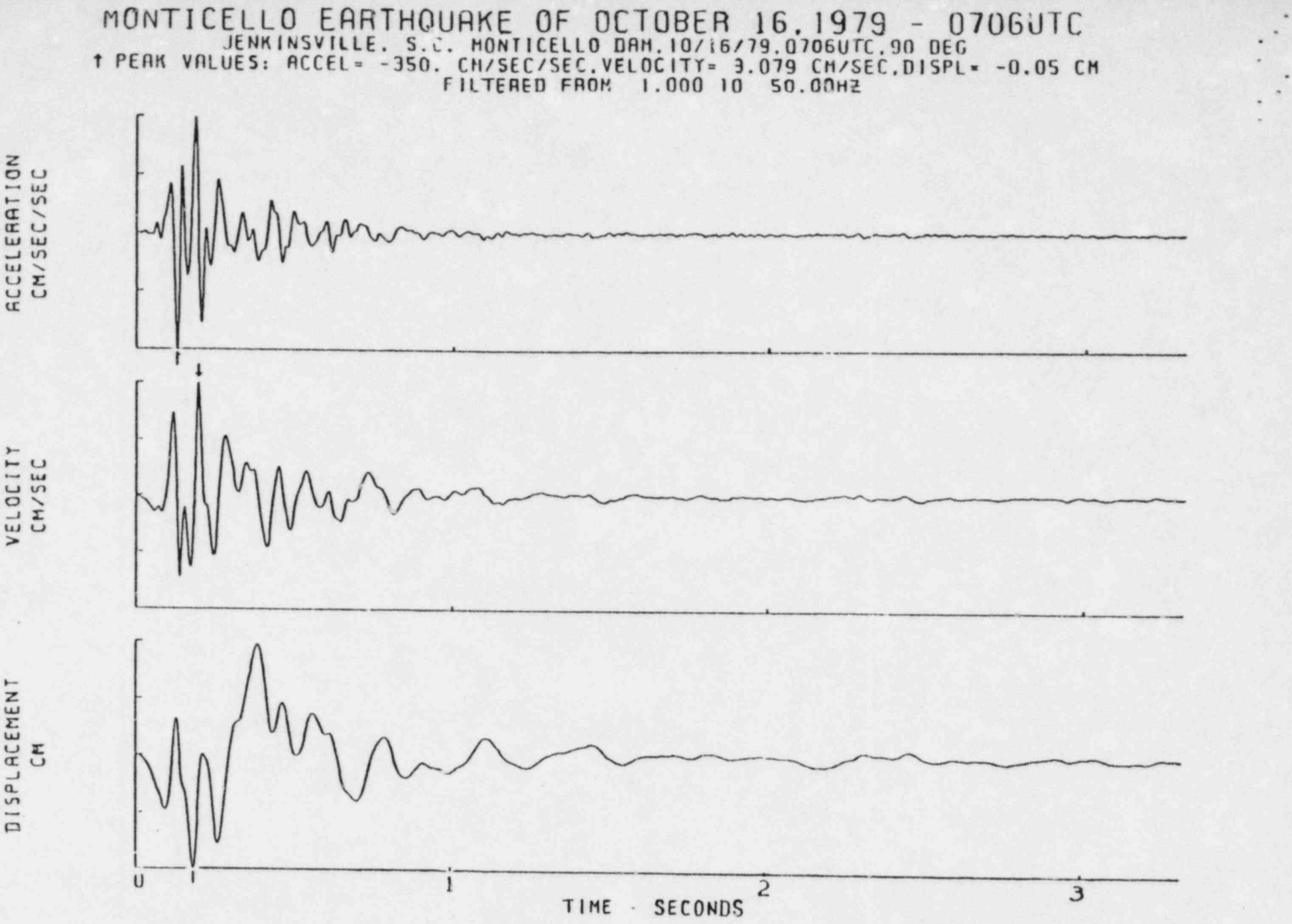

FIGURE 1.30 East component corrected USGS dam abutment record of the M_L 2.8 RIS event of the 07:06 UTC, 10/16/79, with hypocentral depth 0.07 km and epicentral distance 0.78 km.

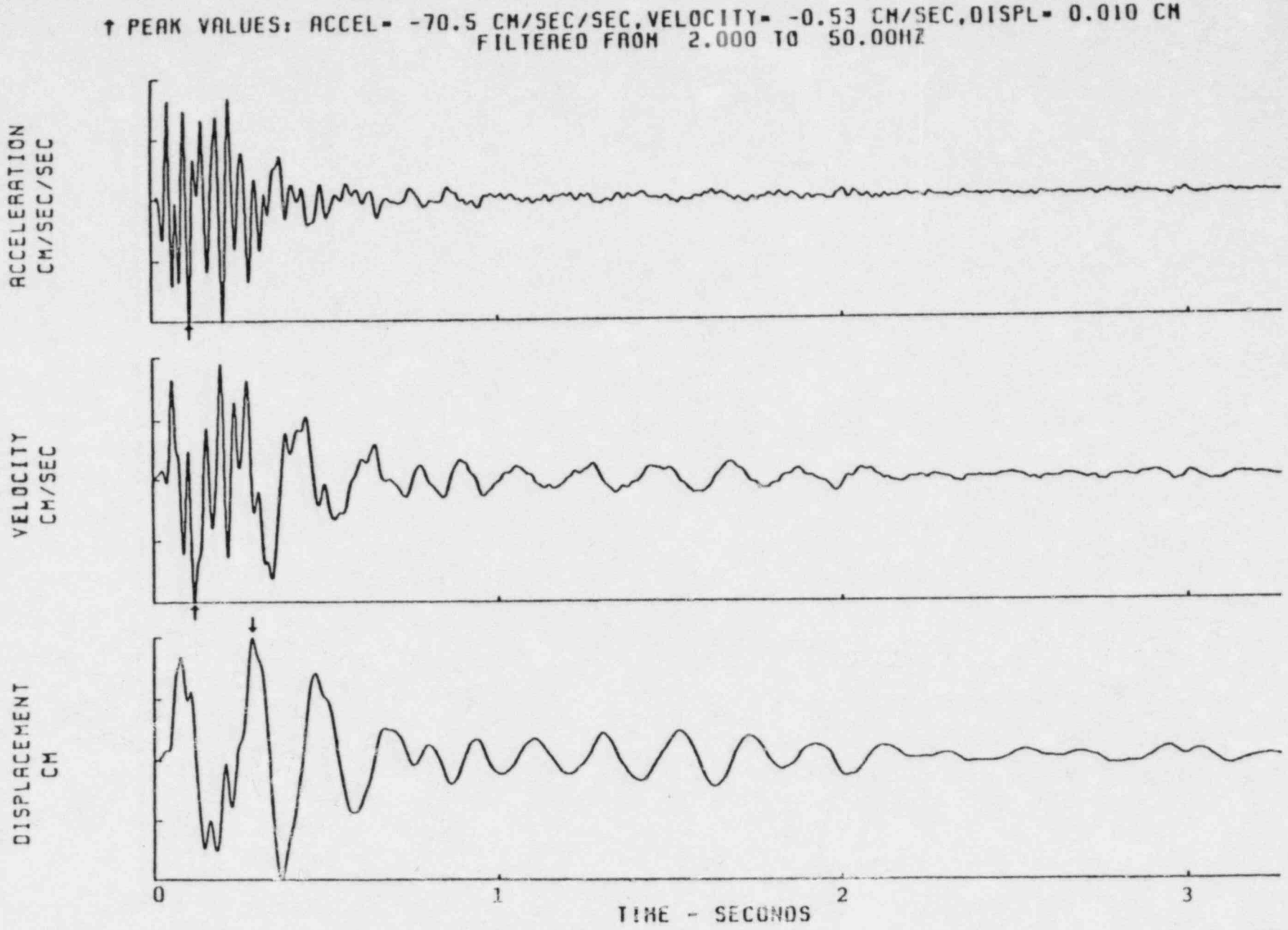

FIGURE 1.31 South component corrected USGS dam abutment record of the M_L 2.2 RIS event of 16:14 UTC, 10/25/78, with hypocentral depth 1.74 km and epicentral distance 0.35 km.

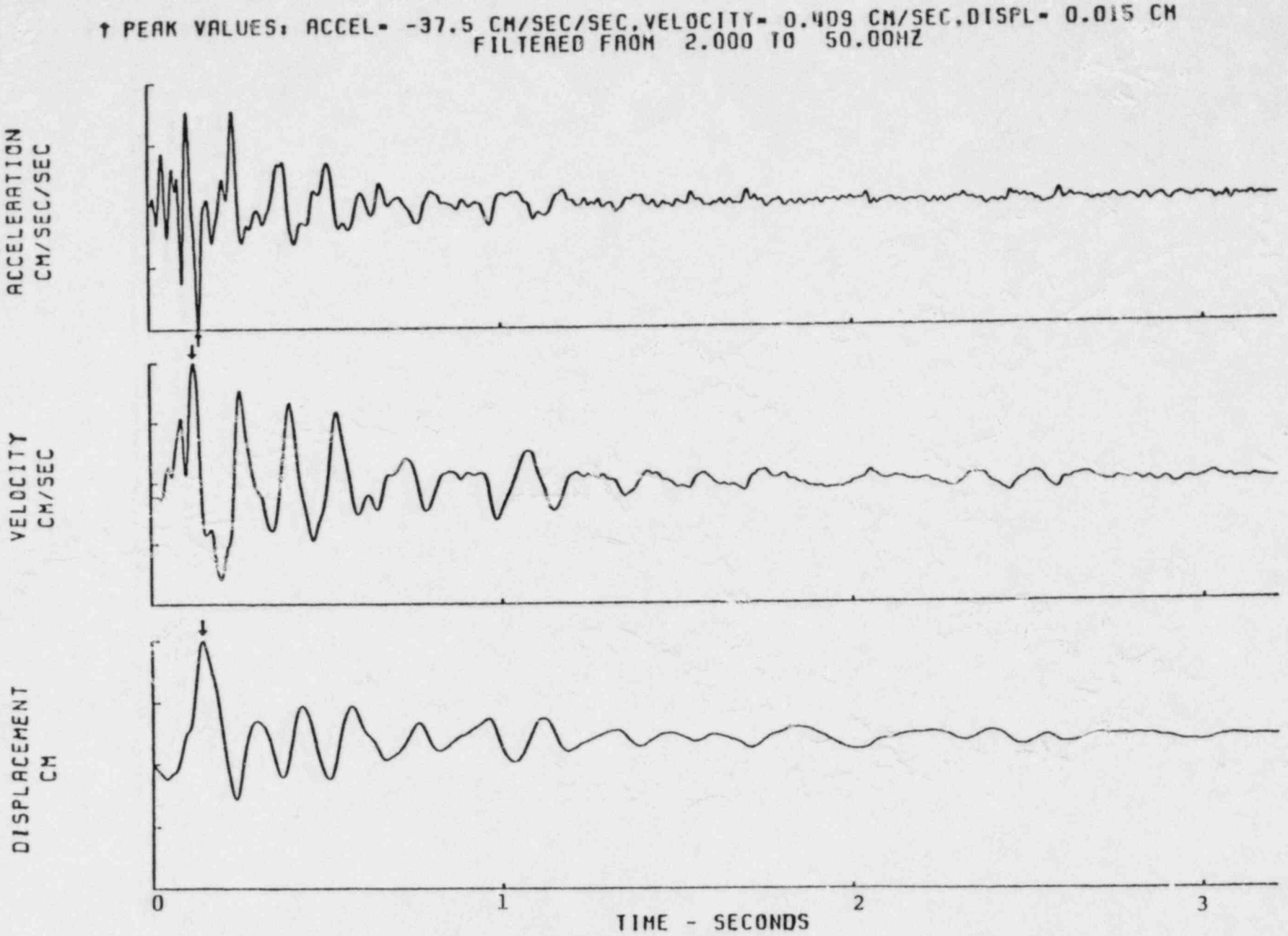

FIGURE 1.32 Vertical component corrected USGS dam abutment record of the M_L 2.2 RIS event of the 16:14 UTC, 10/25/78, with hypocentral depth 1.74 km and epicentral distance 0.35 km.

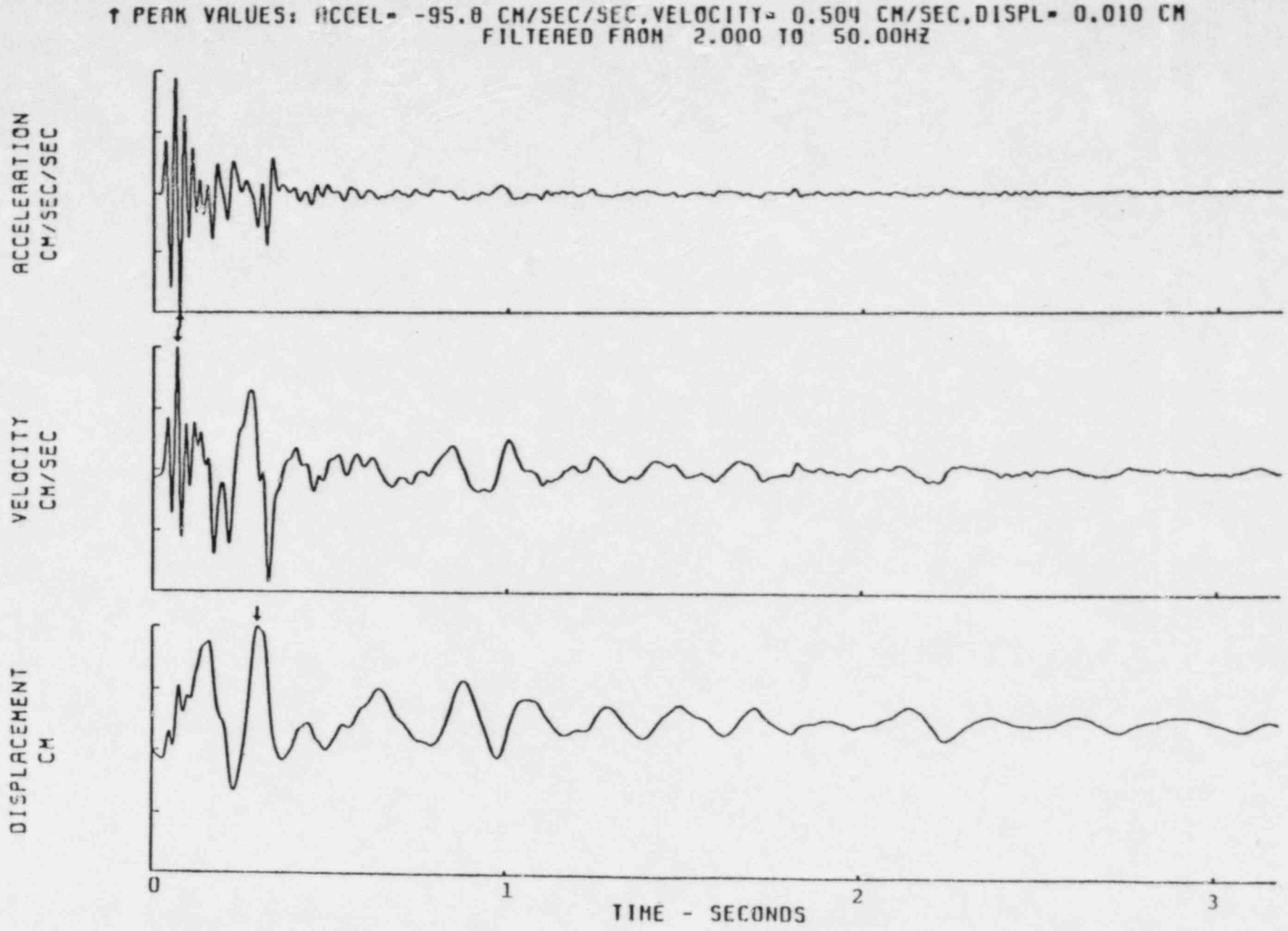

FIGURE 1.33 East component corrected USGS dam abutment record of the M_L 2.2 RIS event of the 16:14 UTC, 10/25/78, with hypocentral depth 1.74 km and epicentral distance 0.35 km.

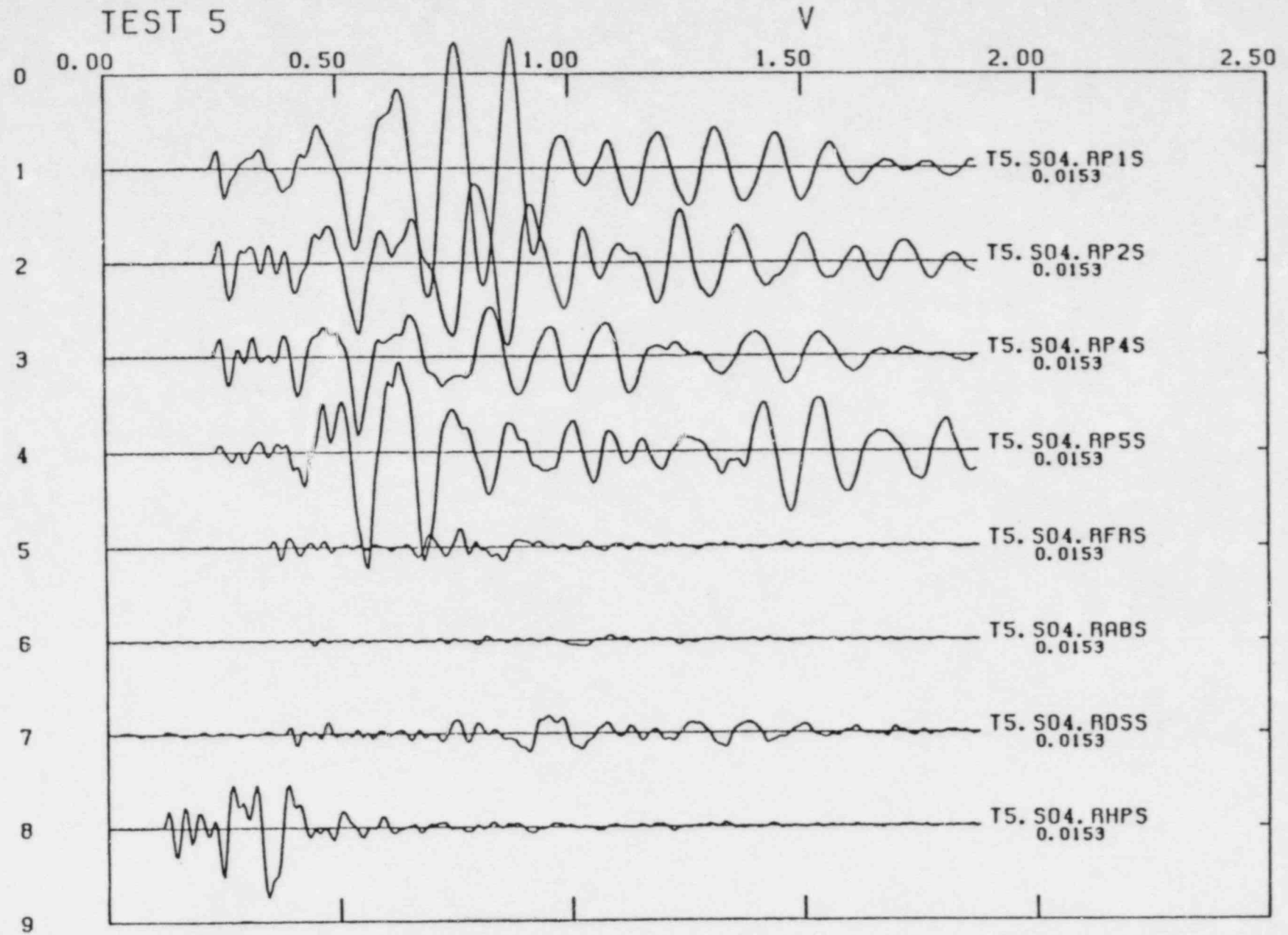

FIGURE 1.34 Vertical component seismograms for Test 5, Shot 4, detonated in rock at a subsurface depth of 116 ft. The accelerograph pad trace (P2) is second from the top. The epicentral distance to the pad is 3100 ft (0.94 km).

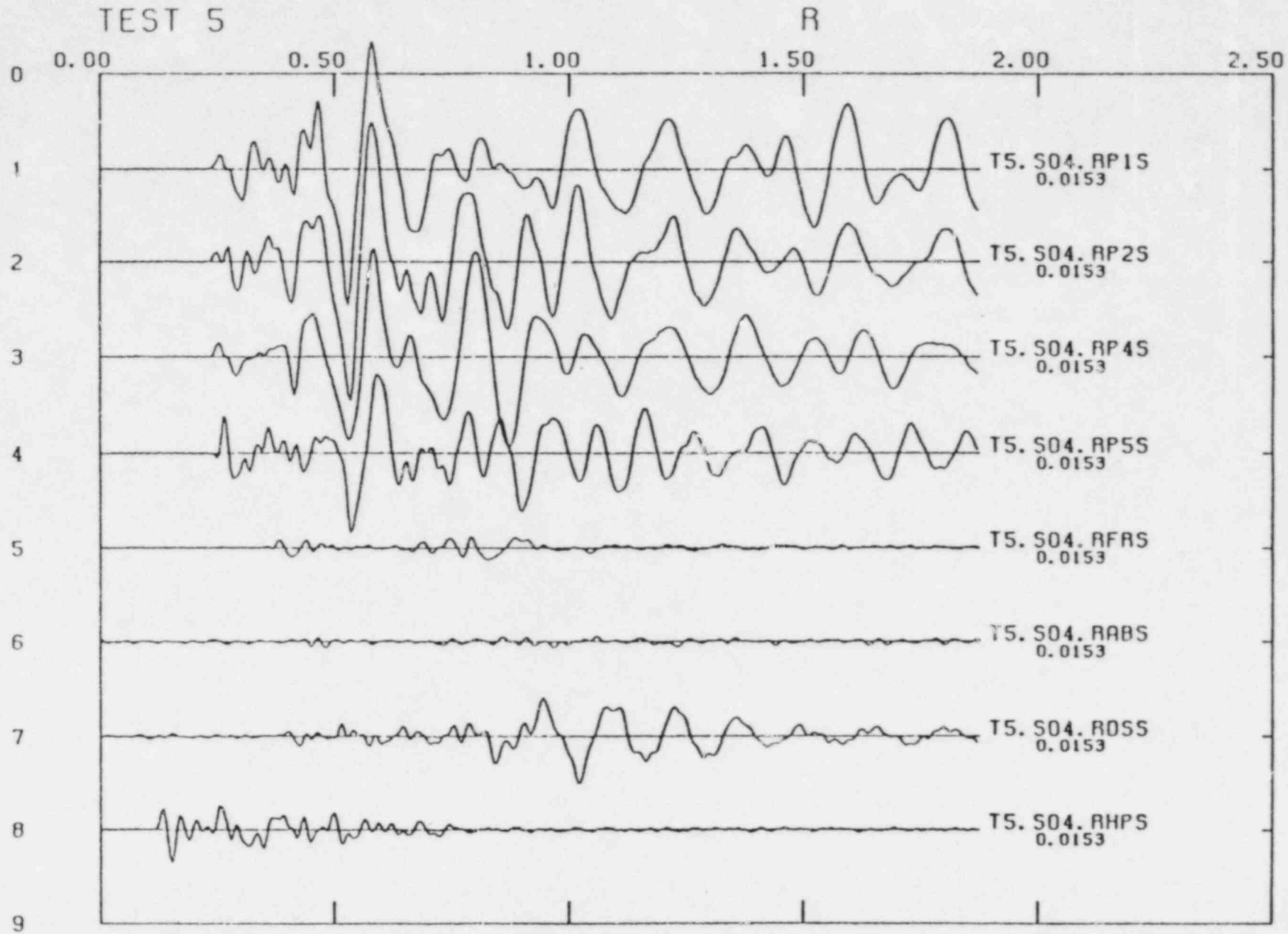

FIGURE 1.35 Radial component seismograms for Test 5, Shot 4, detonated in rock at a subsurface depth of 116 ft. The accelerograph pad trace (P2) is second from the top. The epicentral distance to the pad is 3100 ft (0.94 km).

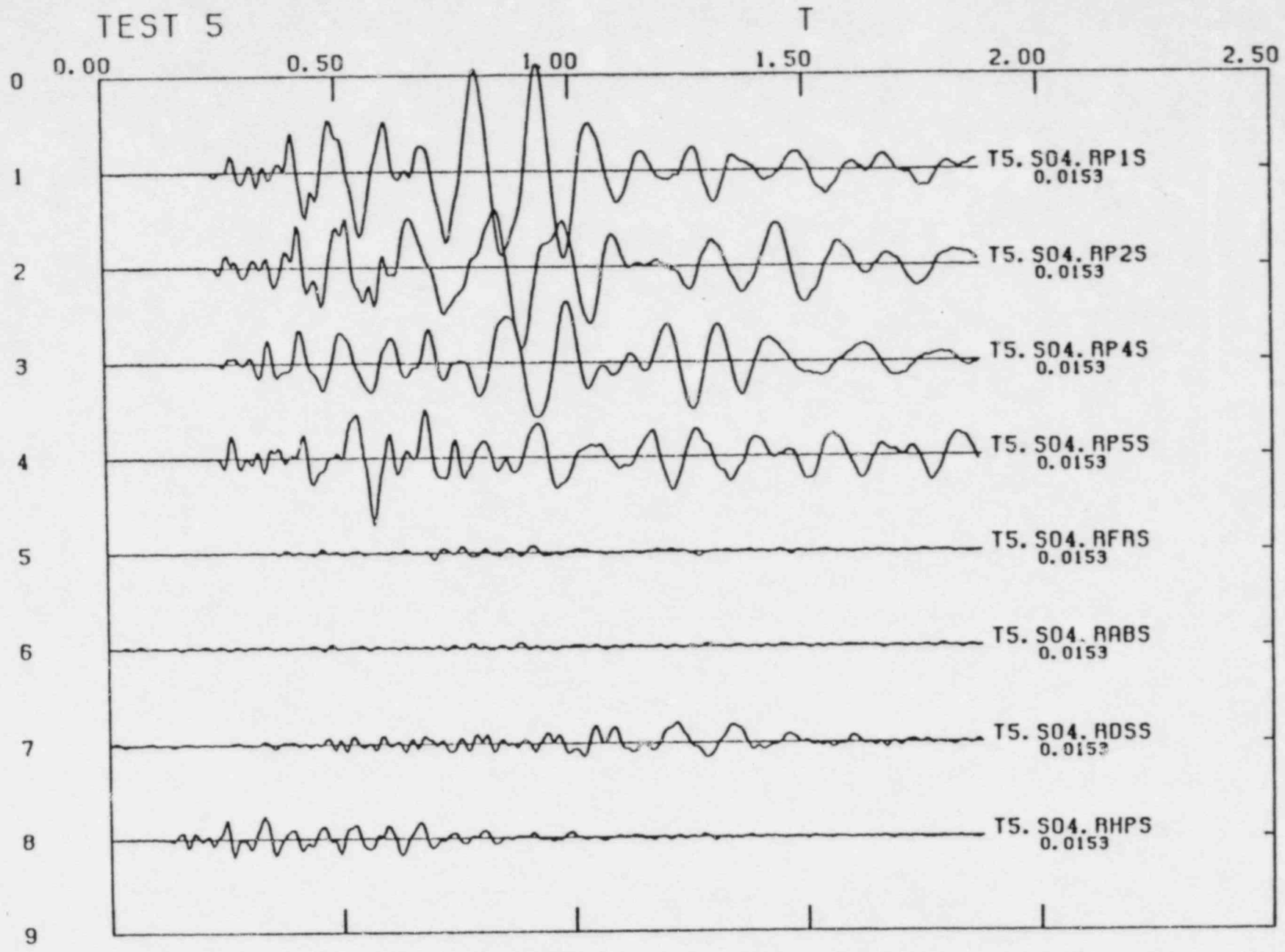

FIGURE 1.36 Transverse component seismograms for Test 5, Shot 4, detonated in rock at a subsurface depth of 116 ft. The accelerograph pad trace (P2) is second from the top. The epicentral distance to the pad is 3100 ft (0.94 km).

Question 2. How sensitive are the final response-spectra reduction factors to the assumption of zero-phase shift for the foundation-to-free-field transfer functions? Justify or modify the estimated reduction factors in light of your answer.

The sensitivity of the foundation response spectra to the assumption of zero-phase shift for the transfer functions is evaluated below by comparing results for three different cases: zero phase, random phase, and the observed phase for the explosion data. The zero-phase and random-phase filters cause minimum and maximum dispersion respectively. Response spectra of foundation accelerograms obtained from transfer functions with the observed phase are bounded by the zero-phase and random-phase cases.

Given below is a description of the procedure by which the 1979 accelerograms are filtered to simulate motion that would have been recorded at foundation recording sites. The construction of such a filter from the smoothed spectral modulus ratios necessitates an assumption about the phase angle as a function of frequency. Of these three possible models, it will be shown that the assumption of zero phase gives a conservative estimate in the sense that the filtered output amplitude tends to have the highest peak value when zero phase is used. In general, response spectra obtained for the zero-phase shift assumption envelope those obtained by other assumptions about the phase. In particular, the zero-phase response spectra always lie above the random-phase response spectra.

Figures 2.1 - 4 illustrate how the filtering process is performed. Figure 2.1 is the input ground acceleration (90 degree component) as recorded at the dam abutment during the October 16, 1979 earthquake (maximum acceleration as shown in the plot is about 330 gals). In Figure 2.2 is plotted the smoothed spectral modulus ratio between the transverse component of ground motion as recorded during Test 4, Shot 4 at the Auxiliary Building and the USGS accelerograph pad. In this case, transverse is in the same direction (E-W) as the earthquake motion input. Because of poor signal-to-noise ratio beyond 50 Hz, the value of the transfer function is set to unity between 50 Hz and the Nyquist frequency so that the spectral amplitudes of the input seismogram will

be passed with no amplitude distortion in that band. The aim is to construct from this amplitude function a time-domain filter with which one can simulate the ground motions as recorded inside the Auxiliary Building during the 1979 earthquake. To do this, the phase information is necessary. The assumption used in Appendix B was that this filter has zero phase response (the straight line shown at 1.5 in Figure 2.2). Inverting this filter to the time domain results in the impulse response given in Figure 2.3. Note that in this plot the onset time of the impulse response has been displaced from the left-hand abscissa for clarity of presentation. The entire response appears to consist of a single spike of amplitude 420 units; however, this is purely an artifact of the zero-phase assumption, and results only in the unaltered transfer of energy (amplitude or phase) between input and filtered seismograms beyond 50 Hz. The information of true interest is the far smaller oscillatory motion shown in Figure 2.3. When the input (Figure 2.1) is convolved with the impulse response (Figure 2.3), the result is the "filtered seismogram" shown in Figure 2.4. Note that the peak amplitude has been reduced from about 330 to 95 gals, which is a reduction factor about equal to the average spectral modulus height in Figure 2.2 between 0 and 50 Hz.

Results for random phase are shown in Figures 2.5 and 2.6. Figure 2.5 shows the filter impulse response which results from using exactly the same spectral modulus as given in Figure 2.2, but now the phase has been taken to be a random number between -pi and pi. Figure 2.5 shows that the character of the filter has changed to random oscillations over the whole record. The effect on the resulting filtered seismogram is pronounced. (Compare Figure 2.6 with the zero-phase result in Figure 2.4.) Note that now the peak amplitude on the filtered seismogram is only about 35 gals.

To investigate further the effect of phase on the simulated seismograms produced, transfer functions using the observed phase are shown in Figures 2.7 and 2.8. Figure 2.7 gives the impulse response from a filter which has the same amplitude characteristics as those of Figures 2.3 and 2.5, but now the phase is selected as follows. At the time the spectral modulus ratios are constructed, a complex transfer function is also computed (in this case

between the pad and the Auxiliary Building). This transfer function has associated with it a phase angle. The impulse response of this filter is given in Figure 2.7. The resulting seismogram, given in Figure 2.8, is seen to have a peak amplitude intermediate between the zero- and random-phase cases (compare Figure 2.8 with Figures 2.4 and 2.6). Figures 2.10 - 2.15 give the filtered seismograms which result when the 180-degree component of the 1979 accelerogram (Figure 2.9) is filtered by a spectral modulus ratio from the radial component as recorded at the Auxiliary Building and the pad. Figures 2.10 - 2.15 compare with Figures 2.3 - 2.8 for the 90-degree component.

In summary, filtered seismograms, each constructed using the same input data and transfer functions which share identical spectral amplitudes, have the highest amplitudes when the filter employed has zero phase.

Figures 2.16 and 2.17 show the result of passing the filtered 90° and 180° component seismograms through a response spectrum algorithm (5 percent damping). The dashed trace gives the response spectrum of the input seismogram. The heavy solid traces show the result produced by the zero-phase filtered seismograms. The other two traces give the results for the observed and random phase seismograms. The zero-phase spectrum almost completely envelopes the other two. In each case the zero-phase spectrum is highest and the random-phase spectrum is lowest. These figures depict the sensitivity of computed response spectra to the phase shift assumption.

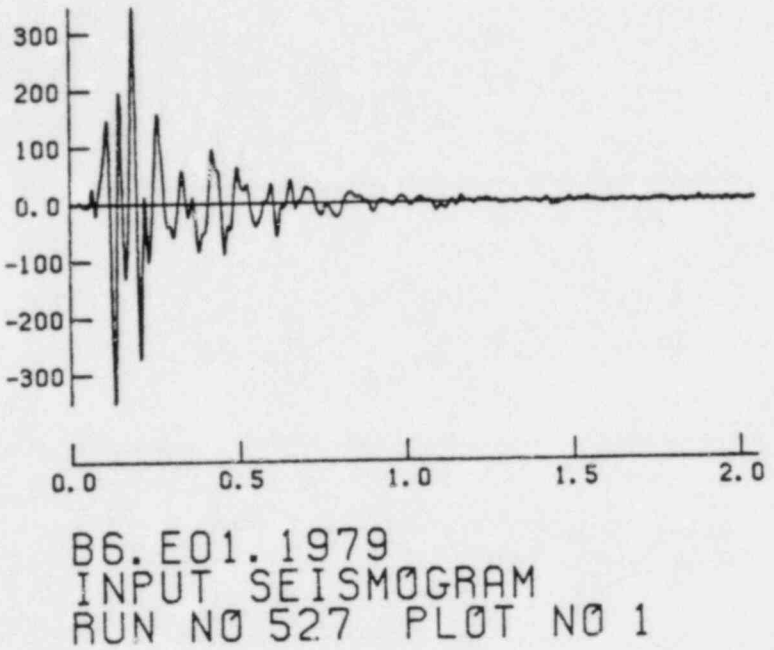

Figure 2.1 90-degree component of the October 16, 1979 earthquake recorded on the USGS accelerograph pad on the dam abutment.

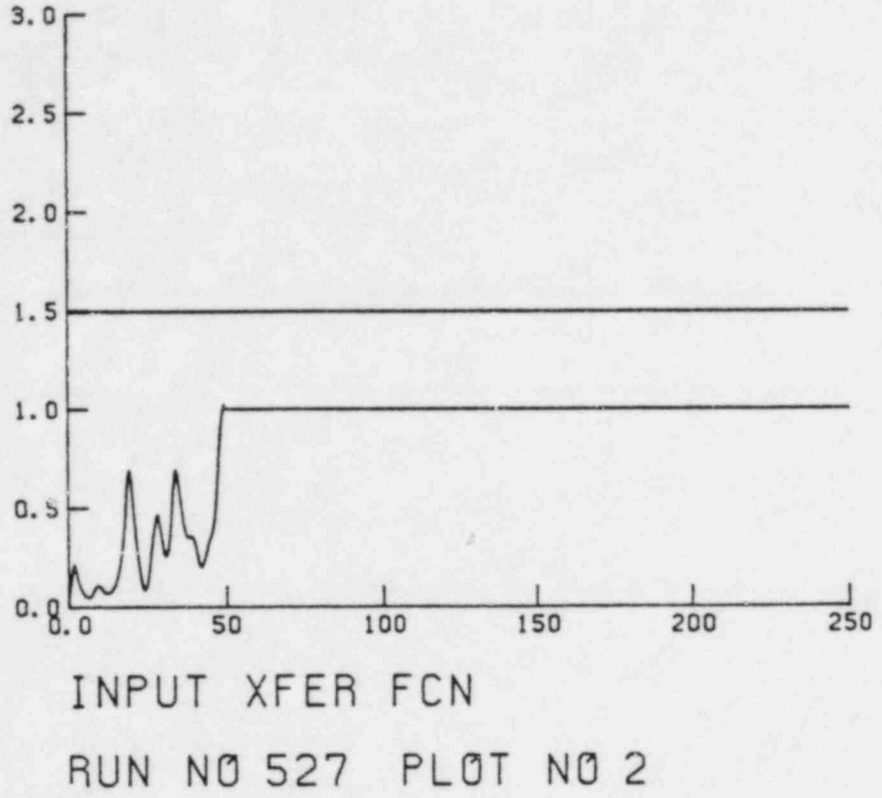

Figure 2.2 Zero phase transfer function, Auxiliary Building foundation/accelerograph pad, transverse component, Test 4, shot 4. Zero phase is plotted as the line at a value of 1.5, while the other line is the modulus of the transfer function in units given along the ordinate scale. Abscissa scale is in Hz.

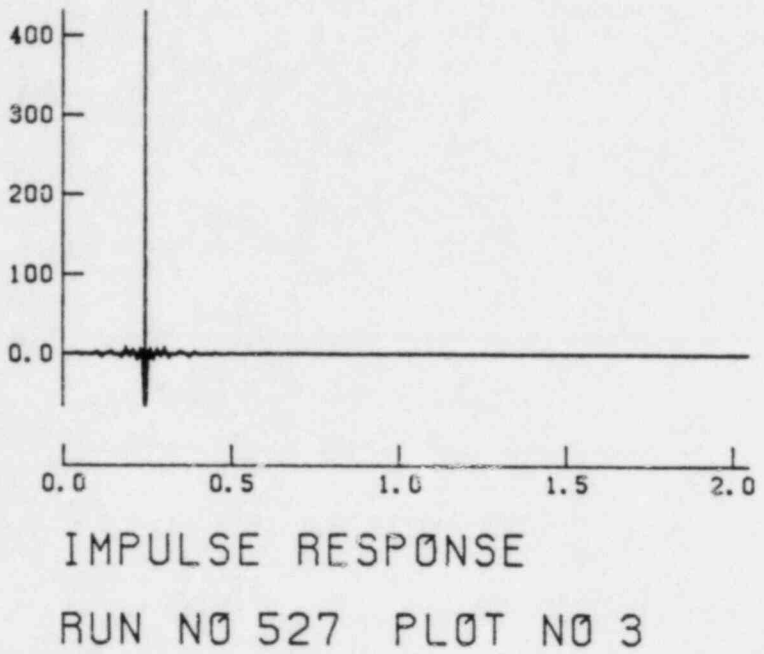

Figure 2.3 Impulse response of the zero-phase transfer function shown in Figure 2.2 (Auxiliary Building/pad, transverse component, Test 4, Shot 4). Abscissa scale is in seconds.

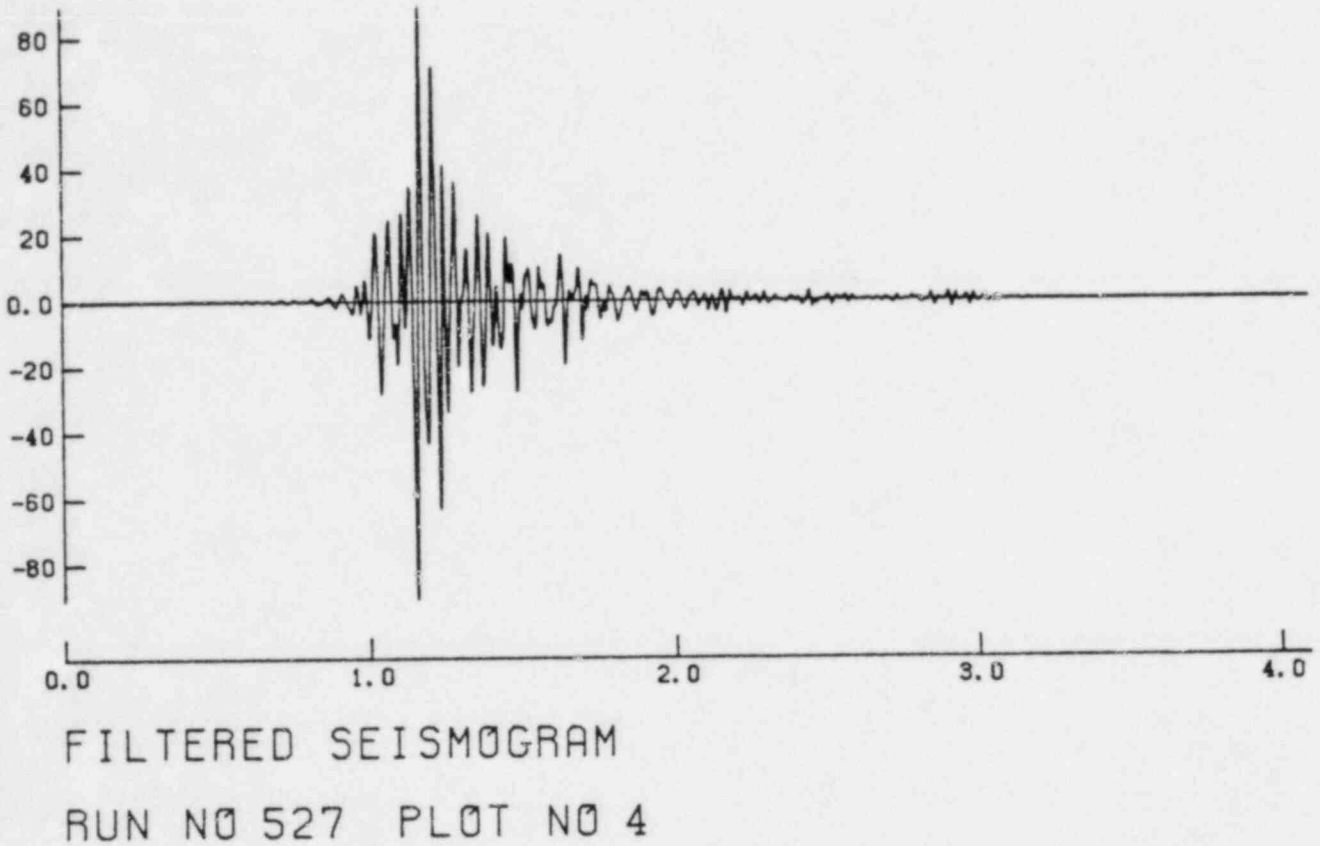

Figure 2.4 Auxiliary Building foundation accelerogram obtained by filtering the 90-degree component of the 1979 accelerogram using the zero-phase transfer function shown in Figure 2.2. Abscissa scale is in seconds.

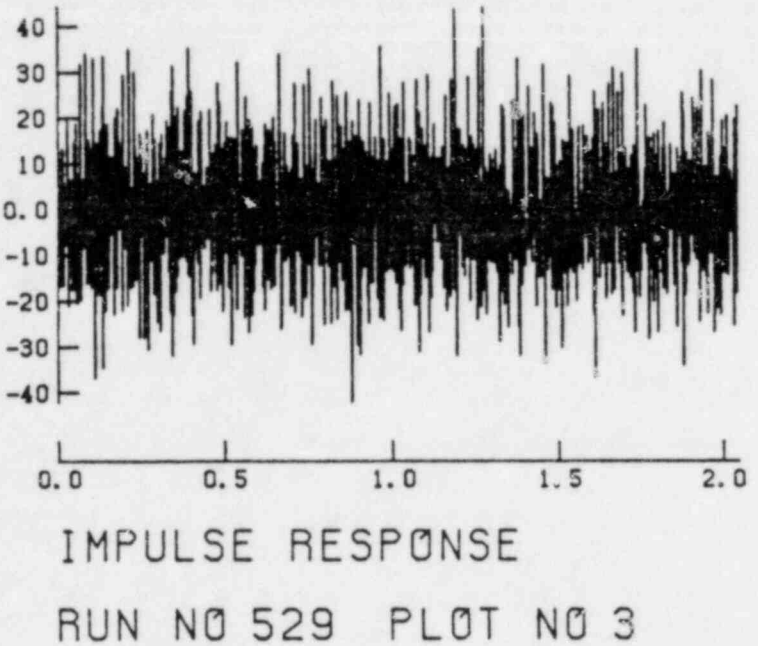

Figure 2.5 Impulse response of a random-phase transfer function with the same spectral modulus as in Figure 2.2. Abscissa scale is in seconds.

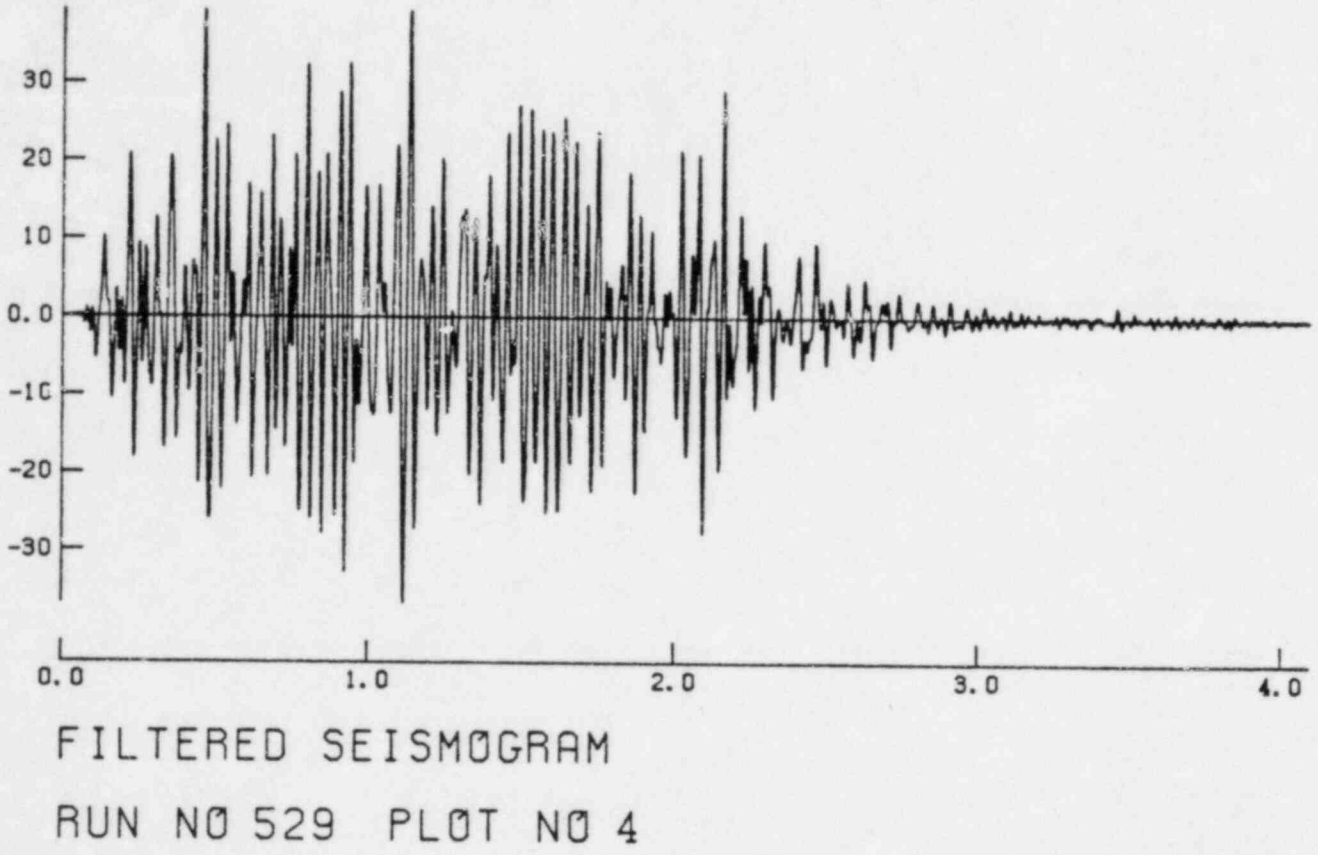

Figure 2.6 Auxiliary Building foundation accelerogram obtained by filtering the 90-degree component of the 1979 accelerogram with the random-phase transfer function whose impulse response is shown in Figure 2.5. Abscissa scale is in seconds.

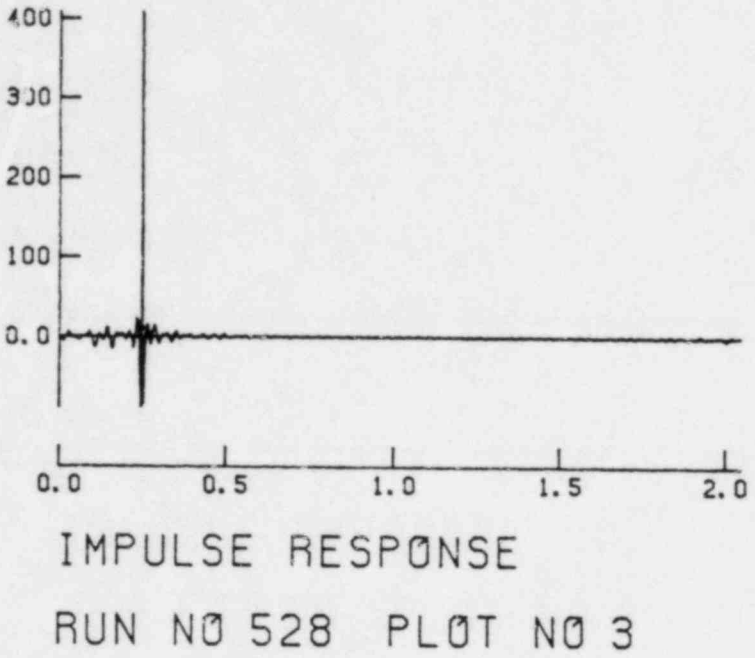

Figure 2.7 Impulse response of the observed-phase transfer function, Auxiliary Building foundation/pad, transverse component, Test 4, shot 4. Abscissa scale is in seconds.

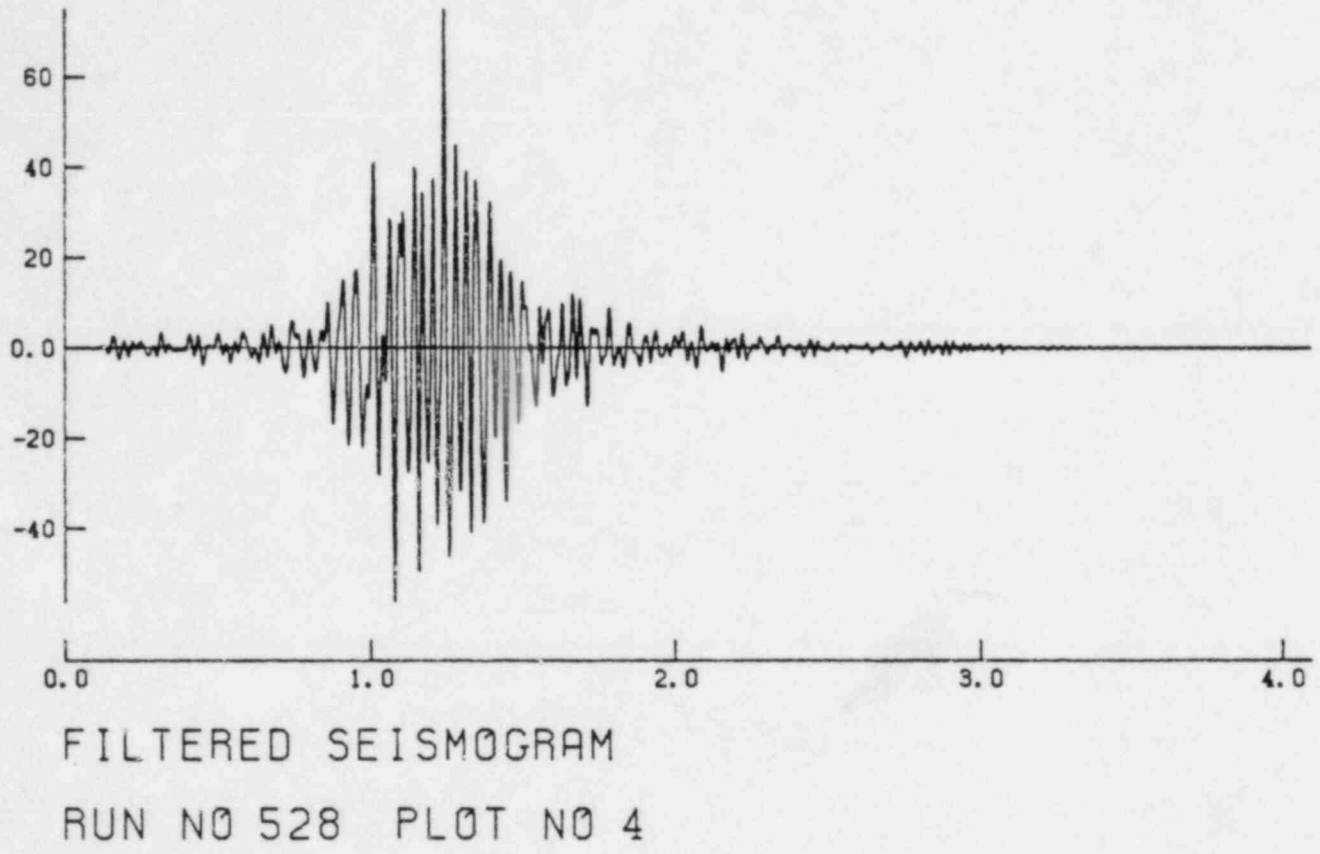

Figure 2.8 Auxiliary Building foundation accelerogram obtained by filtering the 90-degree component of the 1979 accelerogram with the observed phase transfer function whose impulse response is shown in Figure 2.7. Abscissa scale is in seconds.

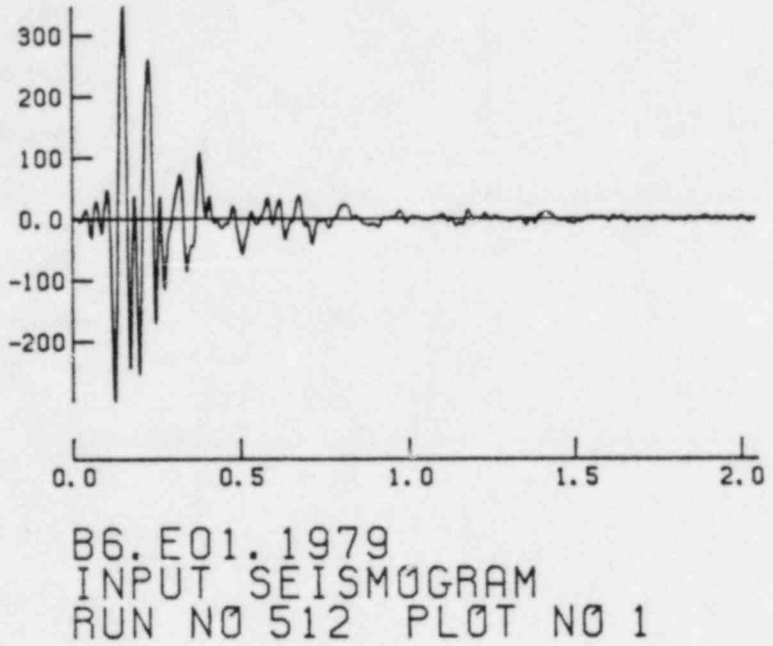

Figure 2.9 180-degree component of the October 16, 1979 earthquake recorded on the USGS accelerograph pad on the dam abutment.

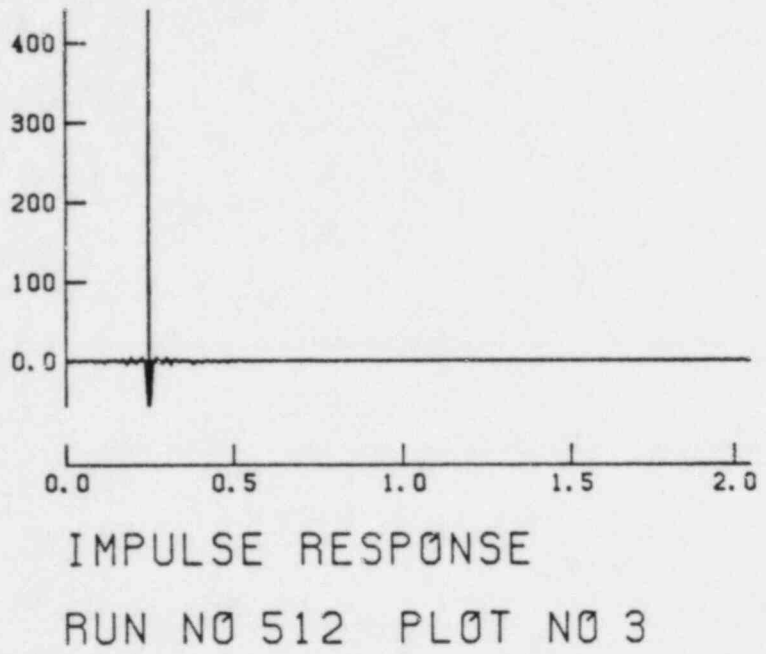

Figure 2.10 Impulse response of the zero-phase transfer function Auxiliary Building foundation/pad, radial component, Test 4, shot 4. Abscissa scale is in seconds.

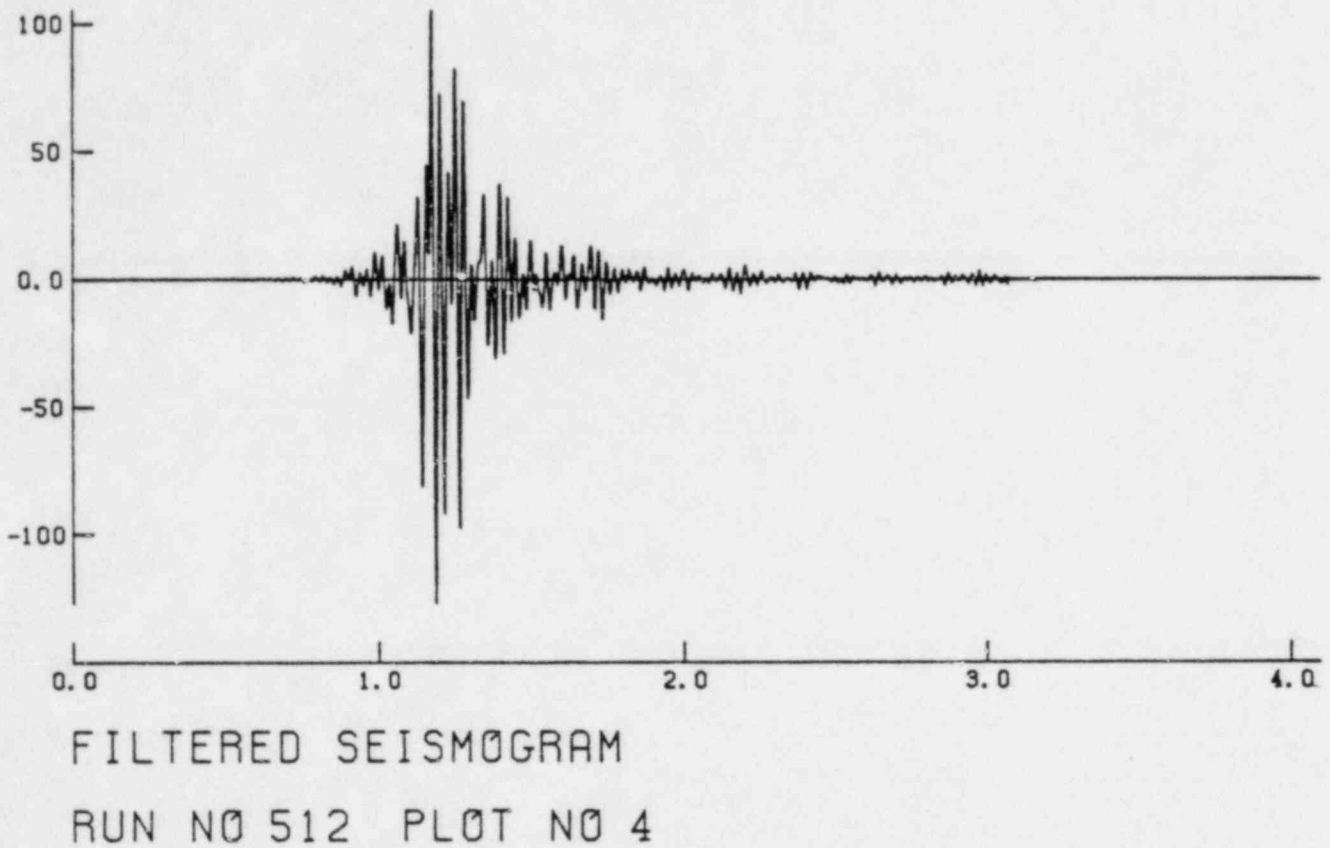

Figure 2.11 Auxiliary Building foundation accelerogram obtained by filtering the 180-degree component of the 1979 accelerogram with the zero-phase transfer function whose impulse response is shown in Figure 2.10. Abscissa scale is in seconds.

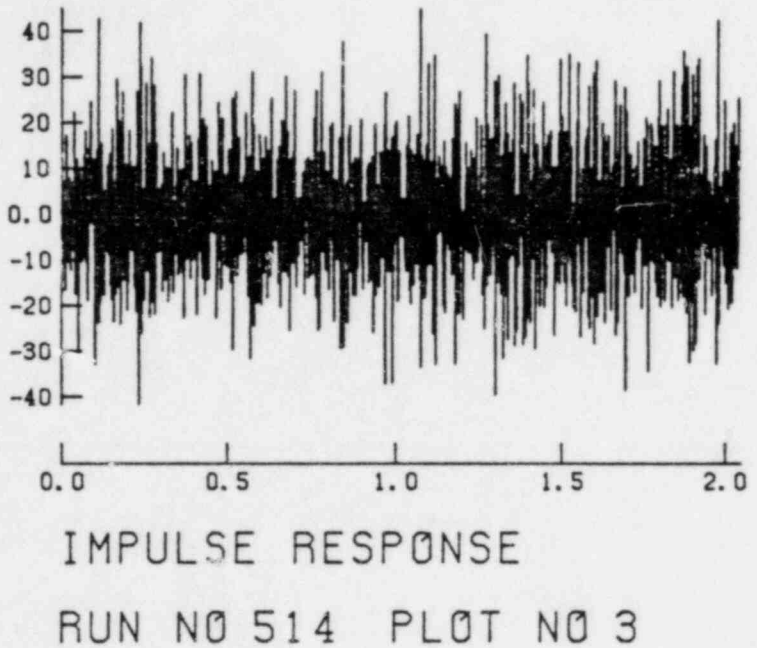

Figure 2.12 Impulse response of a random-phase phase transfer function, Auxiliary Building foundation/pad, radial component, Test 4, shot 4. Abscissa scale is in seconds.

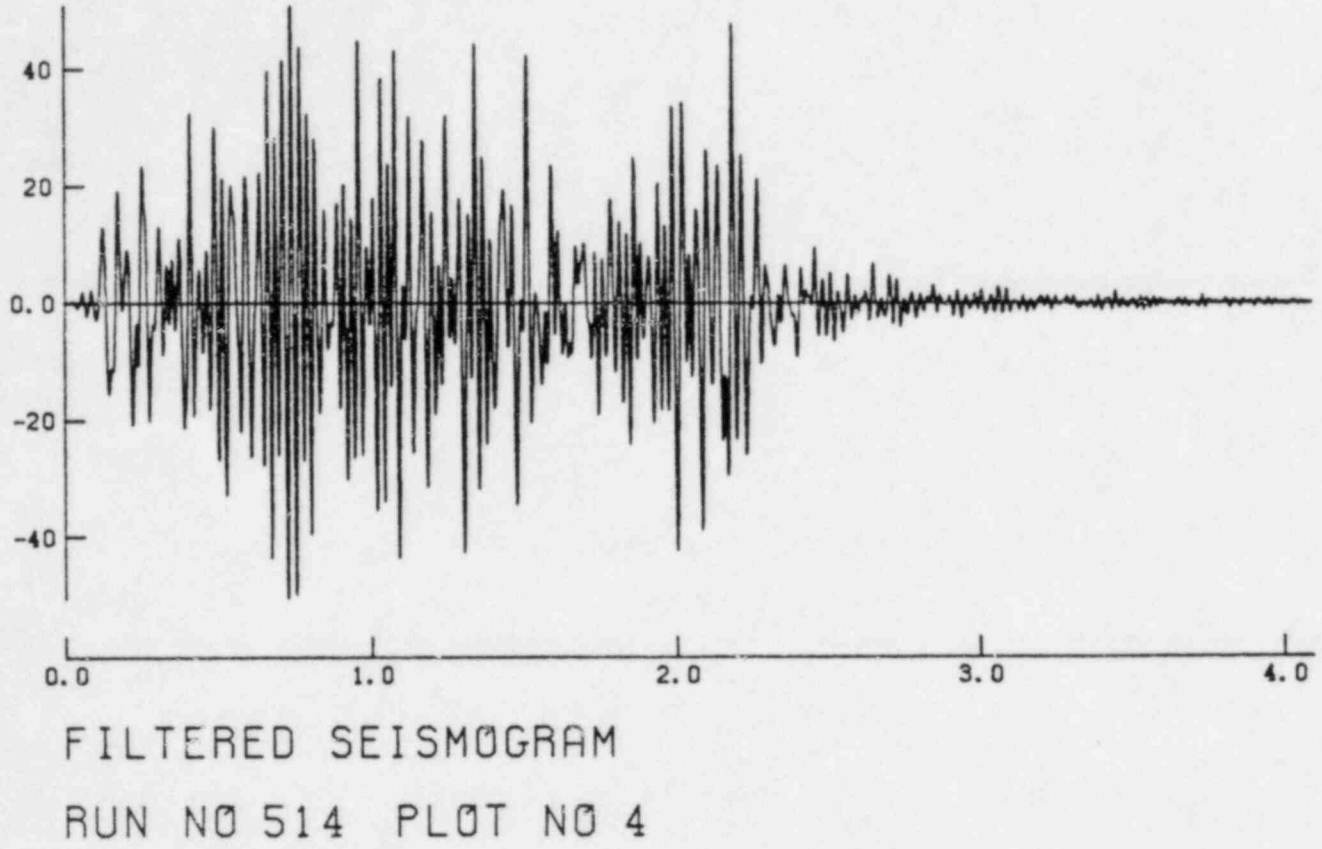

Figure 2.13 Auxiliary Building foundation accelerogram obtained by filtering the 180-degree component of the 1979 accelerogram with the random-phase transfer function whose impulse response is shown in Figure 2.12. Abscissa scale is in seconds.

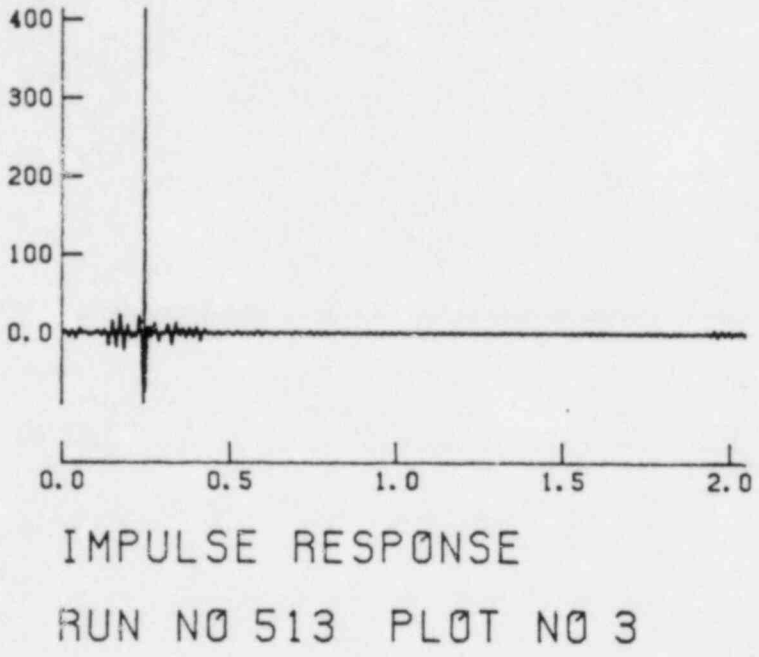

Figure 2.14 Impulse response of the observed-phase transfer function, Auxiliary Building foundation/pad, radial component, Test 4, shot 4. Abscissa scale is in seconds.

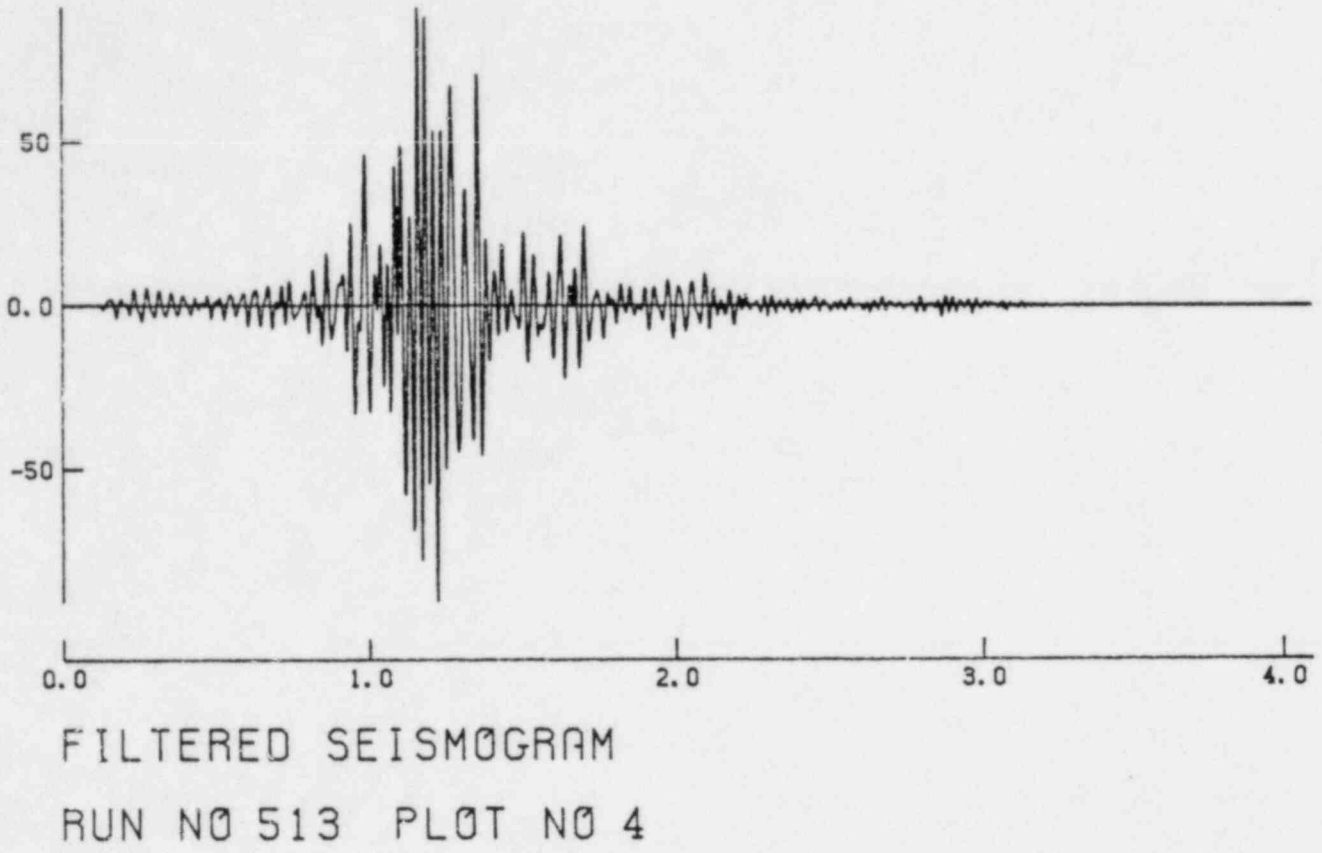

Figure 2.15 Auxiliary Building foundation accelerogram obtained by filtering the 180-degree component of the 1979 accelerogram with the observed-phase transfer function whose impulse response is shown in Figure 2.14. Abscissa scale is in seconds.

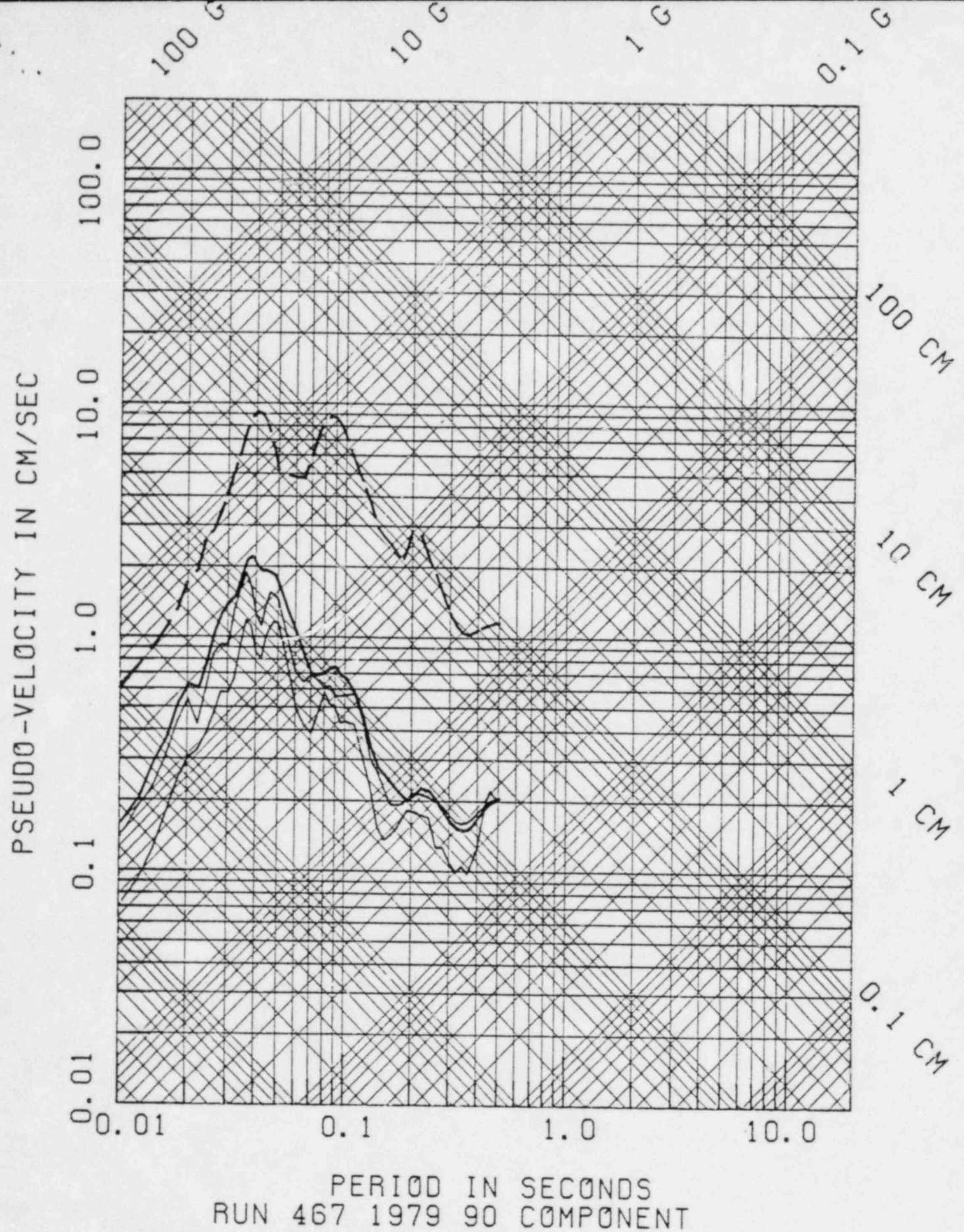

Figure 2.16 Auxiliary Building foundation response spectra obtained from transverse component transfer functions for Test 4, shot 4 with random phase, observed phase and zero phase (in ascending order). Top trace is the response spectrum of the unfiltered 90° component 1979 accelerogram.

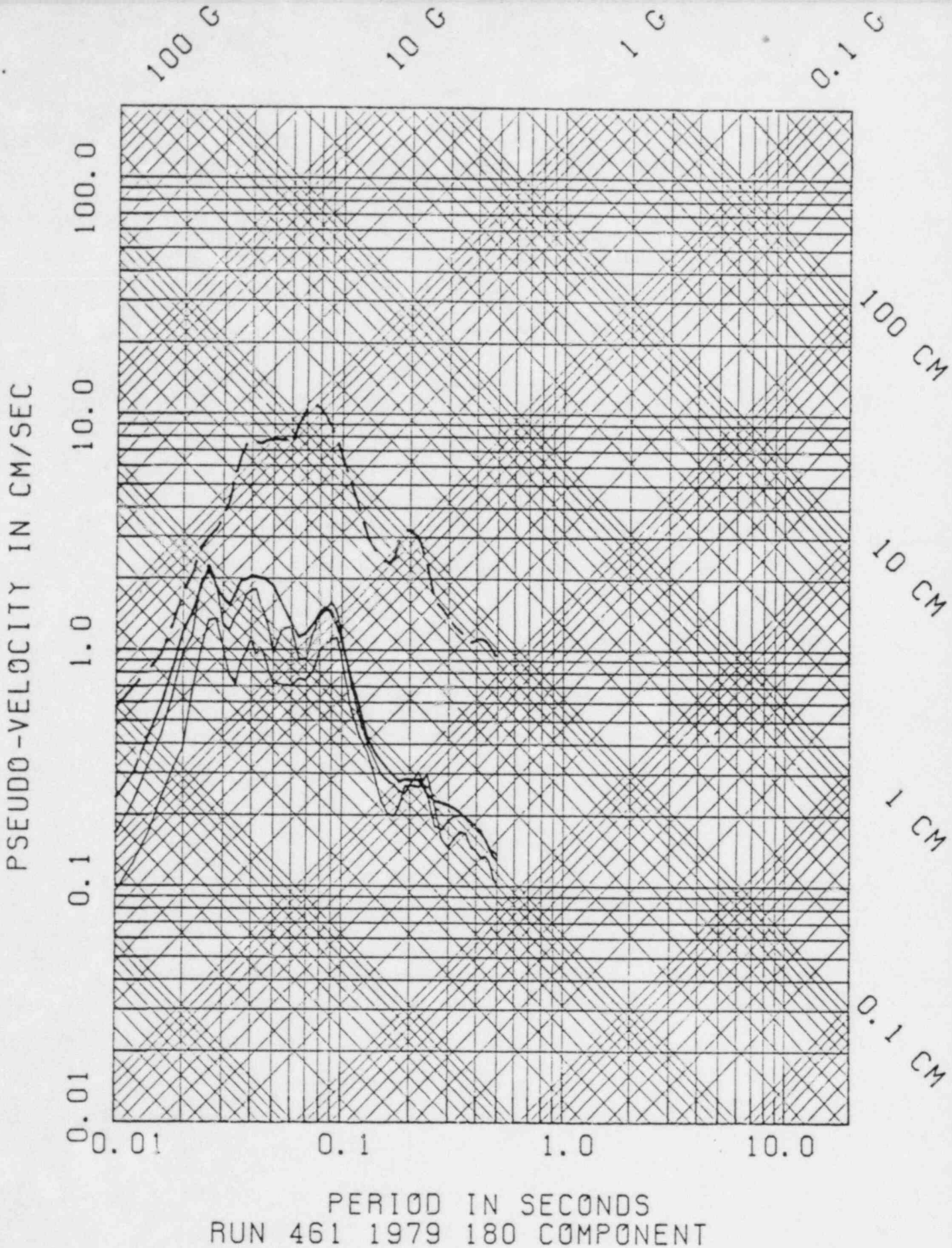

Figure 2.17 Auxiliary Building foundation response spectra obtained from radial component transfer functions for Test 4,shot 4 with random phase, observed phase,and zero phase (in ascending order). Top trace is the response spectrum of the unfiltered 180° component 1979 accelerogram.

Question 2A. (New Q. 2)

Regarding the sensitivity of the results to assumptions about phase response, the Licensee should calculate upper-bound reduced response spectra for computed foundation motions that have been processed with a spiking filter (e.g. Robinson, 1978); the processed signals will have the same amplitude spectra but will be compressed in time as much as possible. Alternatively, the Licensee should demonstrate some other upper bound, given that the pad-to-foundation transfer function may not represent a physically realizable filter.

Robinson, E.A., Multichannel Time Series Analysis with Digital Computer Programs, Revised Edition, Holden Day, San Francisco, 1978.

In assessing assumptions about phase response and the relative durations of input and output signals, it is relevant to compare the durations of foundation and free-field signals. Such a comparison is presented below, and it is found that there is no systematic difference between foundation and free-field signal durations for frequencies above 15 Hz. Below about 15 Hz the free-field durations are longer in some cases, but this is unimportant because the reduced foundation response spectra lie below the M_L 4.5 RIS spectrum at these lower frequencies. The observed similarity of the signal durations justifies the use of the zero-phase shift filter, which preserves signal duration, rather than any other filter which compresses the signal duration.

The premise of the question is that, as an upper bound case, foundation signals should be spike-like and compressed in time as much as possible. How this case could arise physically is not apparent. Both at foundation and free-field sites, the seismograms are composed of P and S groups travelling at bedrock velocities, followed by higher mode surface wave trains. Multipathing and reverbration due to the heterogeneities along the propagation path and near-receiver structure complicate the signals and extend their duration. The character of seismic signatures is alike for the deeper and shallower RIS

events, and for earthquake and explosion sources, as shown in the response to Question 1. Because the seismic signal at any receiver location consists of a multiplicity of arrivals at intervals determined by the velocity structure, it is not reasonable that a spike-like seismic signal of arbitrarily brief duration could be incident upon the structure foundations. Such spike-like signals fabricated with special filters do not provide physically reasonable bounds for the foundation response.

The Robinson spiking filter is inappropriate because it does not preserve the amplitude spectrum. A brief description of this spiking filter and some examples are given below.

An alternative filter that does preserve the amplitude spectrum, and that gives the largest possible peak amplitude, was used. The phase of the output signal is set to zero at all frequencies. This produces a symmetric, non-causal, band-limited impulse that is the most spike-like (maximum amplitude) signal that preserves the original spectral amplitudes. This filter, called here the impulse filter, produces signals that have response spectra only slightly higher than response spectra for the zero-phase shift filter, for frequencies below 40 Hz. However, the zero-phase shift filter is preferable because it preserves the character of the signal, whereas the impulse filter is physically unrealistic; it requires the output signal to be unrelated in phase to the input, spike-like and symmetric in time.

Comparison of foundation and free-field signal durations

The L-22 velocity records of the explosion tests generally have longer durations at free-field sites than at equidistant foundation sites, but this does not mean that the durations are longer at all frequencies. The band pass filter results presented below show that for frequencies above 15 Hz, free-field and foundation signal durations are nearly the same. For frequencies below 15 Hz, the longer durations of the L-22 velocity records at the free-field sites are indicative of lengthier higher-mode surface wave trains: note that the velocity spectra of the explosion records have peaks in the band 10 - 15 Hz so that these lower frequency contributions control the duration of the observed broad-band signals.

Figures 2A.1 - 10 show Hilbert transform envelopes of band pass filtered free-field and foundation seismograms. The band pass filters have width ± 6 Hz to the -30 db point, and were computed for center frequencies from 10 to 32 Hz at 2-Hz intervals. The numbers to the right of the traces give the maximum amplitudes of the envelopes. The envelopes for foundation and free-field records are scaled to the same maximum amplitude in the plots.

Auxiliary Building durations for Test 3, shot 2 are compared with those for free-field sites F1, FR, F6, and F3 in Figures 2A.1 - 4. For frequencies above 15 Hz, there is no systematic difference between Auxiliary Building and free-field durations. The same is the case for the Diesel Generator Building and Service Water Pumphouse data, shown in comparison with free-field site F3 in Figures 2A.5 and 2A.6. Note that in some cases foundation and free-field durations are the same over the entire band 10 - 32 Hz (e.g., Figure 2A.4, transverse component, and Figures 2A.5 and 6, radial components).

Band-pass-filter envelopes for Test 4, shown in Figures 2A.7 - 10, indicate that foundation, free-field, and USGS dam abutment accelerograph pad signal durations are essentially the same above 15 Hz, and in some cases for all frequencies in the band 10 - 32 Hz.

The similarity of foundation, free-field, and accelerograph pad signal durations justifies the use of the zero-phase shift filter, which has no effect on signal duration. While in some cases the free-field durations are longer for frequencies below 15 Hz, this is of no concern because in all cases the reduced foundation response spectra fall below the M_L 4.5 RIS spectrum at these lower frequencies.

The Robinson Spiking filter

Robinson (1978) has described (and given computational algorithms for finding) a "spiking filter," which ideally produces an output signal from an input signal in such a way that the output is a spike located at the most energetic part of the input signal. The spiking filter is intended to resolve the arrival time of a wavelet, and does not preserve the amplitude spectrum. The

output of the filter approaches a value of 1 for the ideal case of a delta function. The spiking algorithm ignores spectral amplitudes, so that, whatever the input, an output near unity for the spike is obtained. In the examples given below, the spiking filter output is normalized to contain the same energy as the input seismogram, so that the effect of using such a filter can be investigated. In Figures 2A.11, 13, and 15 are shown the vertical, 180- and 90-degree components of the 1979 accelerogram as recorded at the dam abutment. Given in Figures 2A.12, 14, and 16 are the spiking filter outputs obtained using Robinson's algorithm.

Note that 256 datum points were used in the construction of the spiking filters, and that the height of the resulting spike is a sensitive function of the number of datum points used in constructing the spiking filter (in this case 20 samples). Therefore, since the resulting high-frequency response spectral output scales with the peak amplitude of the input seismogram, the high-frequency asymptote of any response computed will depend critically on the length of the spiking filter constructed. In any case, this type of spiking filter is totally inappropriate, because it does not preserve the signal spectrum.

Impulse filter

In general no single selection of phase will give a response spectrum which is highest at all frequencies. The phase angle selected here is the one which gives the largest possible peak ground acceleration on the output filtered seismogram, namely zero phase at all frequencies. This filter, called here the impulse filter, is constructed by multiplying the Fourier spectrum of the input seismograms by the real-valued spectral modulus ratio, then replacing the resulting complex-valued spectrum with real values consisting of the Fourier spectral amplitude. It is clear that, for a signal with fixed Fourier amplitude, the impulse filter gives the largest possible peak amplitude, because at zero time, the amplitude consists of a real sum of all of the Fourier components, adding together in phase.

In Figures 2A.17 and 2A.18 the impulse filter results are compared with those for the "zero-phase shift filter" for the 90- and 180-degree components of the 1979 Monticello Reservoir earthquake. Unlike the impulse filter described in the previous paragraph, the zero-phase shift filter sets the phase of the filter, not the output seismogram, to zero. Thus, the result (top trace in these figures) retains the phase information of the output seismogram. In contrast, the impulse filter seismogram has a Fourier transform with zero phase at all frequencies, and therefore the seismogram is symmetric about the origin, where the peak amplitude occurs. Notice that this peak value of acceleration for the bottom traces is almost twice as large as for the zero-phase shift filter results (top traces). Figures 2A.19 and 2A.20 compare the results of passing the filtered seismograms through a 5-percent response spectrum algorithm, for the 90- and 180-degree components of motion respectively. Notice that the impulse filter response is higher at the very high frequencies, but that generally the two traces are fairly close together. From these calculations it is evident that the choice of zero-phase shift or impulse filter does not make a great difference in the computed response spectrum below 40 Hz, although the latter lies generally above the former.

Further comparisons of results for the zero phase shift and impulse filters are shown in Figures 2A.21-23. Foundation envelope response spectra are shown for signals obtained for transfer functions constructed from 50th percentile spectral modulus ratios for the Auxiliary Building, Diesel Generator Building and Service Water Pumphouse.

While the zero-phase shift filter preserves the character of the input signals, the impulse filter does not, requiring instead that circumstances conspire such that the output signal has zero phase at all frequencies. This is not physically reasonable and gives an unrealistically conservative estimate of the foundation response.

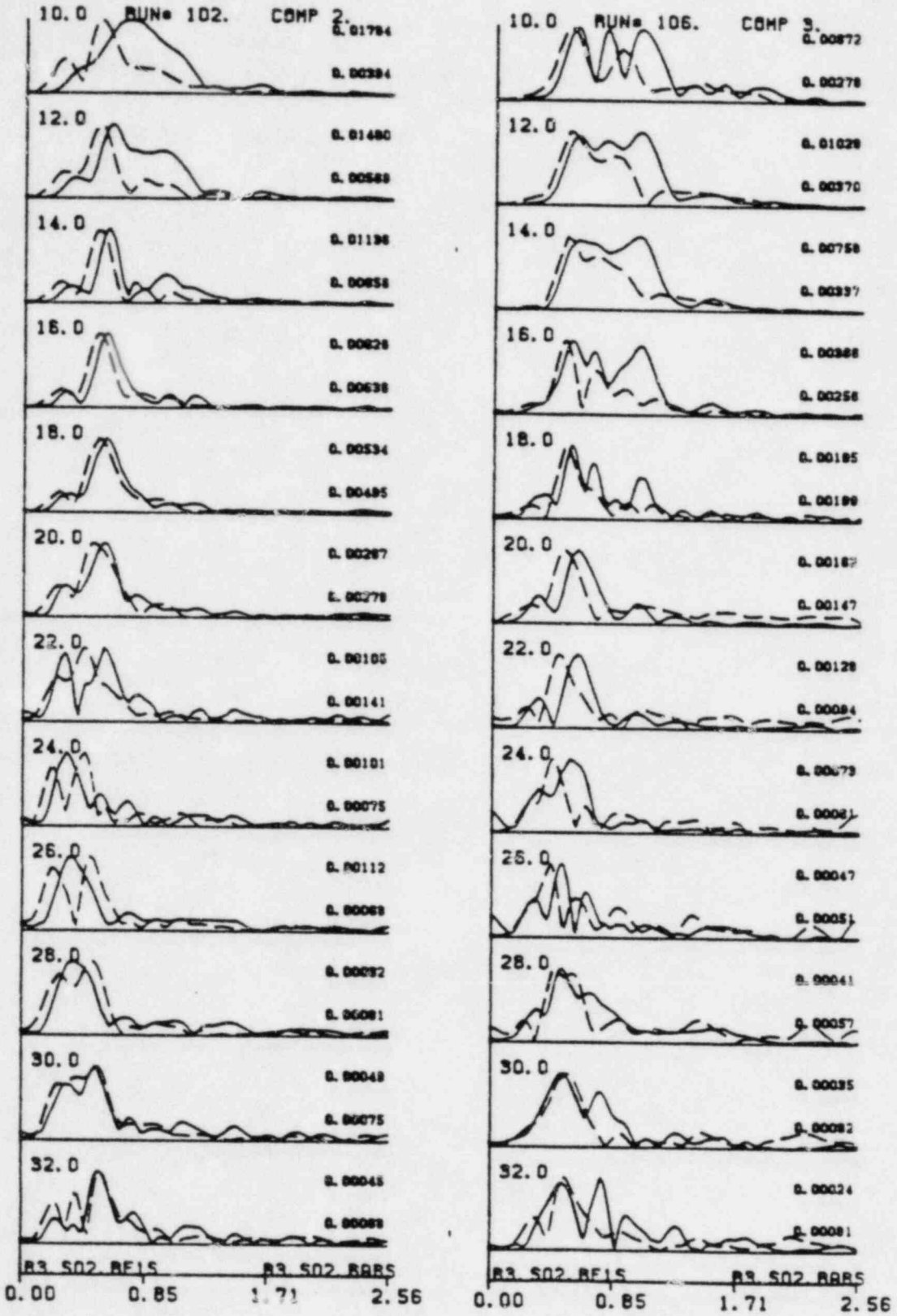

FIGURE 2A.1 Envelopes of band pass filtered records for Test 3, shot 2, at free-field site F1 (solid lines) and Auxiliary Building (dashed lines). Left, radial; right, transverse.

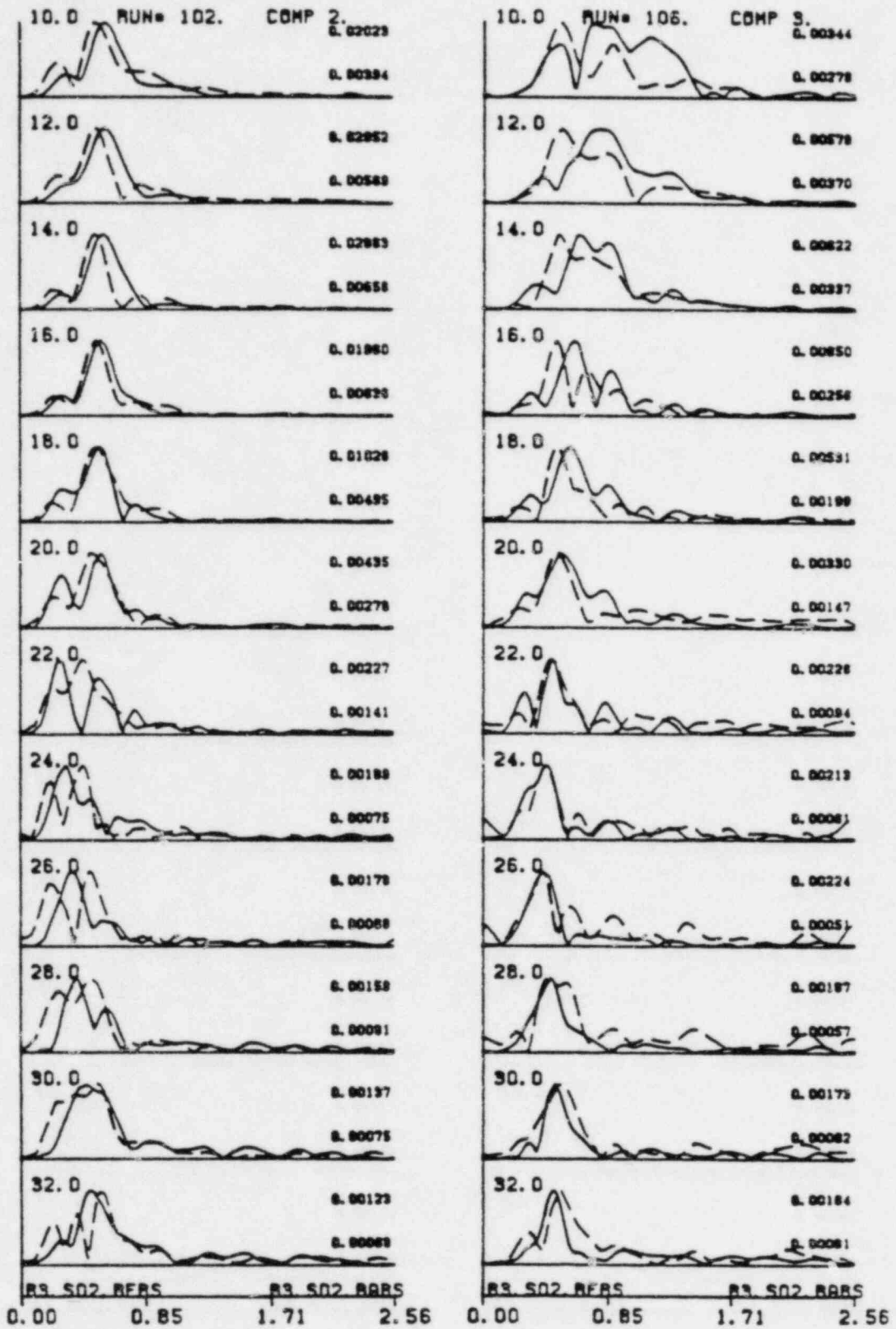

FIGURE 2A.2 Envelopes of band pass filtered records for Test 3, shot 2, at free-field site FR (solid lines) and Auxiliary Building (dashed lines). Left, radial; right, transverse.

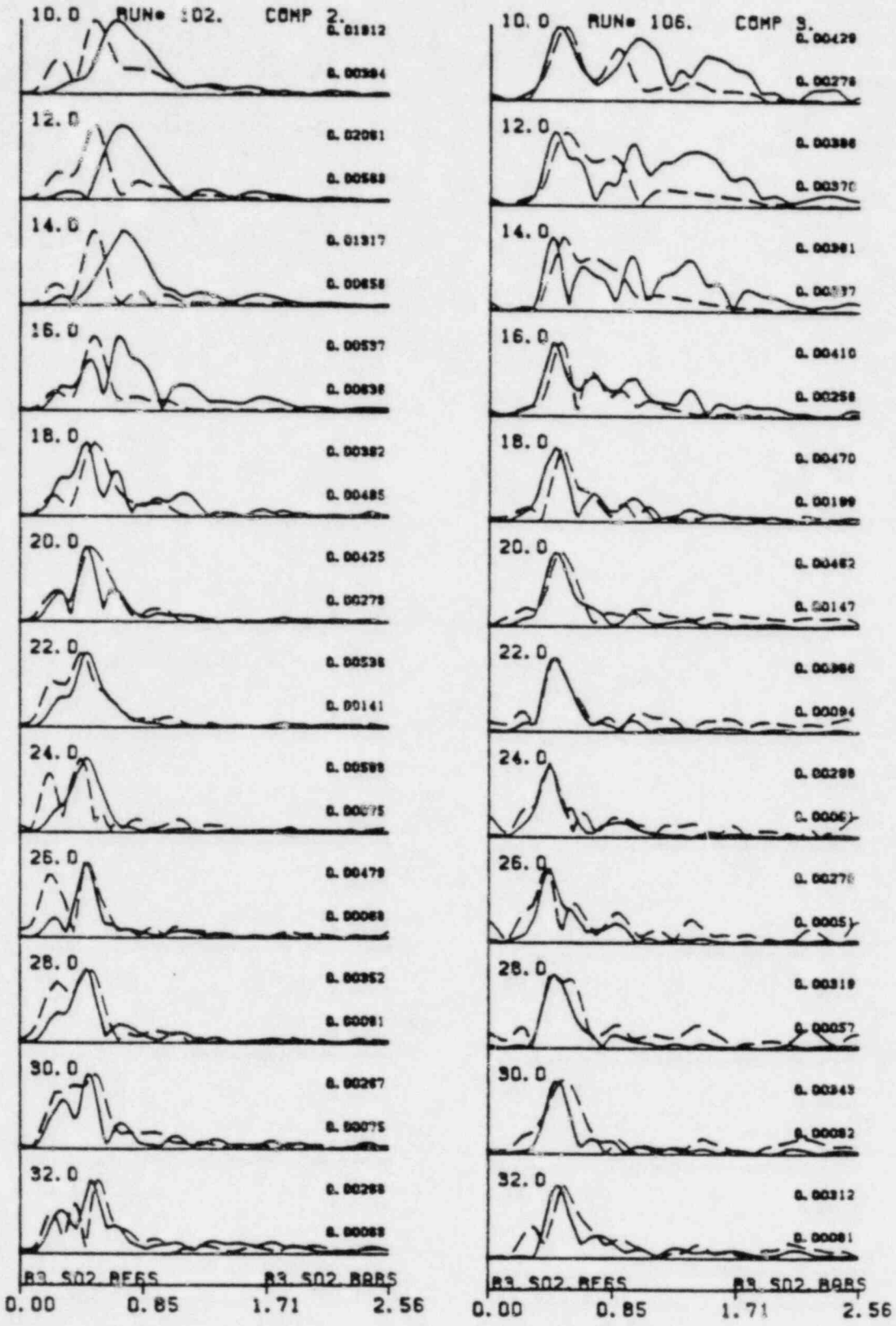

FIGURE 2A.3 Envelopes of band pass filtered records for Test 3, shot 2, at free-field site Ff (solid lines) and Auxiliary Building (dashed lines). Left, radial; right, transverse.

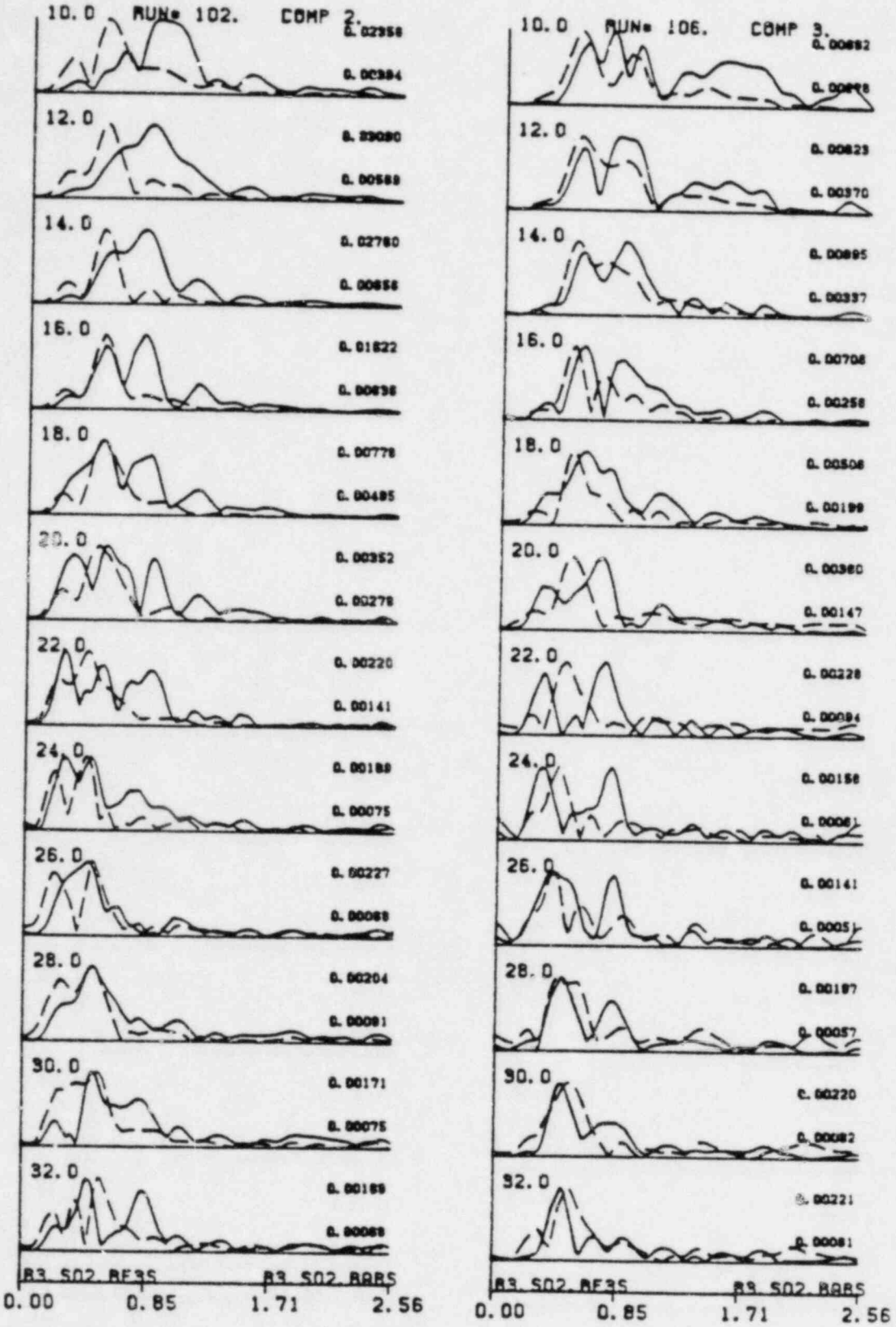

FIGURE 2A.4 Envelopes of band pass filtered records for Test 3, shot 2, at free-field site F3 (solid lines) and Auxiliary Building (dashed lines). Left, radial; right, transverse.

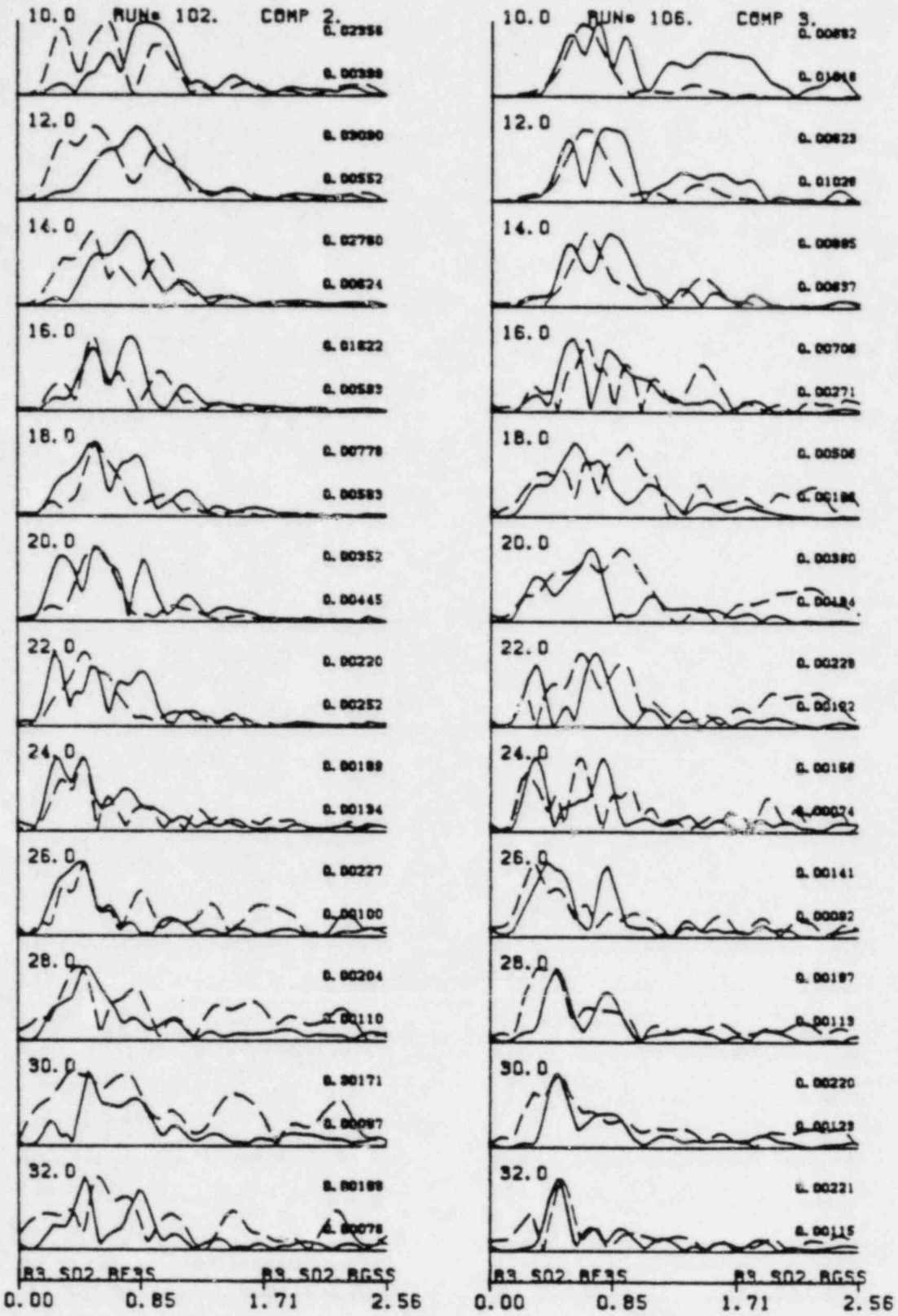

FIGURE 2A.5 Envelopes of band pass filtered records for Test 3, shot 2, at free-field site F3 (solid lines) and Diesel Generator Building (dashed lines). Left, radial; right, transverse.

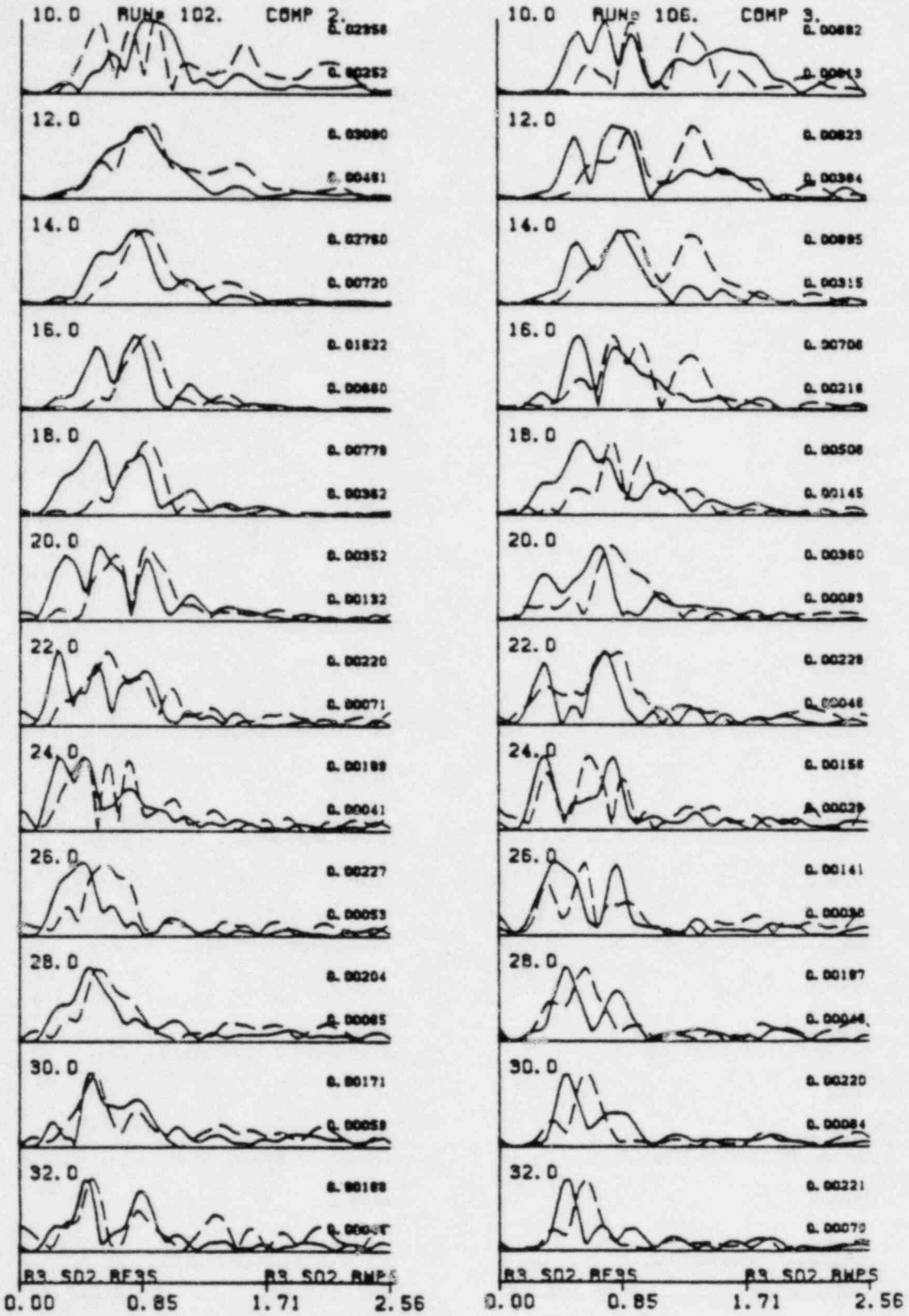

FIGURE 2A.6 Envelopes of band pass filtered records for Test 3, shot 2, at free-field site F3 (solid lines) and Service Water Pumphouse (dashed lines). Left, radial; right, transverse.

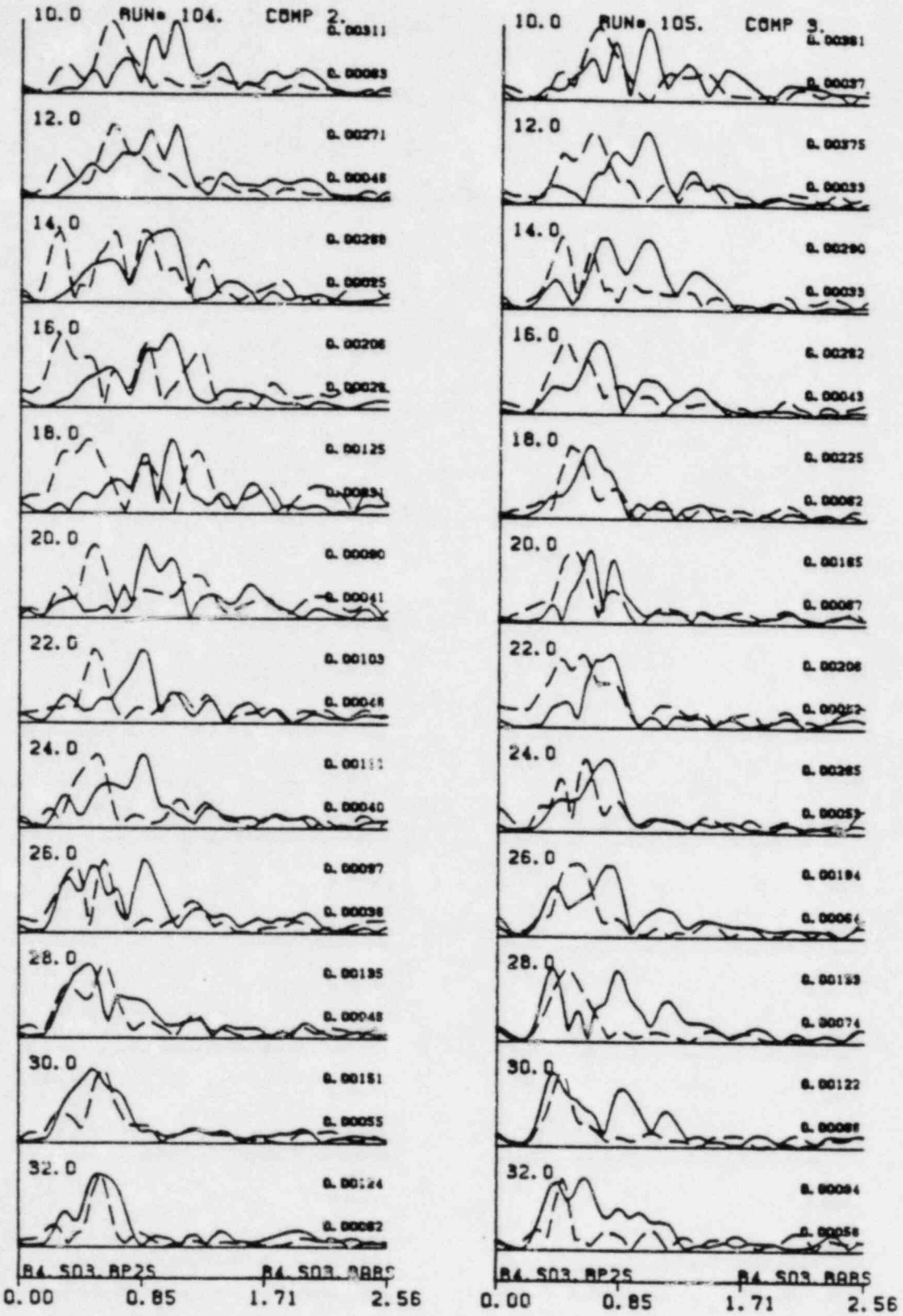

FIGURE 2A.7 Envelopes of band pass filtered records for Test 4, shot 3, at the USGS accelerograph pad (solid lines) and Auxiliary Building (dashed lines). Left, radial; right, transverse.

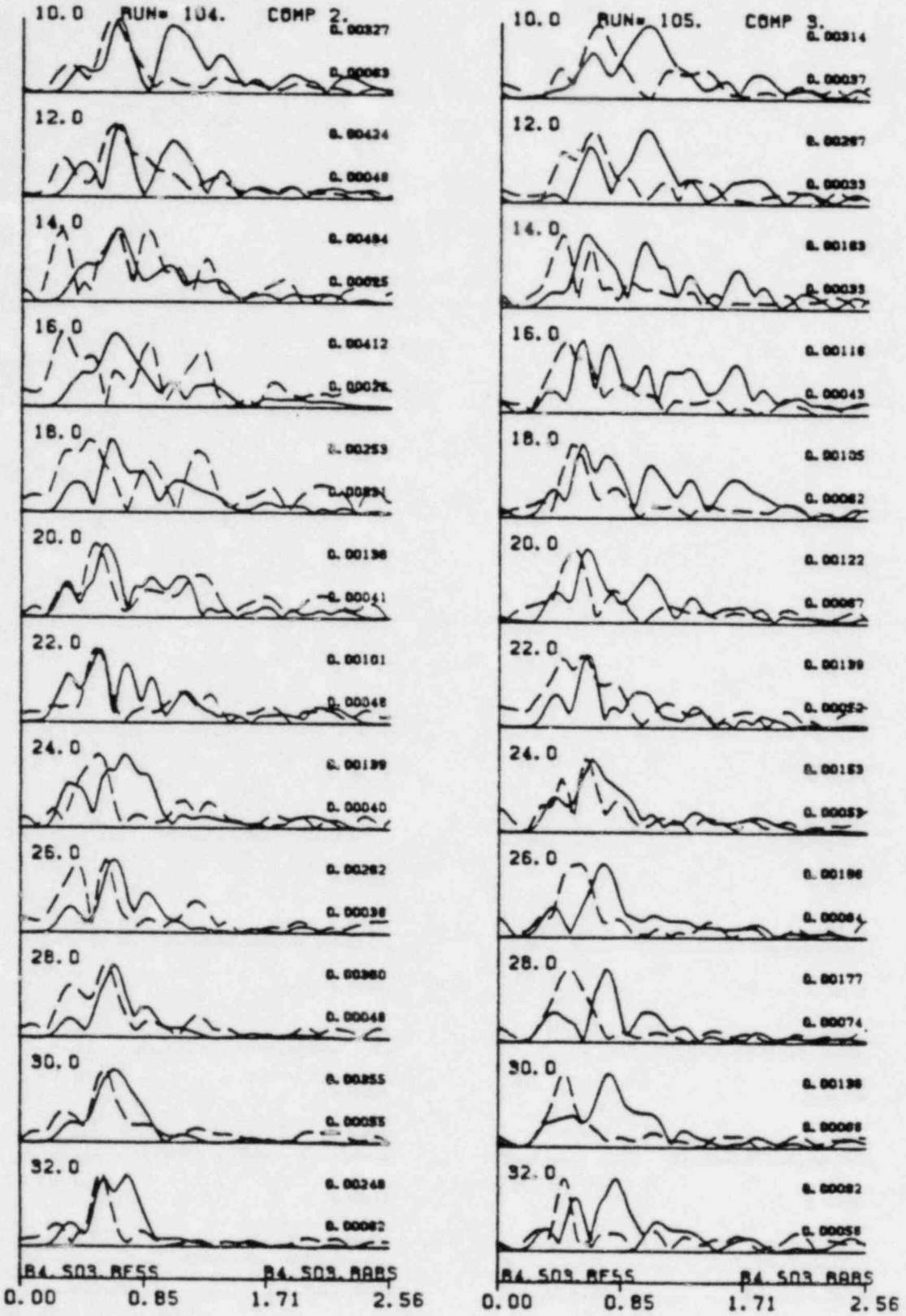

FIGURE 2A.8 Envelopes of band pass filtered records for Test 4, shot 3, at free-field site F5 (solid lines) and Auxiliary Building (dashed lines). Left, radial; right, transverse.

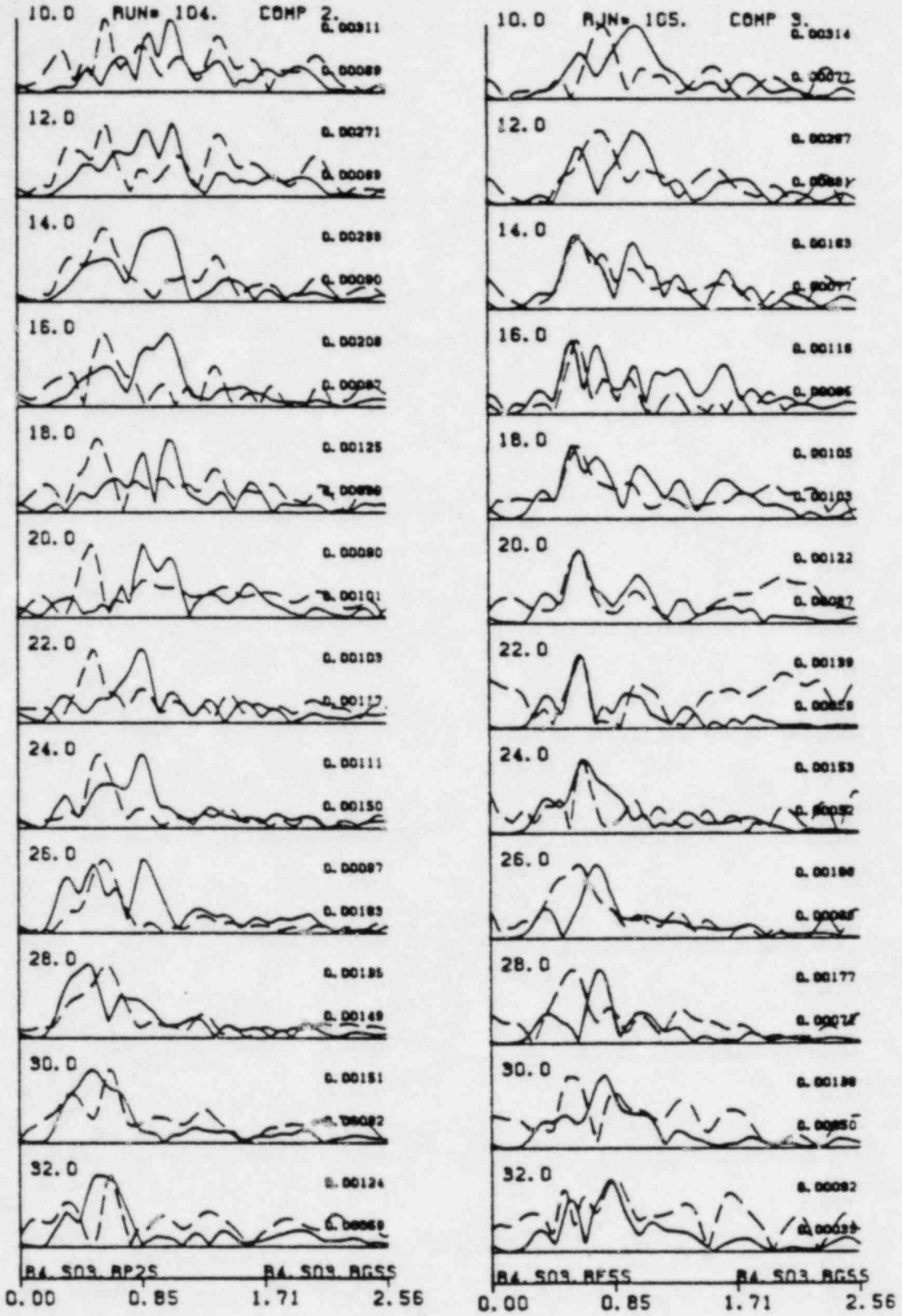

FIGURE 2A.9 Envelopes of band pass filtered records for Test 4, shot 3, at the USGS accelerograph pad (solid lines) and Diesel Generator Building (dashed lines). Left, radial; right, transverse.

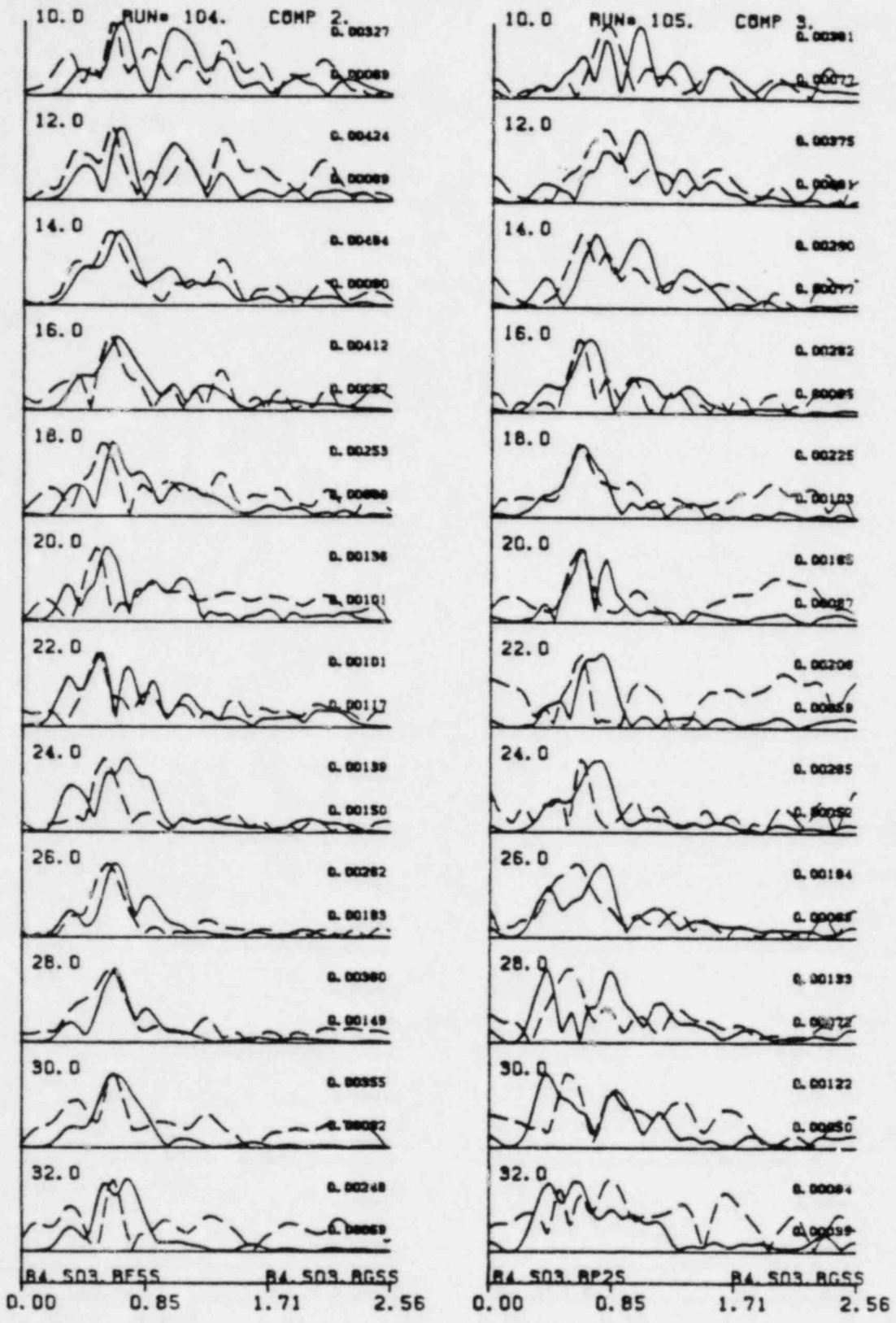

FIGURE 2A.10 Envelopes of band pass filtered records for Test 4, shot 3, at free-field site F5 (solid lines) and Diesel Generator Building (dashed lines). Left, radial; right, transverse.

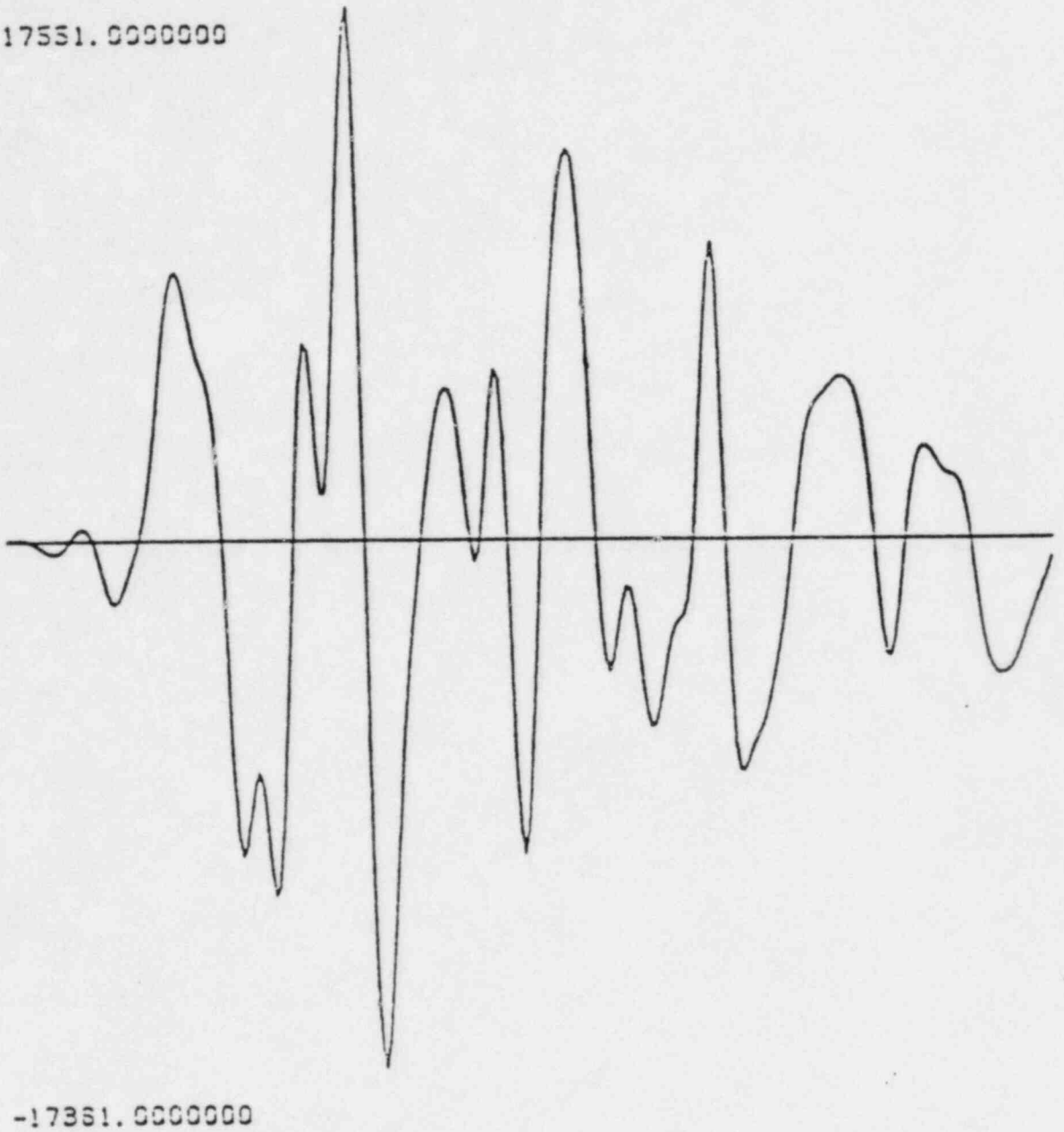

FIGURE 2A.11 Vertical component of the 10/16/1979 Monticello RIS event recorded on the USGS accelerograph pad at the dam abutment. (first 0.512 seconds)

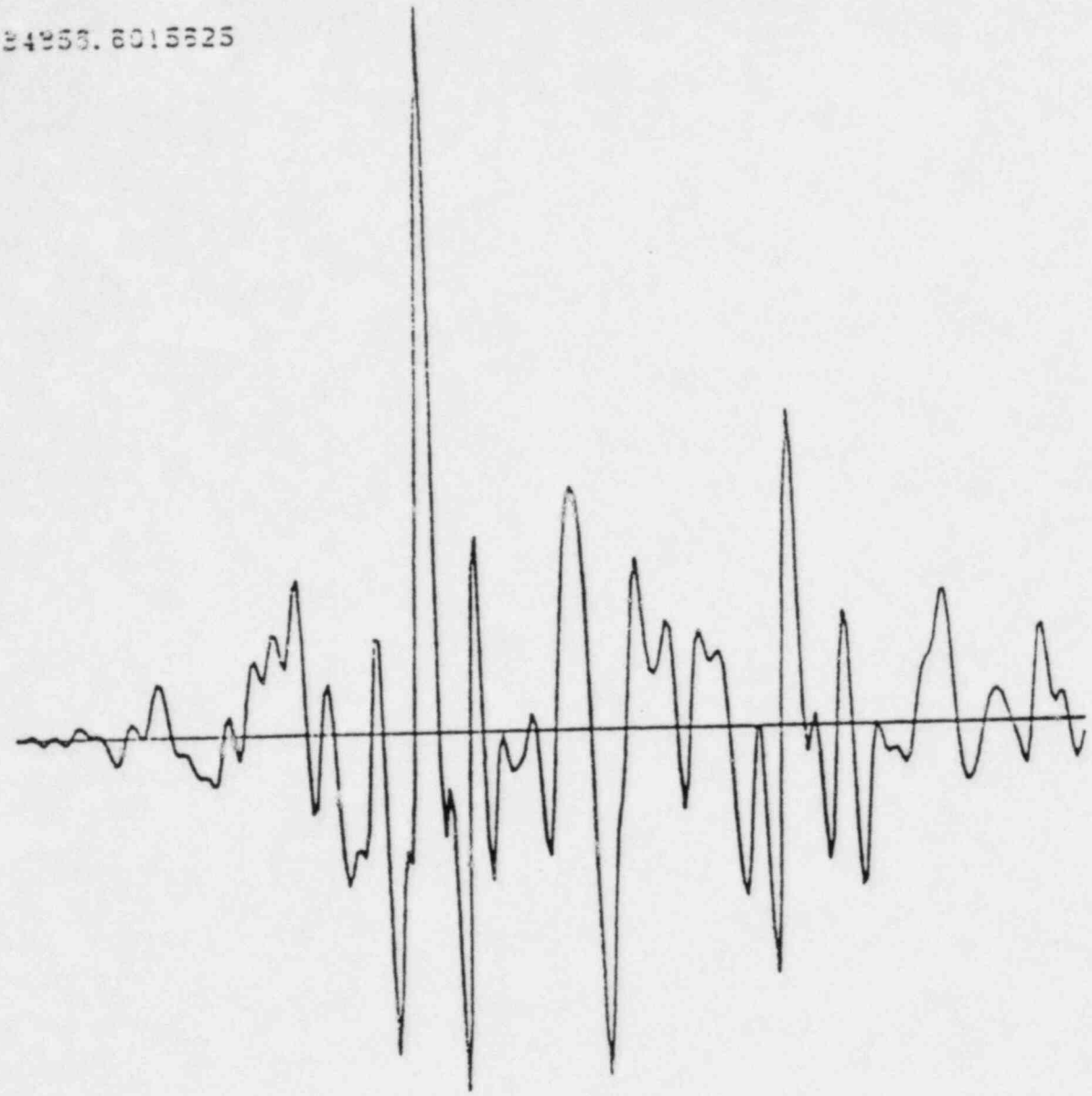

FIGURE 2A.12 Spiking filter output for vertical component of 1979 Monticello event. Spectral amplitudes scaled to provide same total energy as Figure 2A.11.

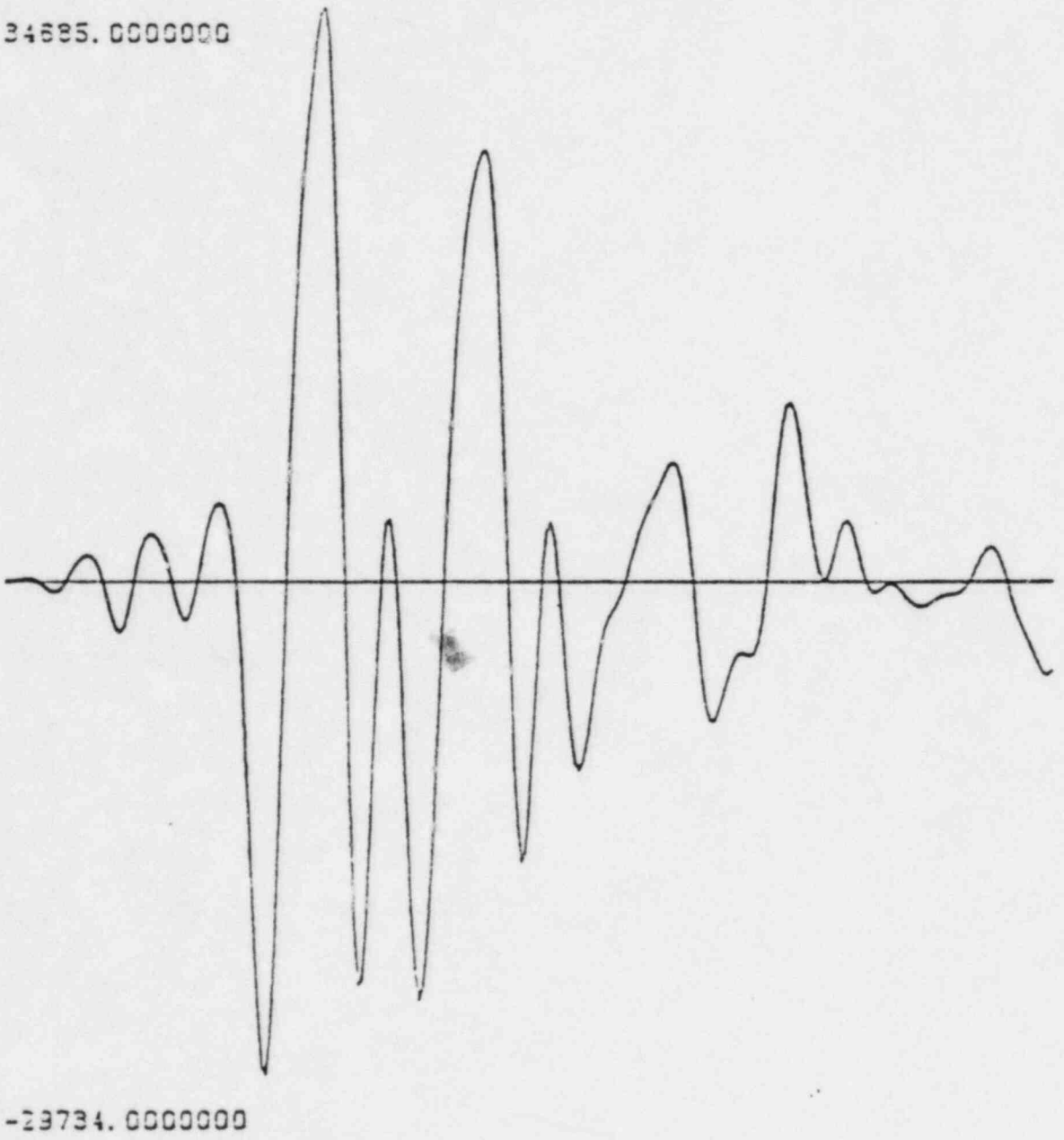

FIGURE 2A.13 180° component of the 10/16/1979 Monticello RIS event (first 0.512 seconds).

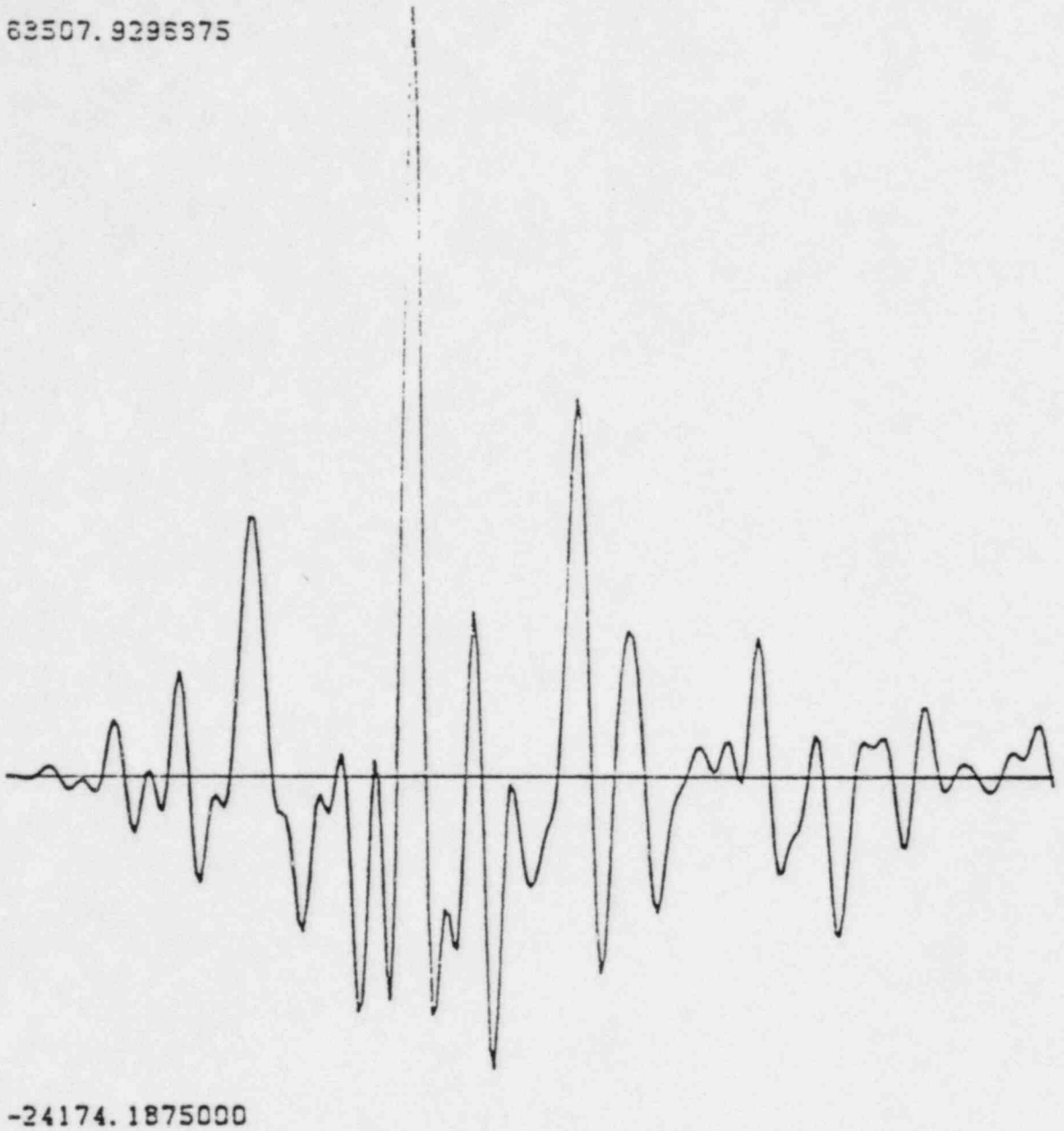

FIGURE 2A.14 Spiking filter output for 180° component of 1979 Monticello event. Spectral amplitudes scaled to provide same total energy as Figure 2A.13.

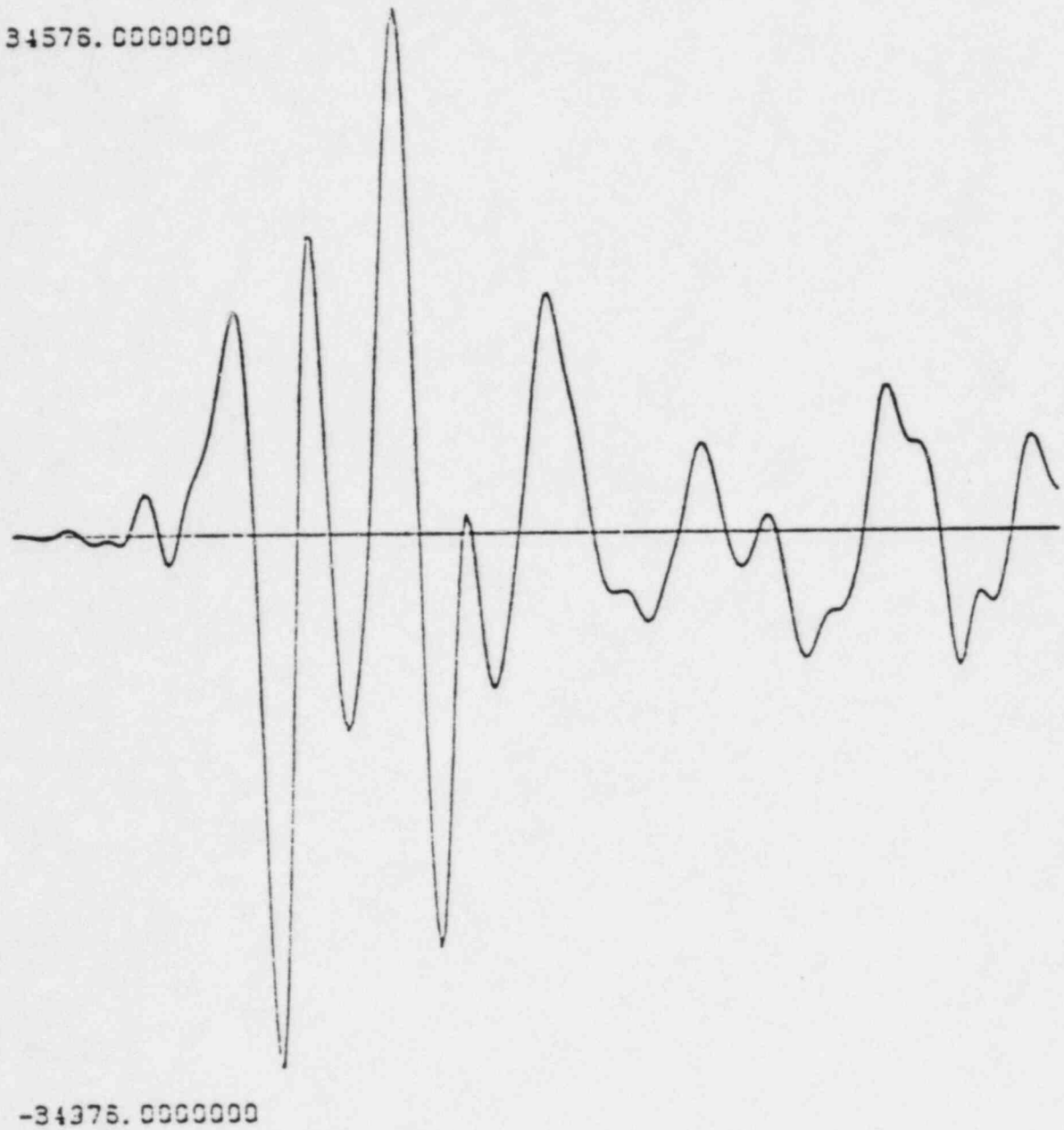

FIGURE 2A.15 90^{o} component of the 10/16/1979 Monticello RIS event (first 0.512 seconds).

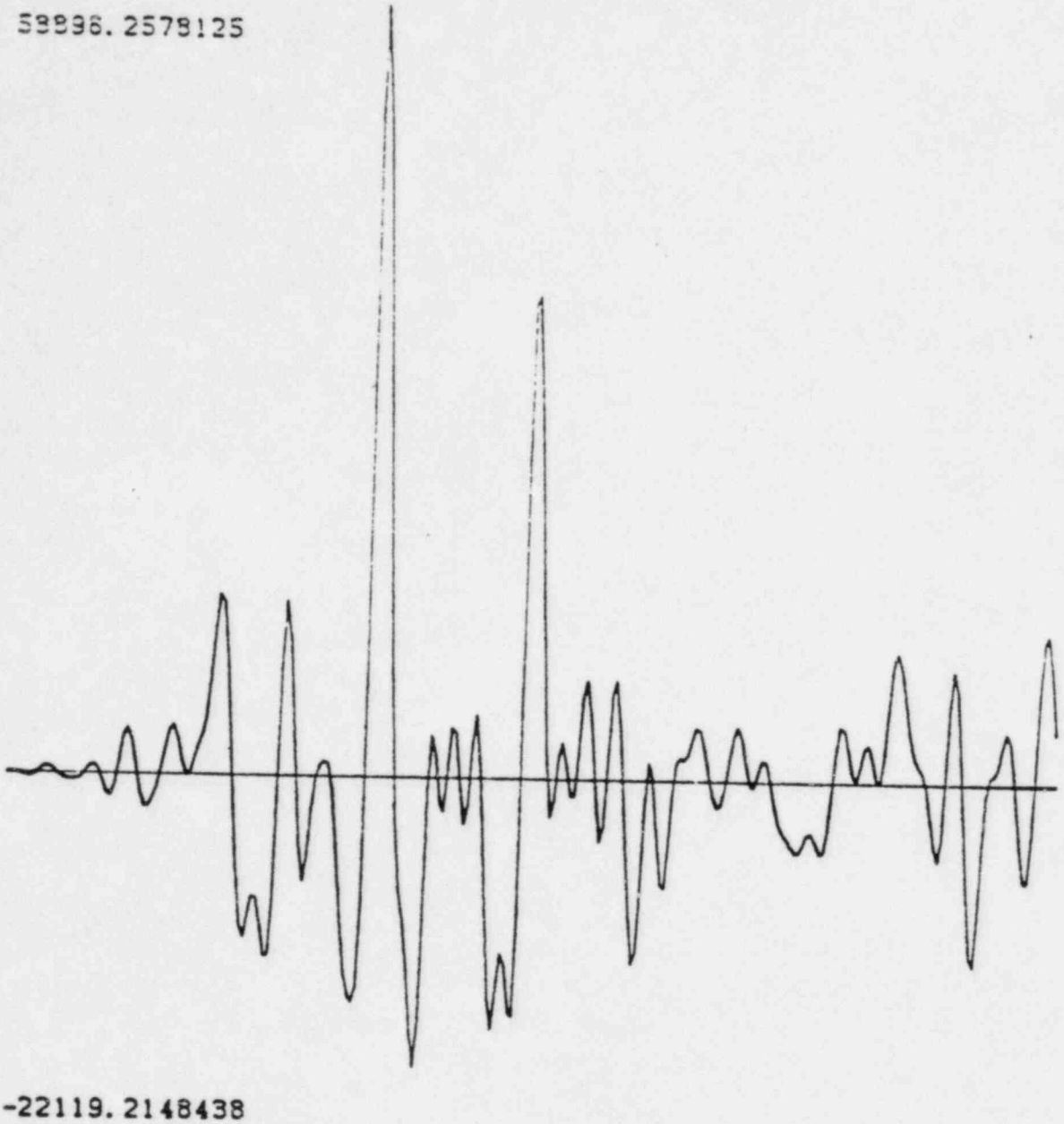

FIGURE 2A.16 Spiking filter output for 90° component of 1979 Monticello event. Spectral amplitudes scaled to provide same total energy as Figure 2A.15.

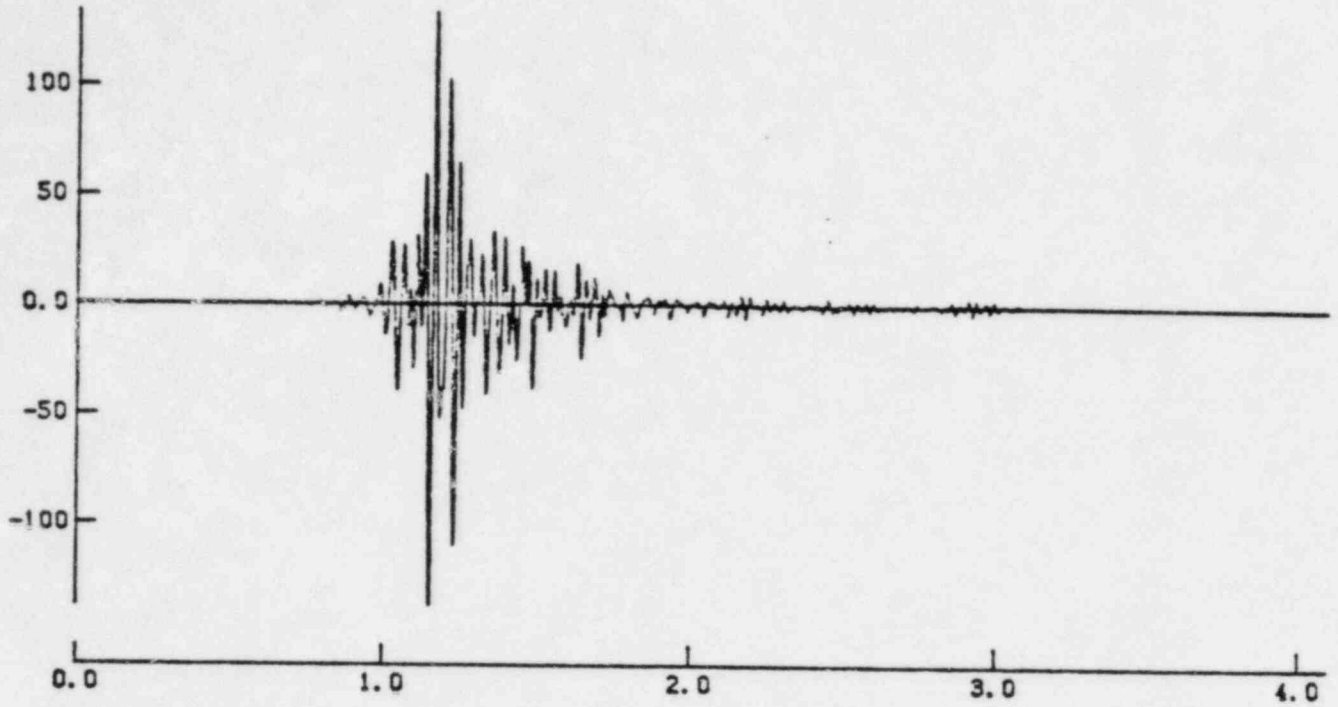

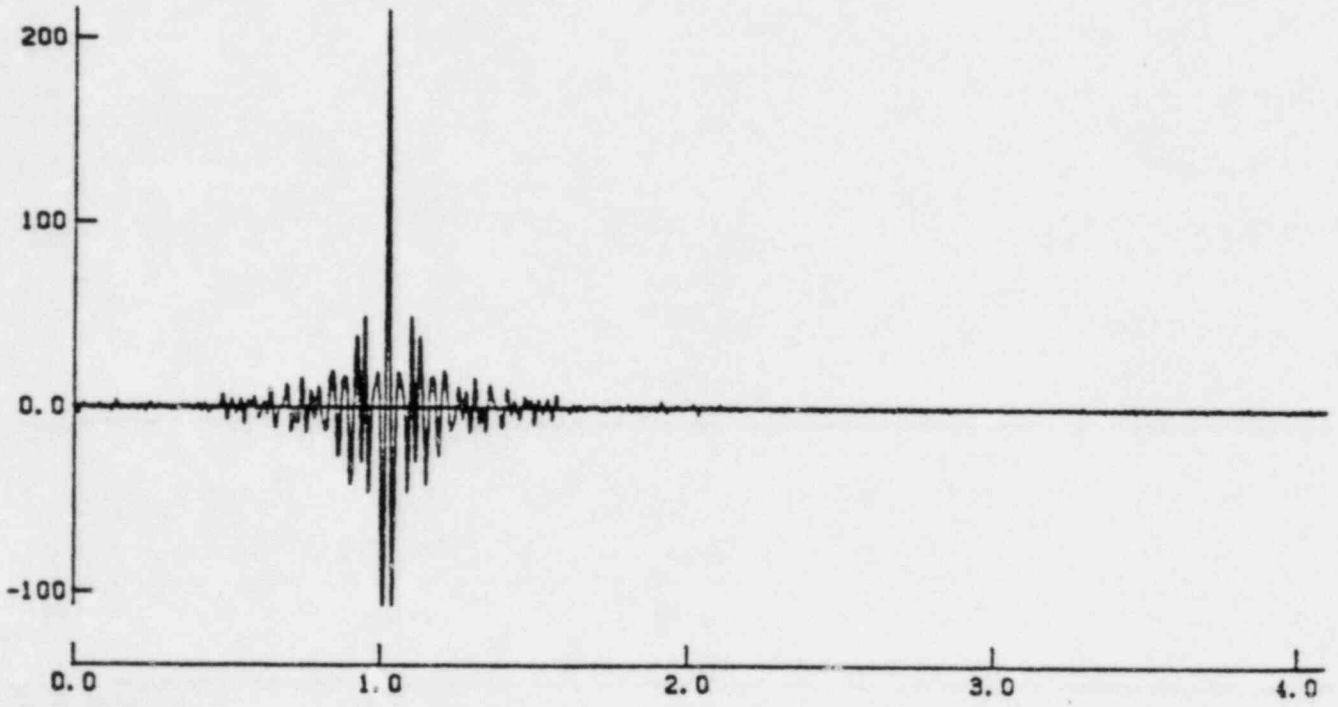

Figure 2A.17 Comparison of filtered 1979 RIS Monticello event, 90° component, using zero-phase (above) and impulse filter (below). Both used AB/P2 zero-phase transfer function.

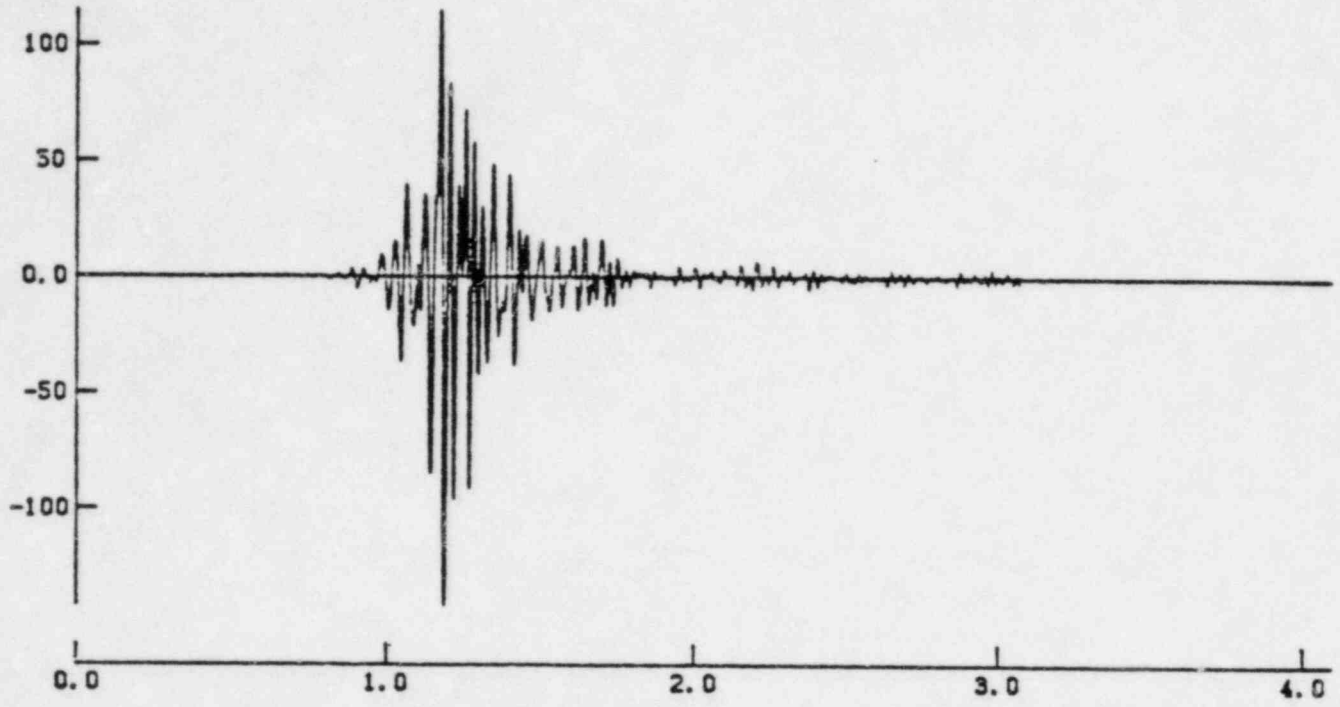

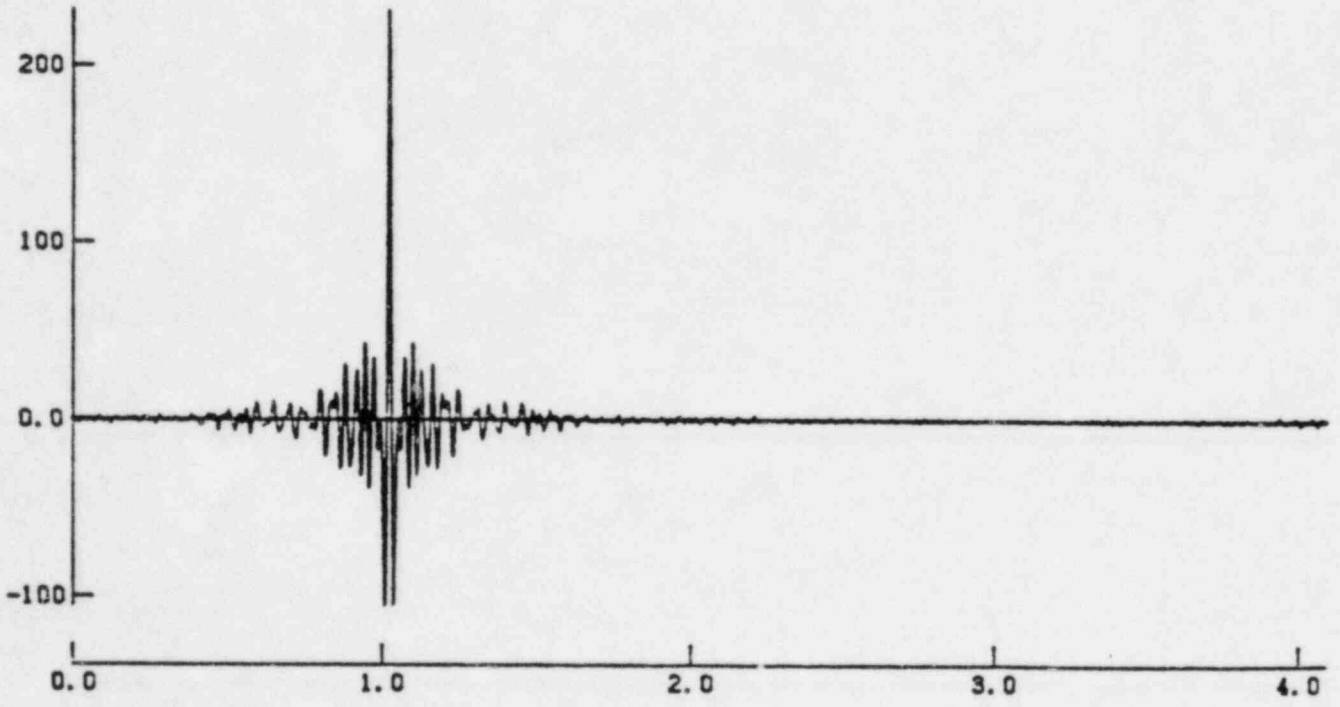

Figure 2A.18 Comparison of filtered 1979 RIS Monticello event, 180° component, using zero-phase (above) and impulse filter (below). Both used AB/P2 zero-phase transfer function.

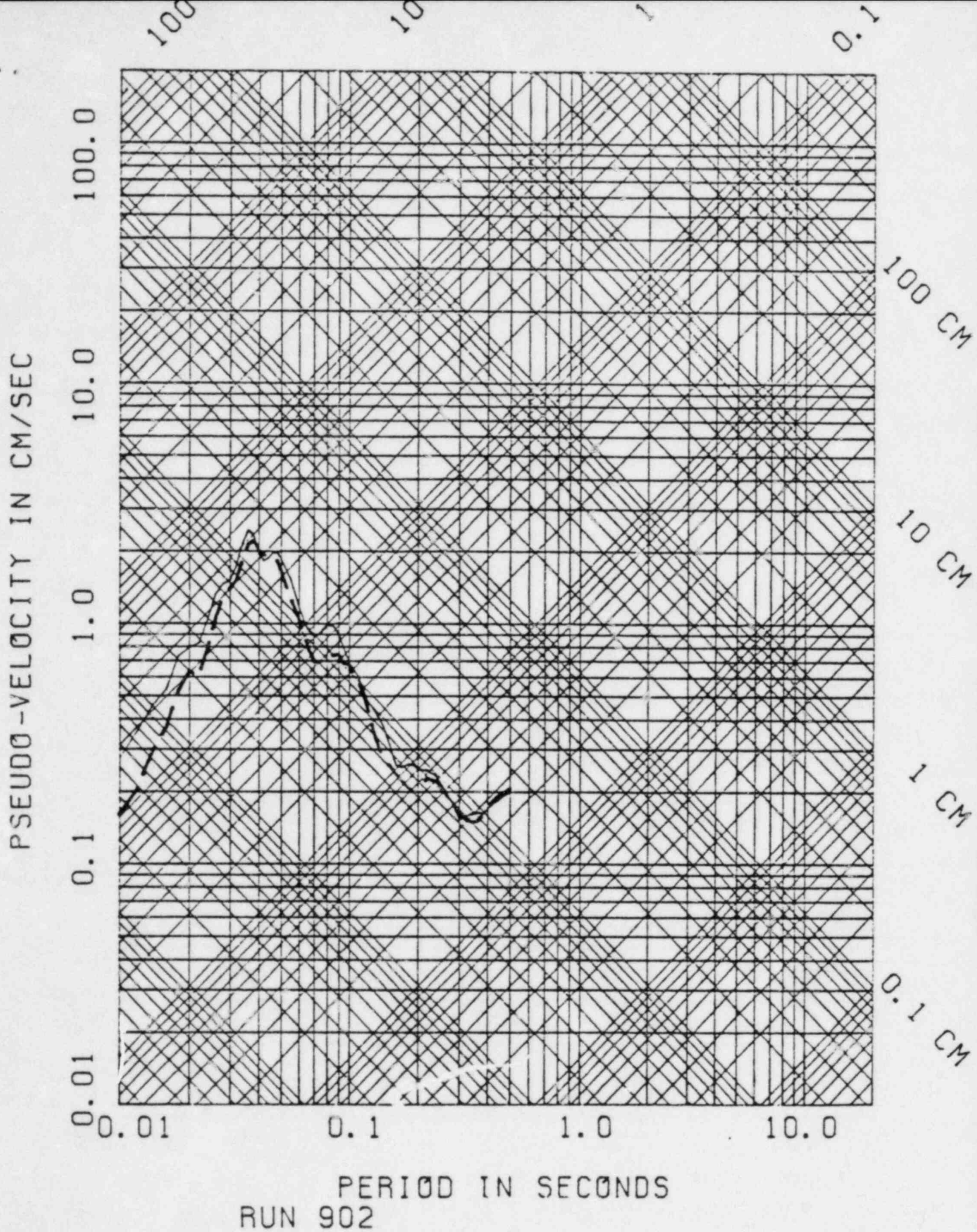

Figure 2A.19 Comparison of response spectra for foundation signals obtained from the impulse filter (solid line) and the zero-phase shift filter (dashed line). The 90° component of the October 16, 1979 accelerogram was filtered with the transverse Auxiliary Building/ accelerograph pad transfer function for Test 4, shot 4.

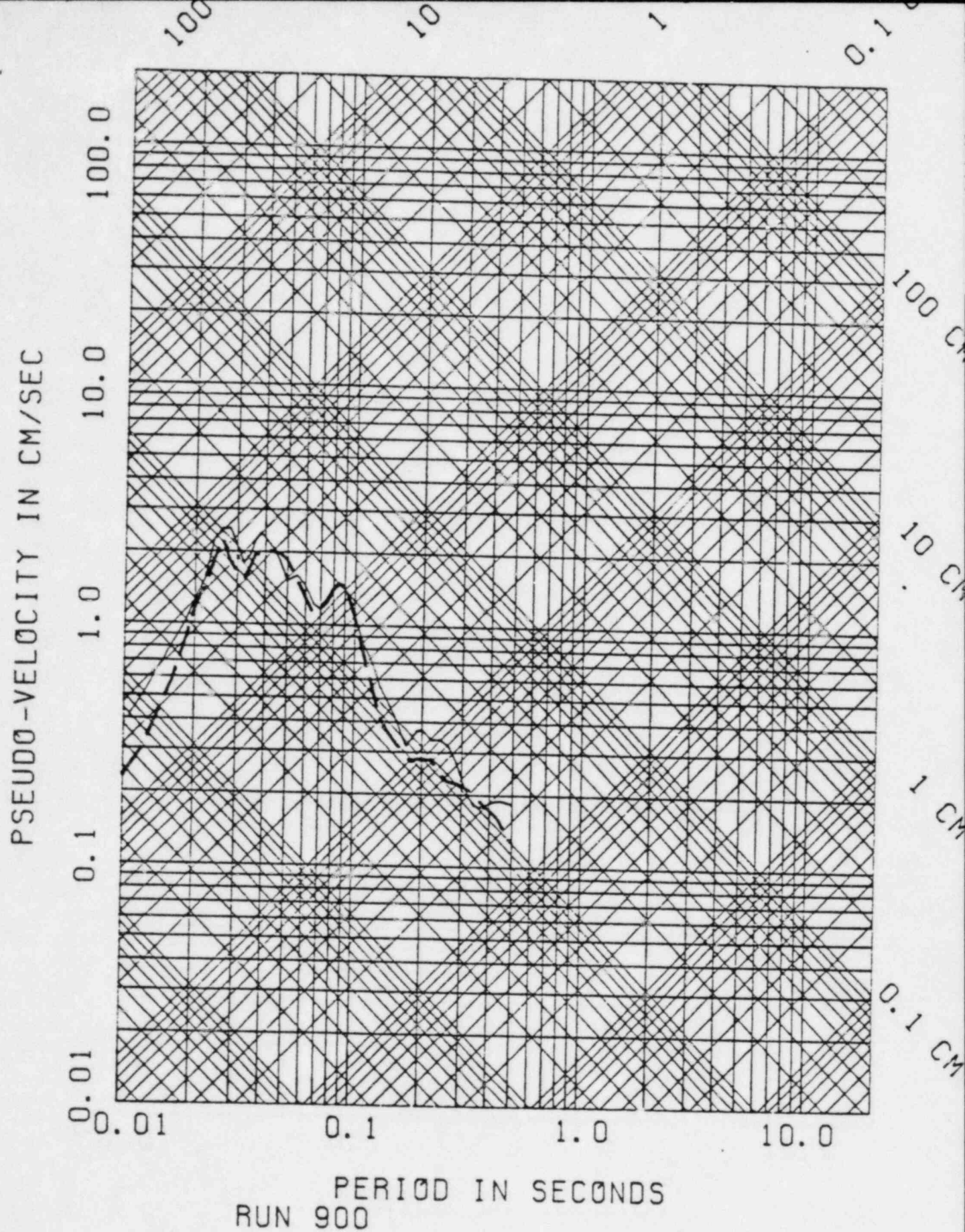

Figure 2A.20 Comparison of response spectra for foundation signals obtained from the impulse filter (solid line) and the zero-phase shift filter (dashed line). The 180° component of the October 16, 1979 accelerogram was filtered with the radial Auxiliary Building/accelerograph pad transfer function for Test 4, shot 4.

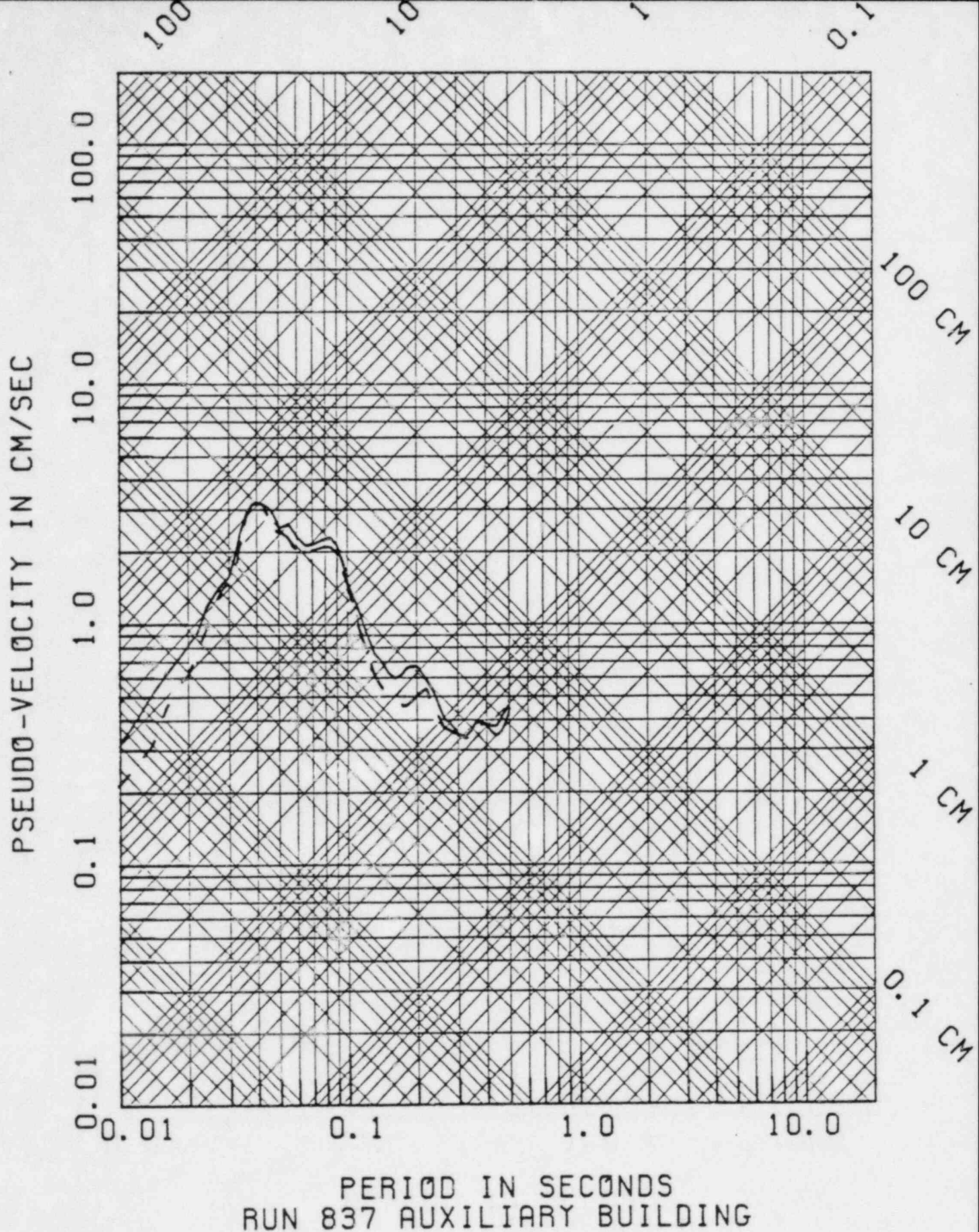

Figure 2A.21 Comparison of Auxiliary Building envelope response spectra of signals obtained for the 50th percentile spectral modulus ratio with the impulse filter (solid line) and the zero-phase shift filter (dashed line).

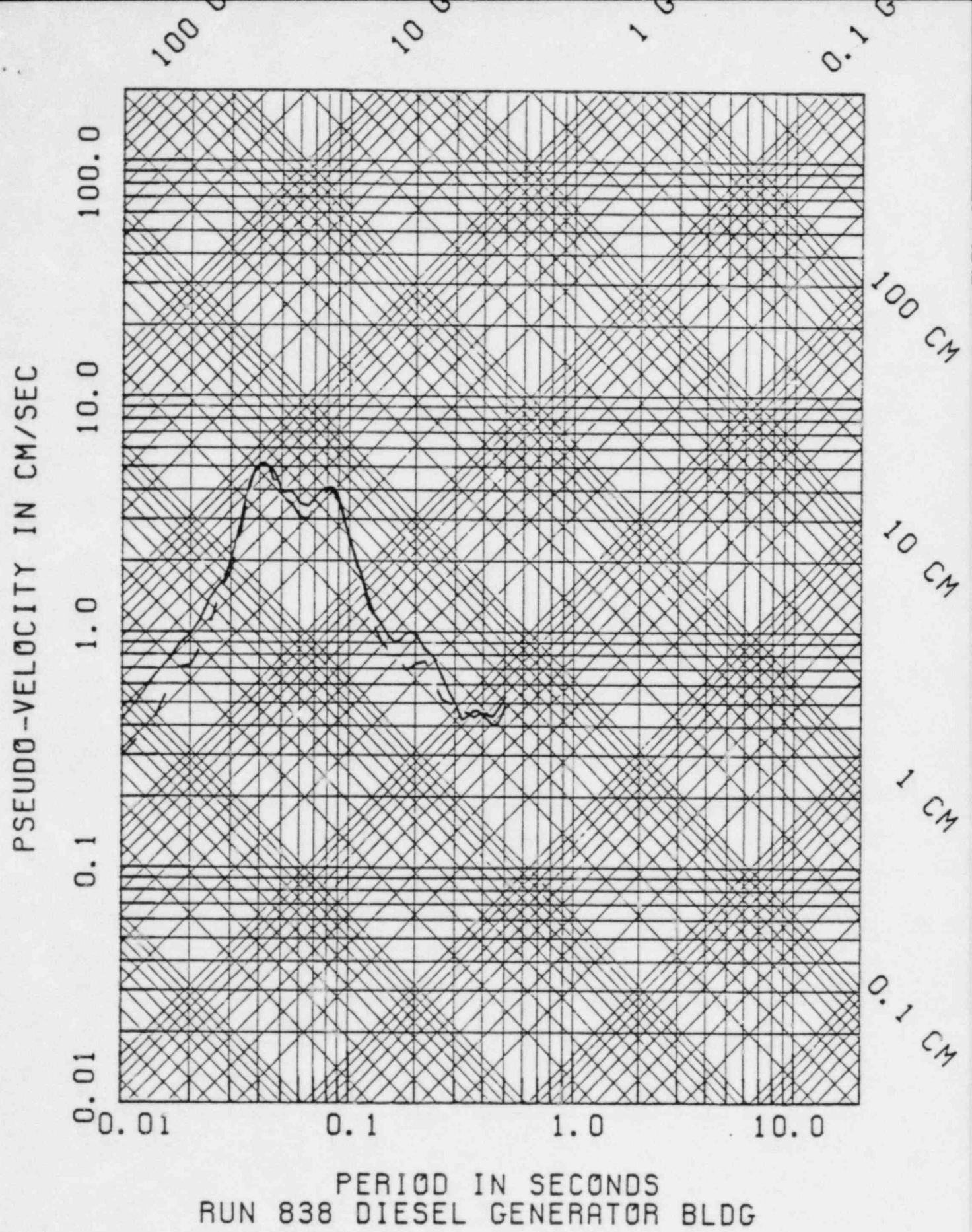

Figure 2A.22 Comparison of Diesel Generator Building envelope response spectra of signals obtained for the 50th percentile spectral modulus ratio with the impulse filter (solid line) and the zero-phase shift filter (dashed line).

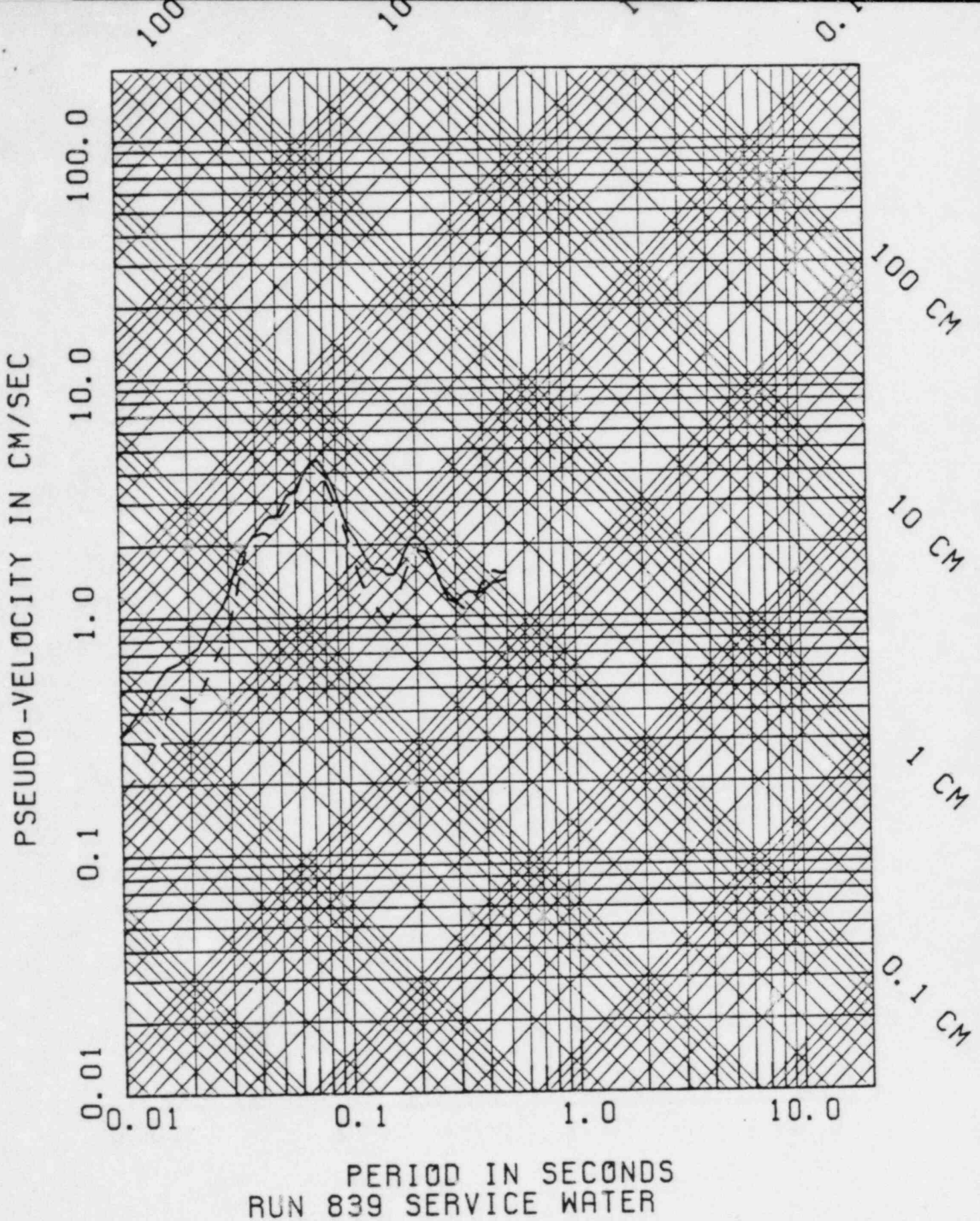

Figure 2A.23 Comparison of Service Water Pumphouse envelope response spectra of signals obtained for the 50th percentile spectral modulus ratio with the impulse filter (solid line) and the zero-phase shift filter (dashed line).

Question 3. Justify the statement on page 28 of Appendix B that "lognormal statistics are appropriate for use here"; document the actual distribution of ratios about the mean. Explain why spectral ratios are averaged geometrically in Appendix B and arithmetically in Appendix A. Justify or modify the estimated reduction factors in light of your answer.

The physical processes which affect wave amplitudes in foundations or on instrument pads as compared to those in the free field on the saprolite surface are expected to be multiplicative in nature, rather than additive. As a result, we expect that the distribution of the ratio of foundation motion or pad motion to free-field motion will be lognormally distributed (or, stated another way, that the logarithm of the ratio will be normally distributed). If the coefficient of variation of the ratio is small, either a lognormal or normal distribution will fit the data adequately; it is only when the coefficient of variation is large that a difference in distribution fit will be obvious.

In the case of the soil-pad interaction study (Appendix A), the coefficient of variation of the pad/free-field spectral ratio is small at each frequency. Thus the average reduction factors can be computed either arithmetically or geometrically, and similar results will be obtained. This is illustrated in Figure 3.1, which shows average spectral ratios computed by each method.

For explosion test data (Appendix B), the justification of a lognormal distrifution for the foundation/free-field motion can be examined from the experimental spectral modulus ratios obtained. Figure 3.2a shows observed values of the logarithm of Auxiliary Building/free-field spectral modulus at 25 Hz for Test 3, plotted on normal probability scale. There are 40 data available for this test series (5 shots, 4 free-field sites, 2 horizontal components). Also shown is a line indicating the fitted distribution. The linearity of the data, and the good fit to the straight line, demonstrate that the lognormal assumption is appropriate. For comparison, Figure 3.2b shows the same data

but plotted as the arithmetic ratio (not the logarithm) on normal probability scale. The non-linearity of the data on this plot show that a normal distribution is inappropriate.

Figures 3.3 and 3.4 show equivalent plots of data for Test 3 at 14.8 Hz and 30 Hz, respectively. While the data are not as well behaved as at 25 Hz, the lognormal assumption is still the appropriate distribution choice.

For the Test 4 series, there are 16 ratios of Auxiliary Building/free-field available at each frequency. Plots of these data in logarithmic form on a normal probability scale are shown in Figures 3.5, 3.6, and 3.7 for 25, 14.8 and 30 Hz, respectively. The data do not fit a lognormal distribution exactly, in particular because of the fewer number of points available, but the assumption of a lognormal distribution is justified, since there are no systematic departures from the fitted distribution over all data sets.

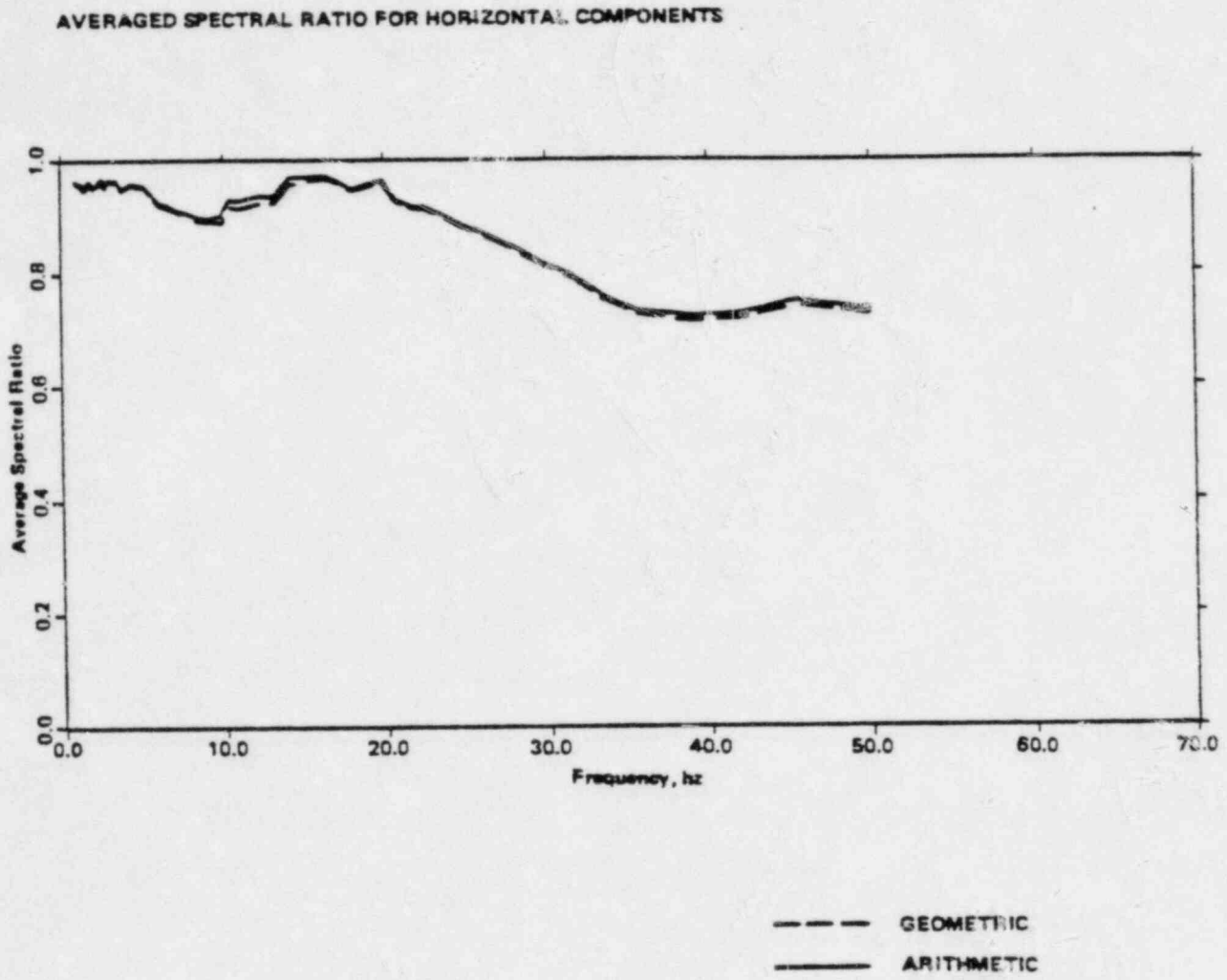

Figure 3.1
FREE-FIELD / PAD SPECTRAL RATIO,
COMPUTED GEOMETRICALLY AND ARITHMETICALLY

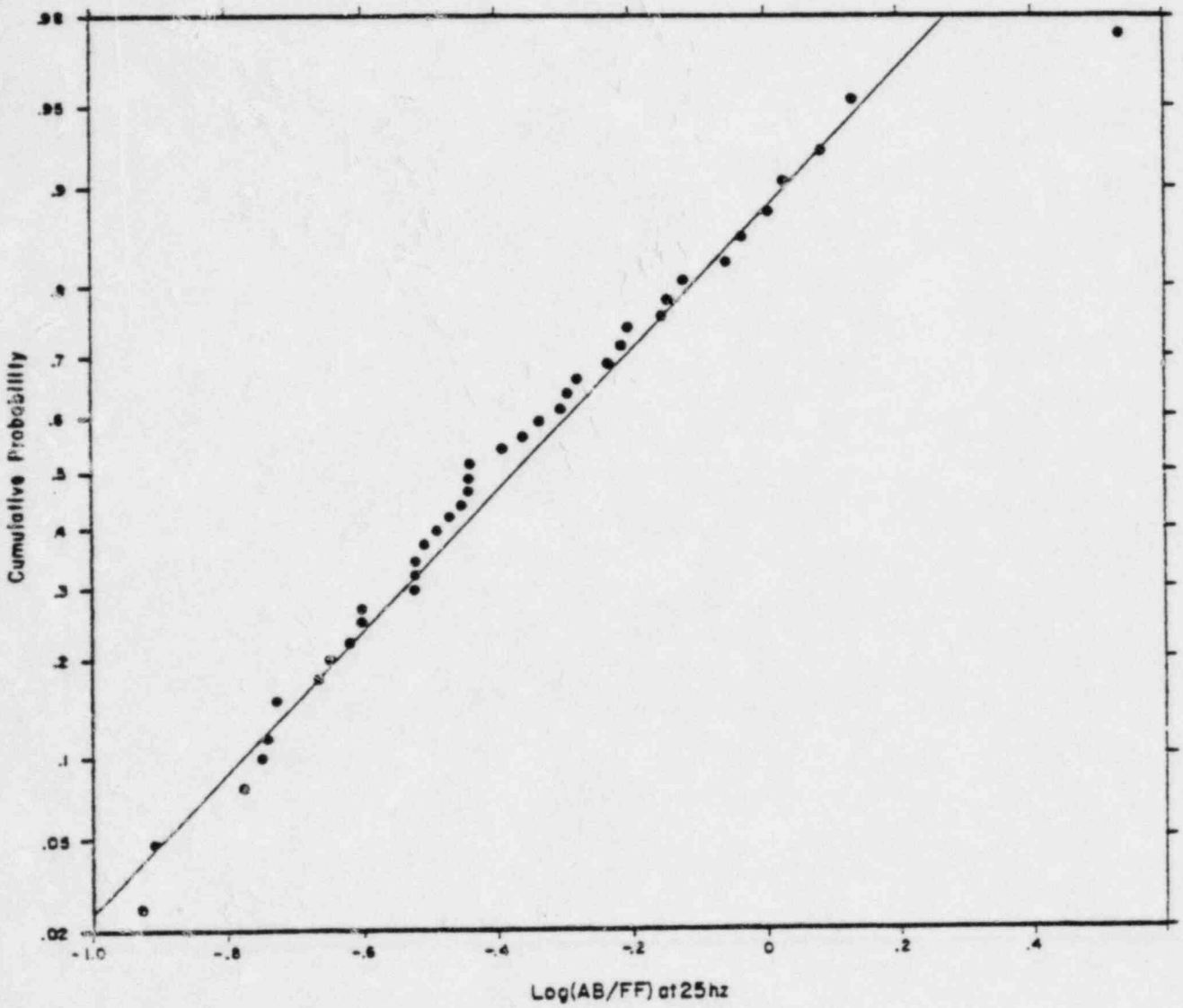

Figure 3.2a

LOG OF AUXILIARY BUILDING/FREE-FIELD SPECTRAL MODULUS (25 HZ), TEST 3, PLOTTED ON NORMAL PROBABILITY SCALE

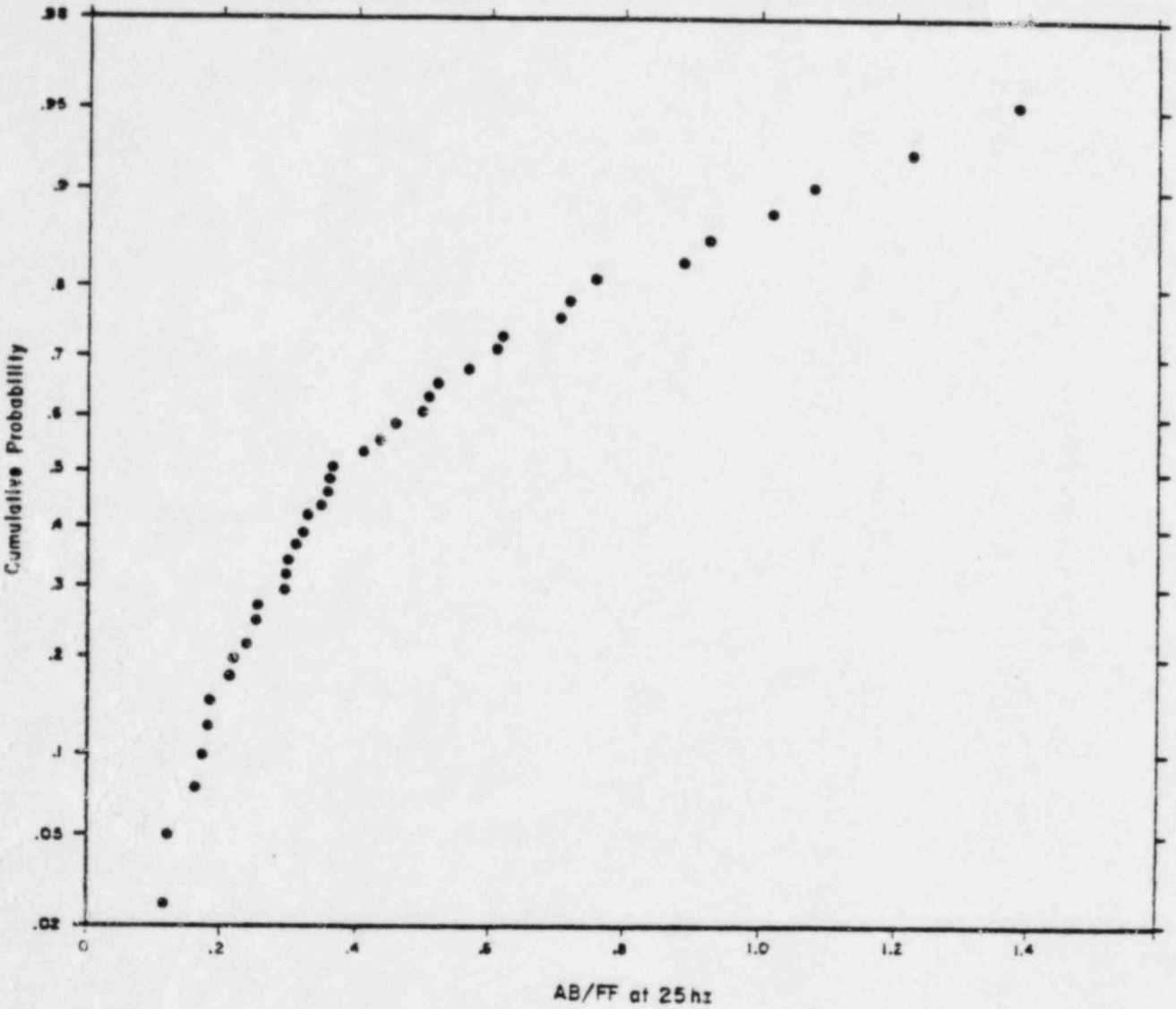

Figure 3.2b
AUXILIARY BUILDING/FREE-FIELD SPECTRAL MODULUS (25 HZ), TEST 3, PLOTTED ON NORMAL PROBABILITY SCALE

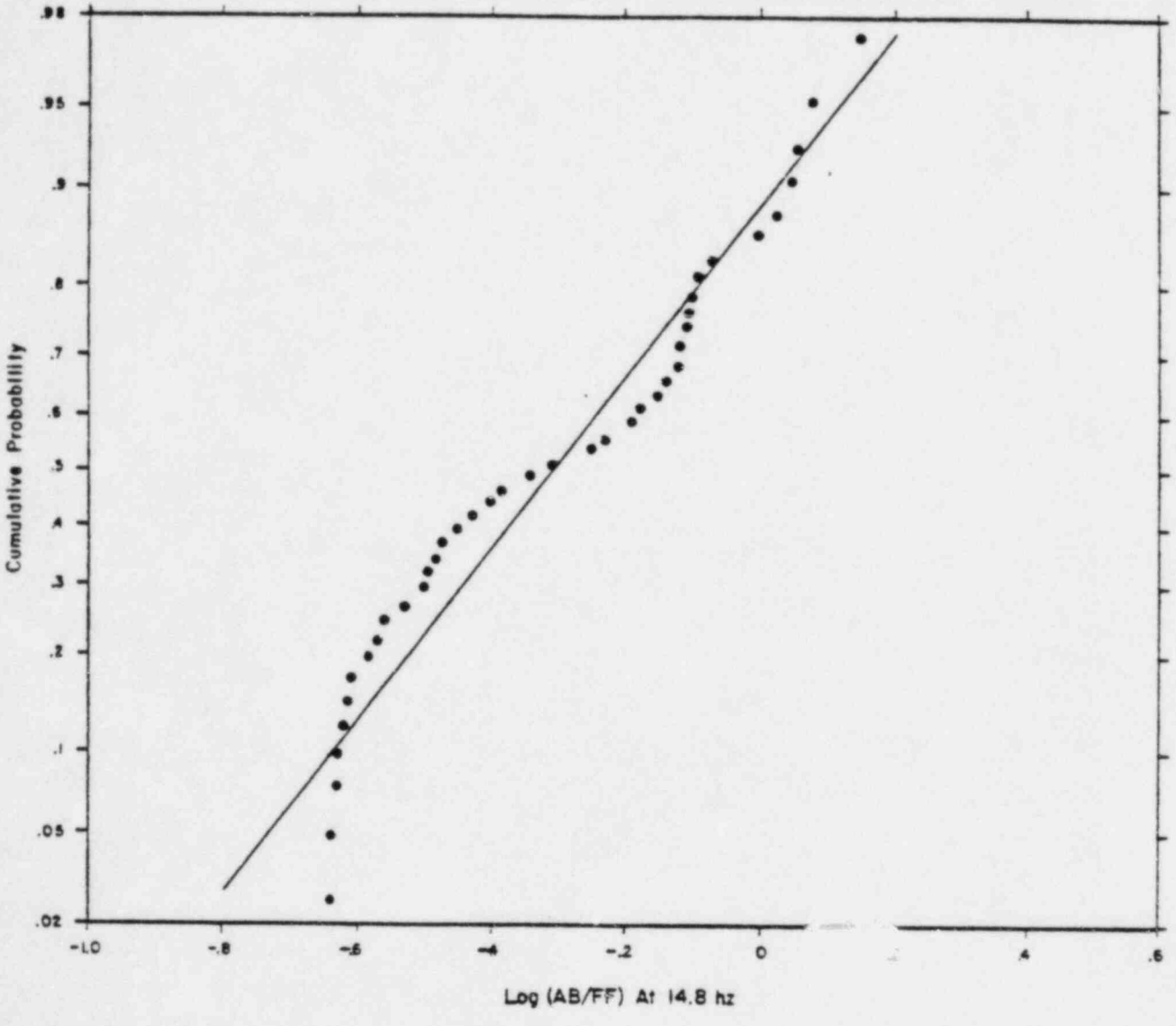

Figure 3.3

LOG OF AUXILIARY BUILDING / FREE-FIELD SPECTRAL MODULUS (14.8 hz), TEST 3, PLOTTED ON NORMAL PROBABILITY PAPER

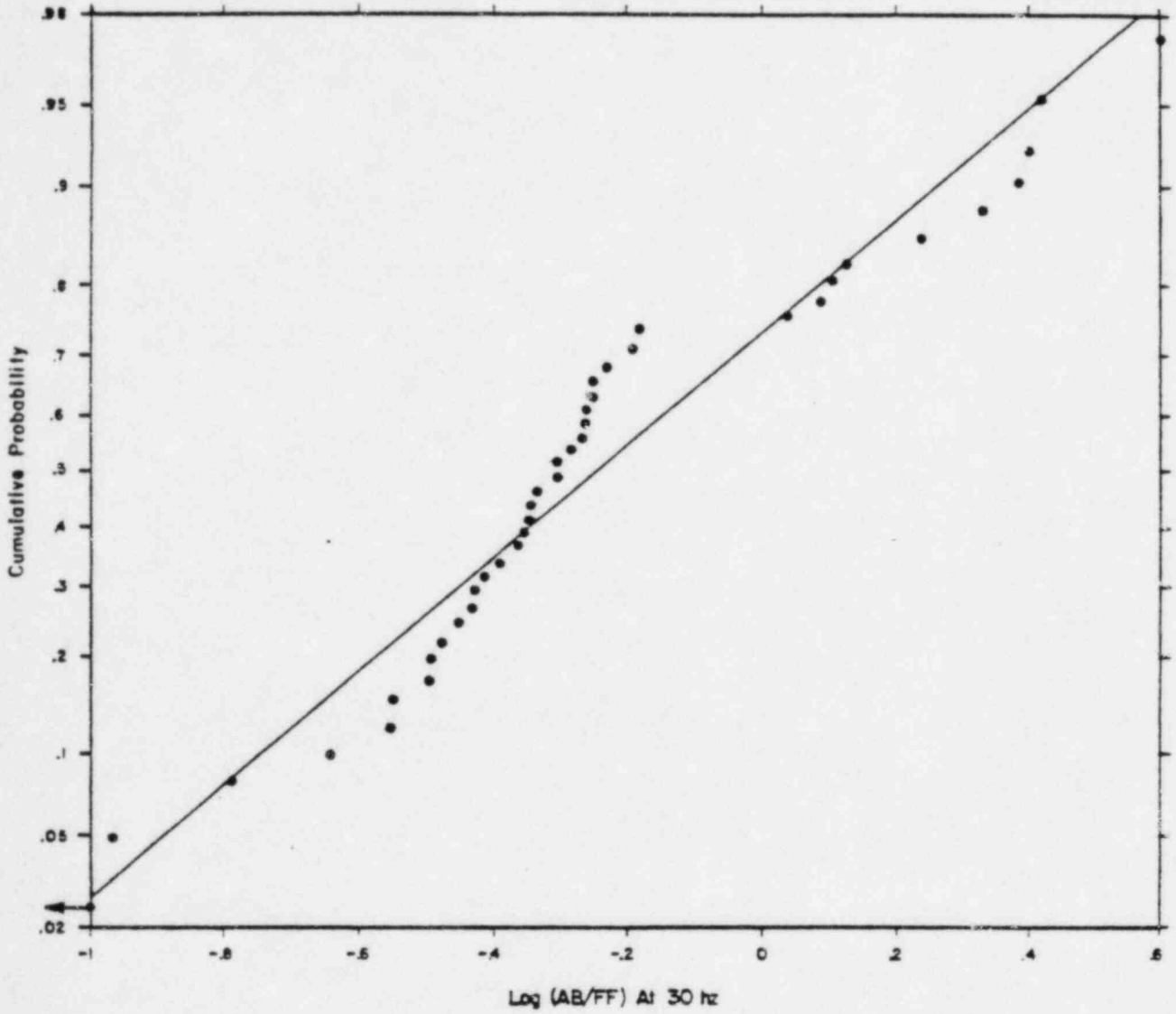

Figure 3.4

LOG OF AUXILIARY BUILDING / FREE FIELD SPECTRAL MODULUS (30 hz), TEST3, PLOTTED ON NORMAL PROBABILITY SCALE

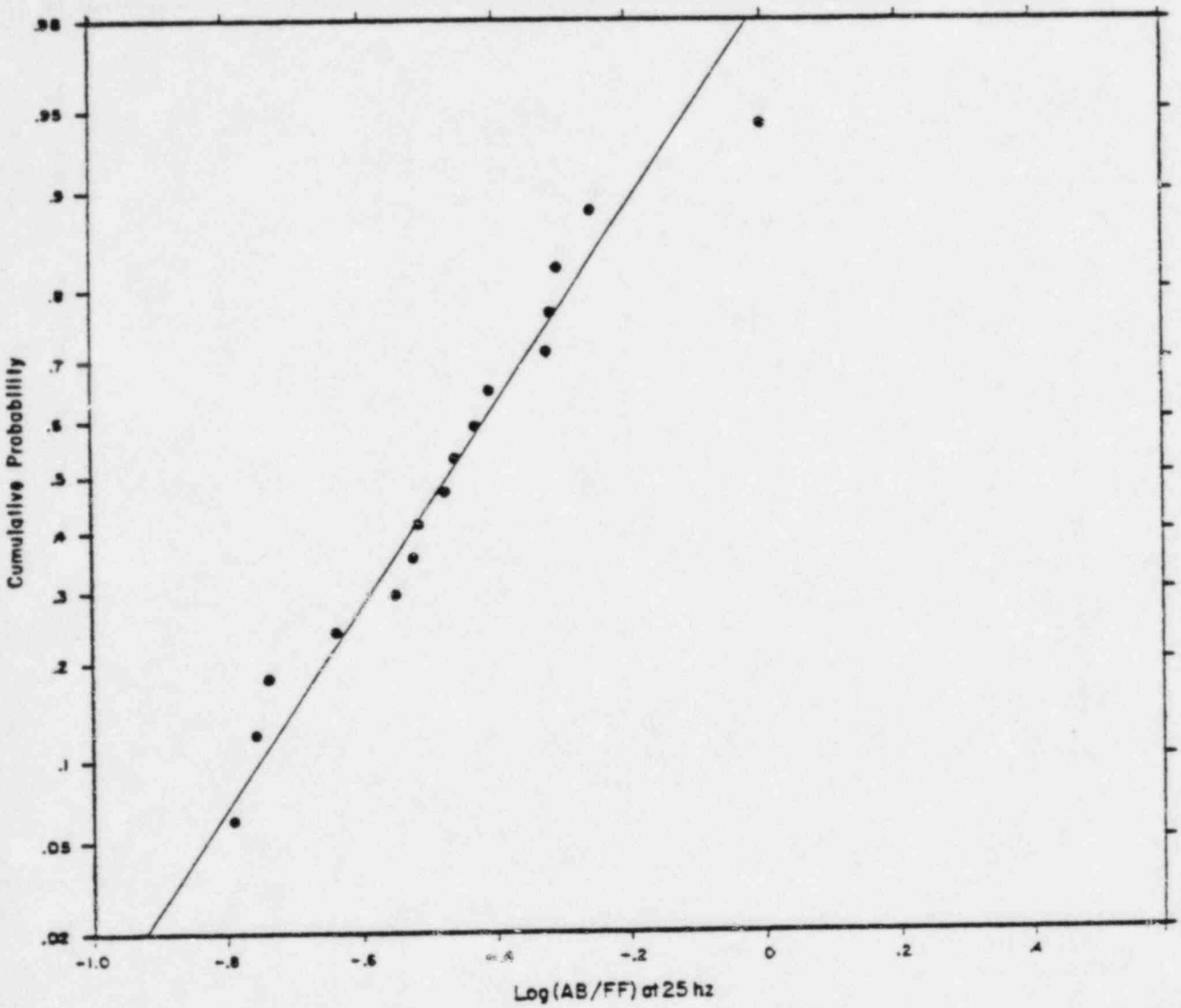

Figure 3.5

LOG OF AUXILIARY BUILDING/FREE-FIELD SPECTRAL MODULUS (25 HZ), TEST 4, PLOTTED ON NORMAL PROBABILITY SCALE

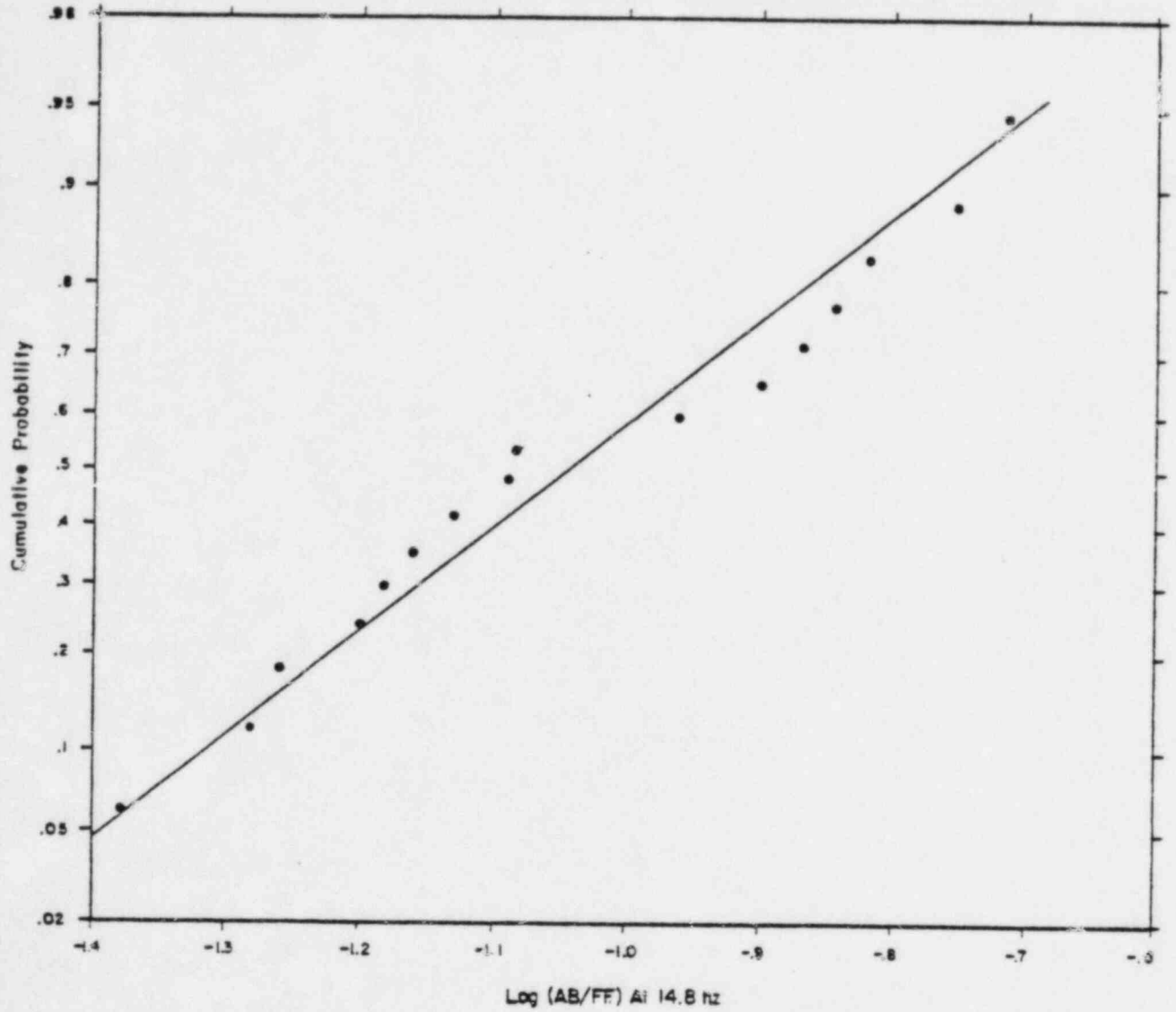

Figure 3.6
LOG OF AUXILIARY BUILDING / FREE-FIELD SPECTRAL MODULUS (14.8 hz), TEST 4, PLOTTED ON NORMAL PROBABILITY SCALE

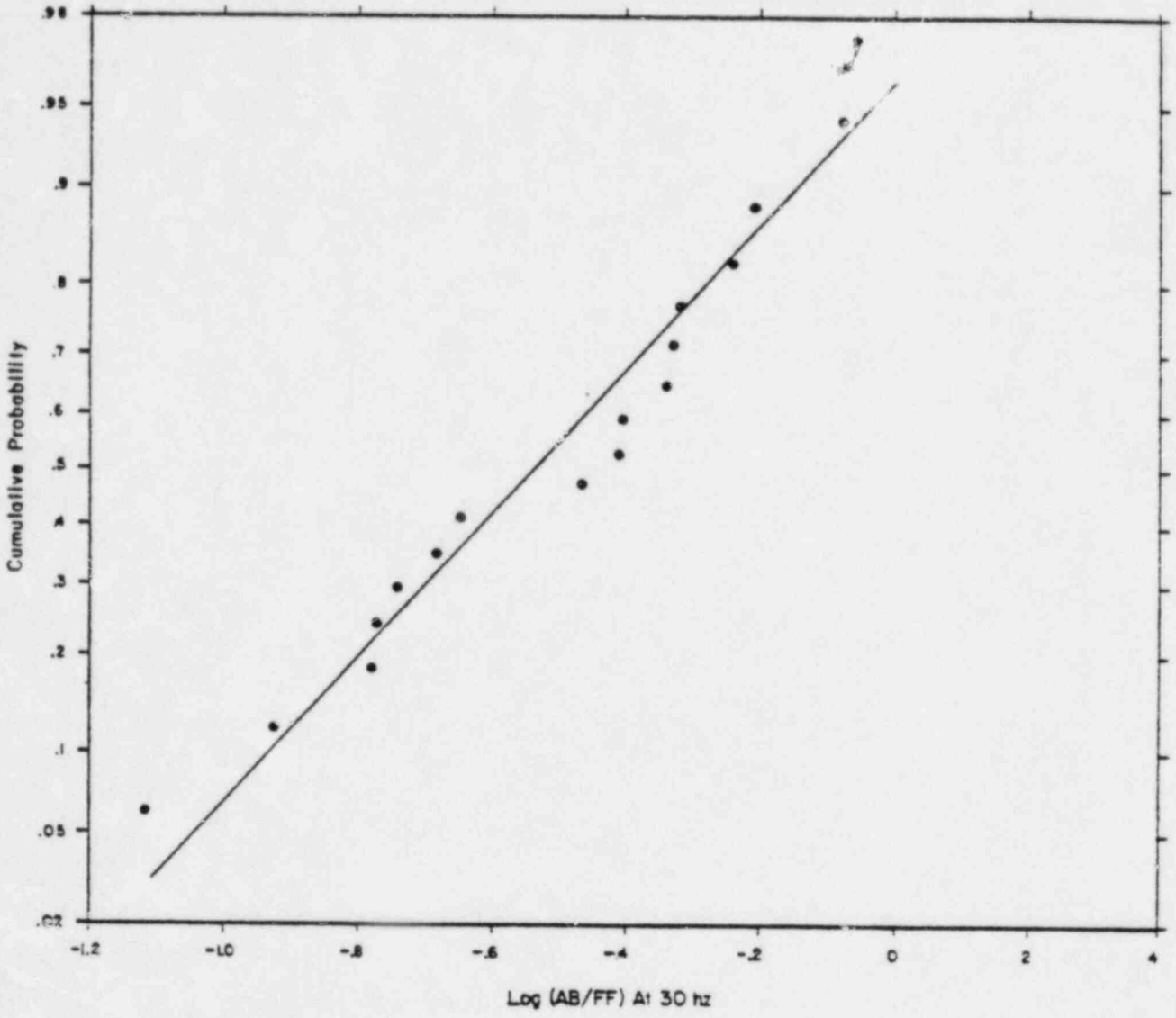

Figure 3.7

LOG OF AUXILIARY BUILDING / FREE-FIELD SPECTRAL MODULUS (30 hz), TEST 4, PLOTTED ON NORMAL PROBABILITY SCALE

Question 3A. (New Q. 1)

The Licensee should document the actual distribution of spectral ratios and justify empirically the use of lognormal statistics. Based on the actual distribution, the Licensee should calculate foundation/free-field spectral ratios for percentiles ranging from, at least, the 50th through the 90th, in 10-percentile steps, for the total site-to-site and shot-to-shot variability. Reduced envelope spectra corresponding to these percentiles should be calculated, using the results from the pad-shaking tests.

Distribution of spectral modulus ratios

The distribution of spectral modulus ratios is documented in the response to Question 3, and it is shown that the lognormal distribution adequately represents the data.

Discussion of the response spectrum criterion

The calculation and proper interpretation of reduced (foundation) envelope spectra corresponding to various percentiles requires consideration of what the original envelope spectrum represents. In particular, if the envelope spectrum represents ground motion at a specific site, percentiles of foundation response should not be developed as though the envelope spectrum were applicable to an unknown, randomly-chosen site. Hence a discussion of the possible interpretations of the envelope criterion is appropriate.

The criterion specified in the Safety Evaluation Report, SER, (NUREG-0717, Supplement No. 4) is the envelope of response spectra of accelerograms recorded at the USGS accelerograph site on the dam abutment. The criterion can be interpreted in different ways that may or may not be mutually exclusive. The most direct interpretation is that

(1) the criterion is specific to the USGS accelerograph site, where the strong motion data were recorded.

Another interpretation that is consistent with the language of the SER is that

(2) the criterion is referenced to representative site conditions, with the implication that

(a) the dam abutment site is representative of an average free-field site, or further that

(b) free-field sites are indistinguishable in terms of seismic response.

These interpretations of the criterion were taken into account in the design of the 1982 explosion tests. The outcome is that, while there is substantial variability in site response, the dam abutment accelerograph site is in fact representative of the instrumented free-field sites in that it exhibits average site response. This is documented in Appendix B, and is discussed at length below. Thus interpretations (1) and (2a) are equivalent for practical purposes, while interpretation (2b) is not supported by the data.

The question being addressed implies yet a third interpretation of the criterion, namely that

(3) the criterion is referenced to an unspecified site chosen at random.

This interpretation is neither stated nor implied in the SER, and was not considered in the design of the explosion tests. Because both the data forming the criterion and the explosion test data are keyed to a common reference site, variability of site response at different locations should not contribute to the experimental uncertainty in estimating foundation response corresponding to the criterion.

Results for individual recording sites

To illustrate the importance of the site effect, and therefore the need to apply the criterion in a site-specific manner, results obtained by applying the envelope response spectrum criterion to individual recording sites are given below. These calculations demonstrate that the criterion from the dam abutment accelerograph data cannot be applied indiscriminately to other sites without regard to differences in site response. Application of the criterion in this manner introduces extraneous dispersion in the calculated foundation spectra that would not appear if site differences were taken into account.

For each site, a zero phase shift transfer function was obtained from the 50th percentile foundation/site spectral modulus ratio for the shot sequence. For both the Auxiliary and Diesel Generator Buildings, Tests 3 and 4 provide a total of seven transfer functions. For the six free-field sites, foundation accelerograms were calculated by filtering the ERTEC free-field accelerograms computed for the October 16, 1979 RIS event, while for the accelerograph site (P2), the USGS accelerograms were filtered to produce foundation accelerograms directly. In the case of the Service Water Pumphouse, the ERTEC free-field accelerograms were filtered with the four transfer functions from Test 3.

Results for the Auxiliary Building, Diesel Generator Building, and Service Water Pumphouse are shown in Figures 3A.1, 3A.2 and 3A.3. The calculated foundation response spectra differ significantly, depending on which site is chosen as that to which the envelope response spectrum criterion is applied. The actual foundation response measured in the explosion tests is of course not a function of free-field site location. The scatter in the computed foundation response spectra illustrates the extraneous dispersion that is introduced when the criterion is applied without regard to differences in site response.

Note that the amplitude of the calculated foundation response is inversely related to the spectral amplitude of the signal recorded in the field. Thus the site with the lowest signal amplitude, F1, has the highest calculated foundation response. But if the accelerograph pad had been located at site F1, the envelope response spectrum criterion would have been much lower.

To examine site differences in further detail, shot sequence statistics were calculated for Auxiliary Building/site spectral modulus ratios for sites F1 and P2 (the USGS accelerograph site). Figure 3A.4 compares Auxiliary Building foundation response spectra calculated for the 16th and 84th percentiles of the spectral modulus ratios for F1 and P2. The separation of the results for the two sites demonstrates the significance of the site effect. Although there may be a contribution due to path differences, this is a relatively small effect as can be seen by comparing Figures VI.C.47 and VI.C.48 of Appendix B, which show very similar Auxiliary Building/dam abutment spectral modulus ratios for Tests 4 and 1.

Because saprolite propagation effects are site-dependent, it is inappropriate to apply the criterion from the dam abutment data to other sites without regard to site differences. However, comparison of the results for different sites in Figures 3A.1 and 3A.2 shows that the USGS accelerograph site is representative of an average of free-field sites in terms of site response. This can also be seen by comparing the results for the accelerograph site (P2) in Figures 3A.1 and 3A.2 with the 50th percentile results in Figures 3A.5 and 3A.6, respectively. In the latter two figures, the criterion is referenced to the geometric average of horizontal component spectral amplitudes at equidistant free-field sites. This comparison shows that results obtained by referencing the criterion specifically to the accelerograph site (interpretation (1)) are nearly the same as when the criterion is referenced to average free-field site conditions (interpretation (2a)). Interpretation (1) yields calculated foundation response spectra that are slightly lower than for interpretation (2a) for frequencies up to 30 Hz, and slightly higher at higher frequencies. To a good approximation, the accelerograph site can be taken as representative of an average free-field site, thus validating interpretation (2a). This finding is consistent with the observation that the saprolite thickness of 56 ft at the accelerograph site is representative of the average saprolite thickness in the Monticello Reservoir region.

Appropriate percentiles for reduced envelope spectra

Consistent with the above observations, it is appropriate to calculate percentiles of foundation motion incorporating only source and path variability. This corresponds to interpretation (2a) above, which is equivalent to interpretation (1). Figures 3A.5, 3A.6 and 3A.7 show percentiles for reduced envelope spectra in the Auxiliary Building, Diesel Generator Building, and Service Water Pumphouse, respectively. These response spectra were calculated from accelerograms obtained by filtering the free-field accelerograms derived for the October 16, 1979 RIS event from the pad-shaking tests with zero-phase transfer functions of percentiles 50, 60, 70, 80, and 90. Data for Tests 3 and 4 were given equal weight in computing the spectral modulus ratio statistics for the Auxiliary and Diesel Generator Buildings. It is the Licensee's

position that Figures 3A.5, 3A.6 and 3A.7 are the appropriate representation of dispersion for reduced envelope spectra.

Percentiles for reduced envelope spectra according to interpretation (3)

The overall dispersion of the foundation response spectra shown in Figures 3A.8, 3A.9 and 3A.10 expresses the uncertainty that would apply if the location of the USGS accelerograph site were unknown, corresponding to interpretation (3) which is inappropriate. The results in Figures 3A.8, 3A.9 and 3A.10 do not apply to the criterion and are included only to complete the response to Question 3A as stated.

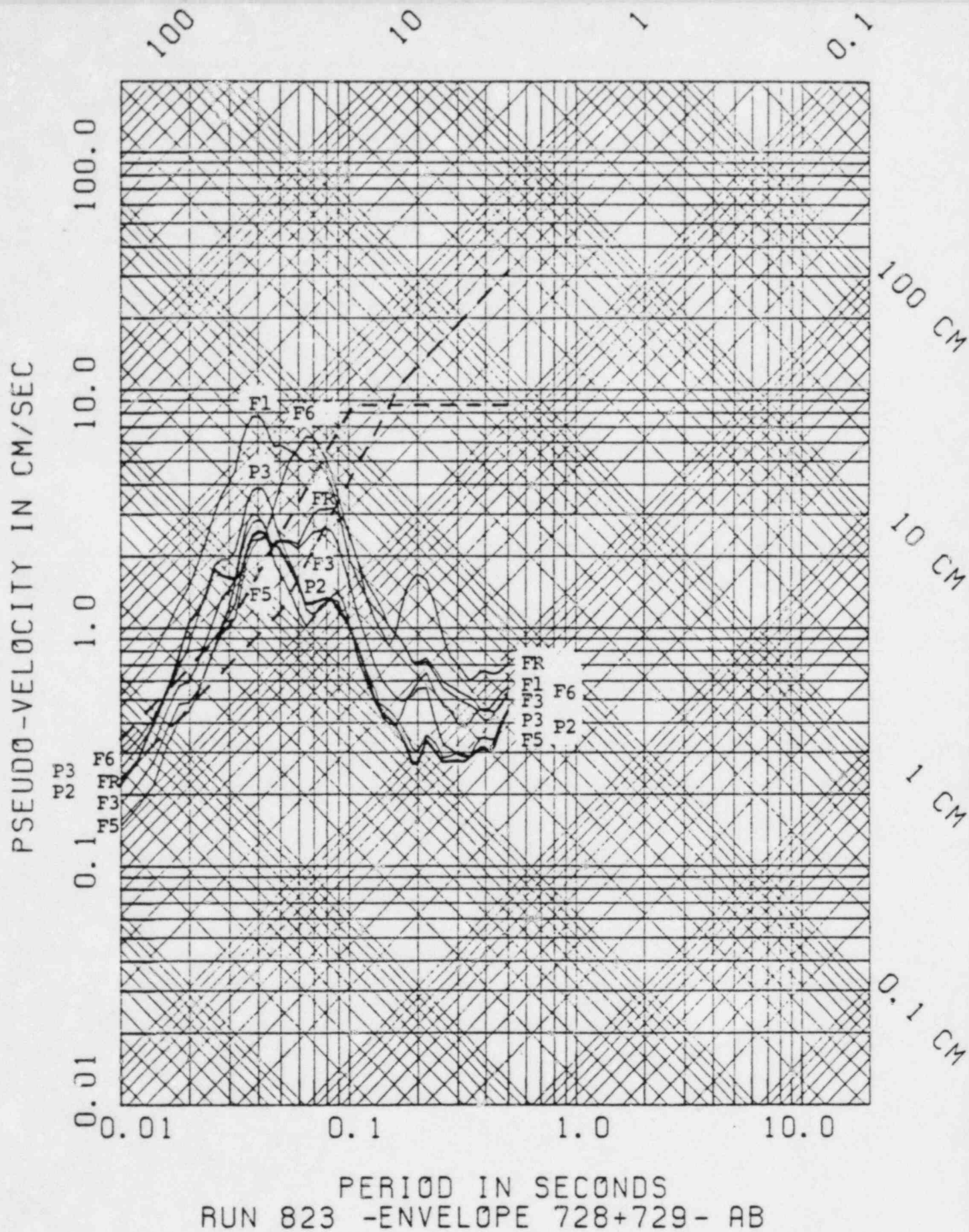

Figure 3A.1 Auxiliary Building envelope response spectra obtained by filtering free-field accelerograms from the pad-shaking tests with zero phase shift transfer functions for free-field sites F1, FR, F3, F5, F6, and P3. For the accelerograph site (P2, heavier line), the USGS accelerograms were filtered.

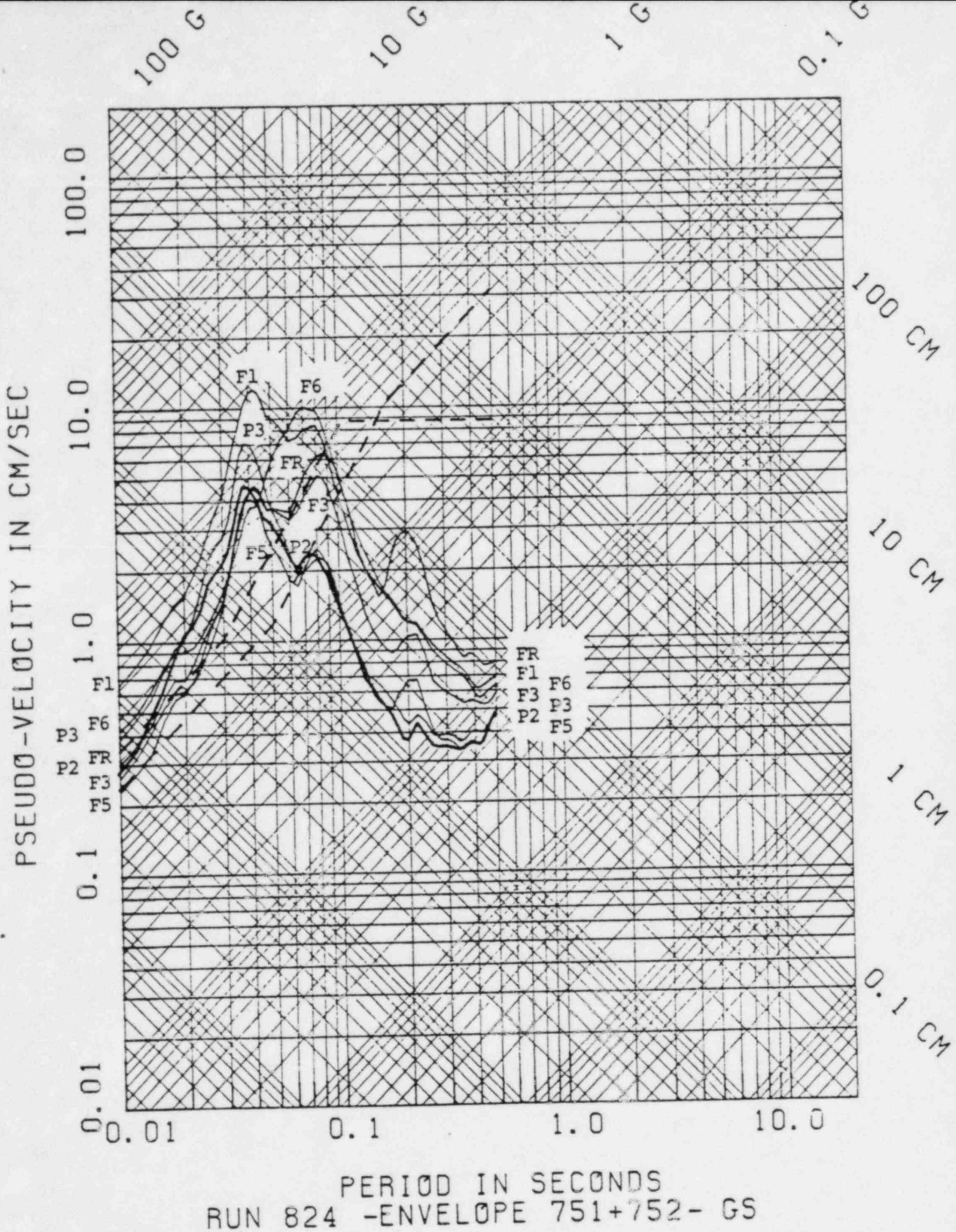

Figure 3A.2 Diesel Generator Building envelope response spectra obtained by filtering free-field accelerograms from the pad-shaking tests with zero phase shift transfer functions for free-field sites F1, FR, F3, F5, F6, and P3. For the accelerograph site (P2, heavier line), the USGS accelerograms were filtered.

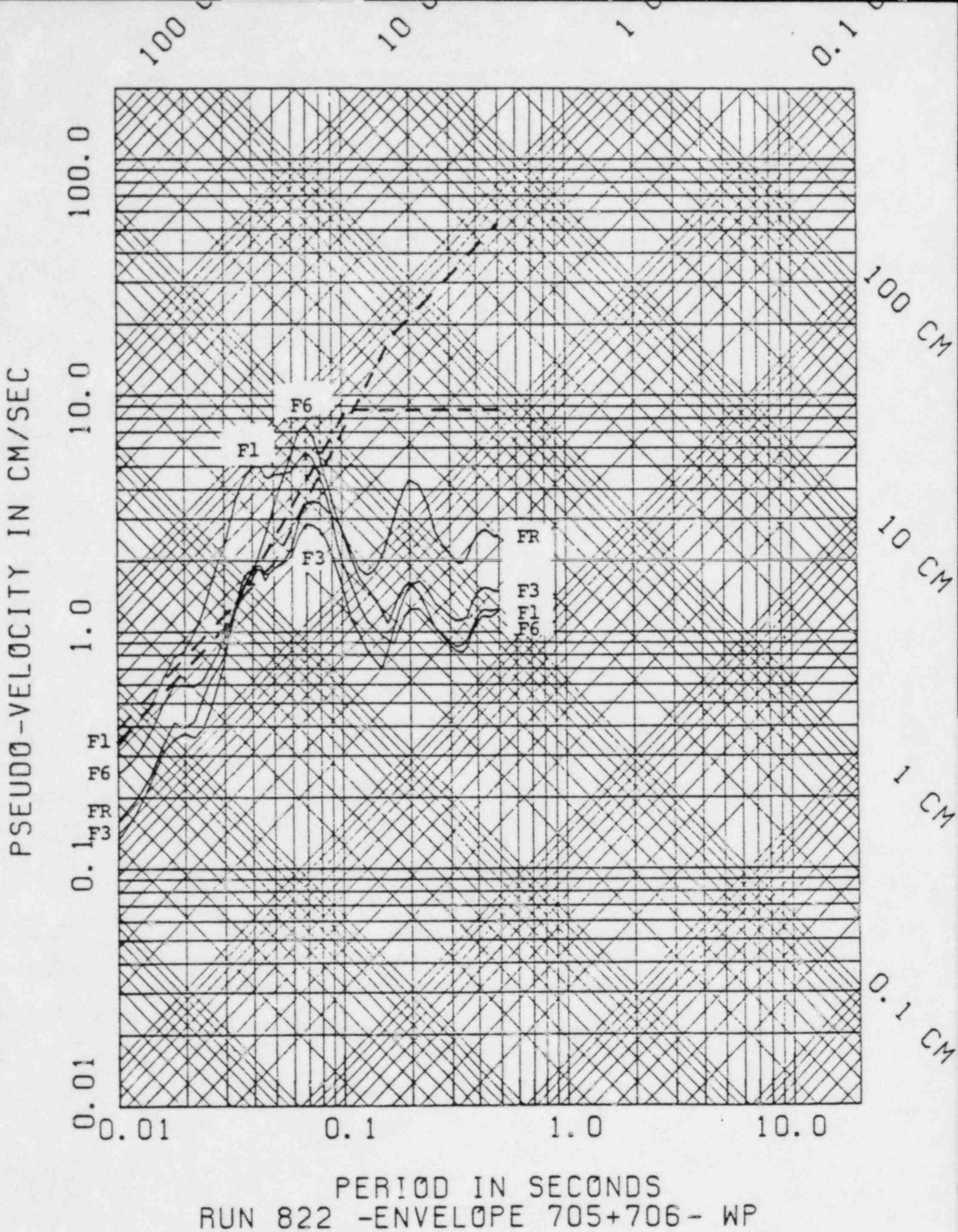

Figure 3A.3 Service Water Pumphouse envelope response spectra obtained by filtering free-field accelerograms from the pad-shaking tests with zero phase shift transfer functions for free-field sites F1, FR, F3, and F6.

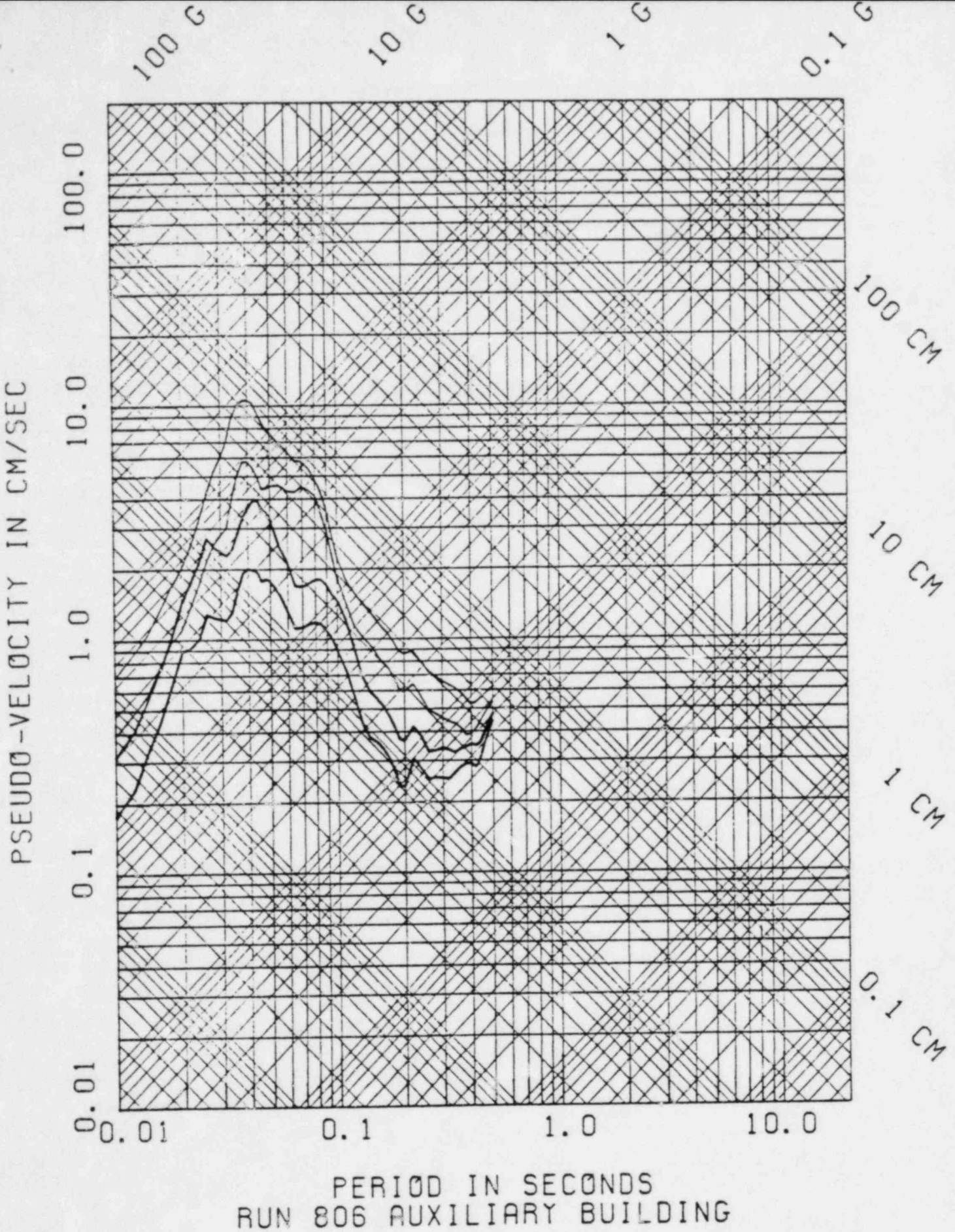

Figure 3A.4 Comparison of calculated Auxiliary Building response spectra obtained for the 84th and 16th percentile spectral modulus ratios for site F1 (upper two traces) and site P2 (lower two traces).

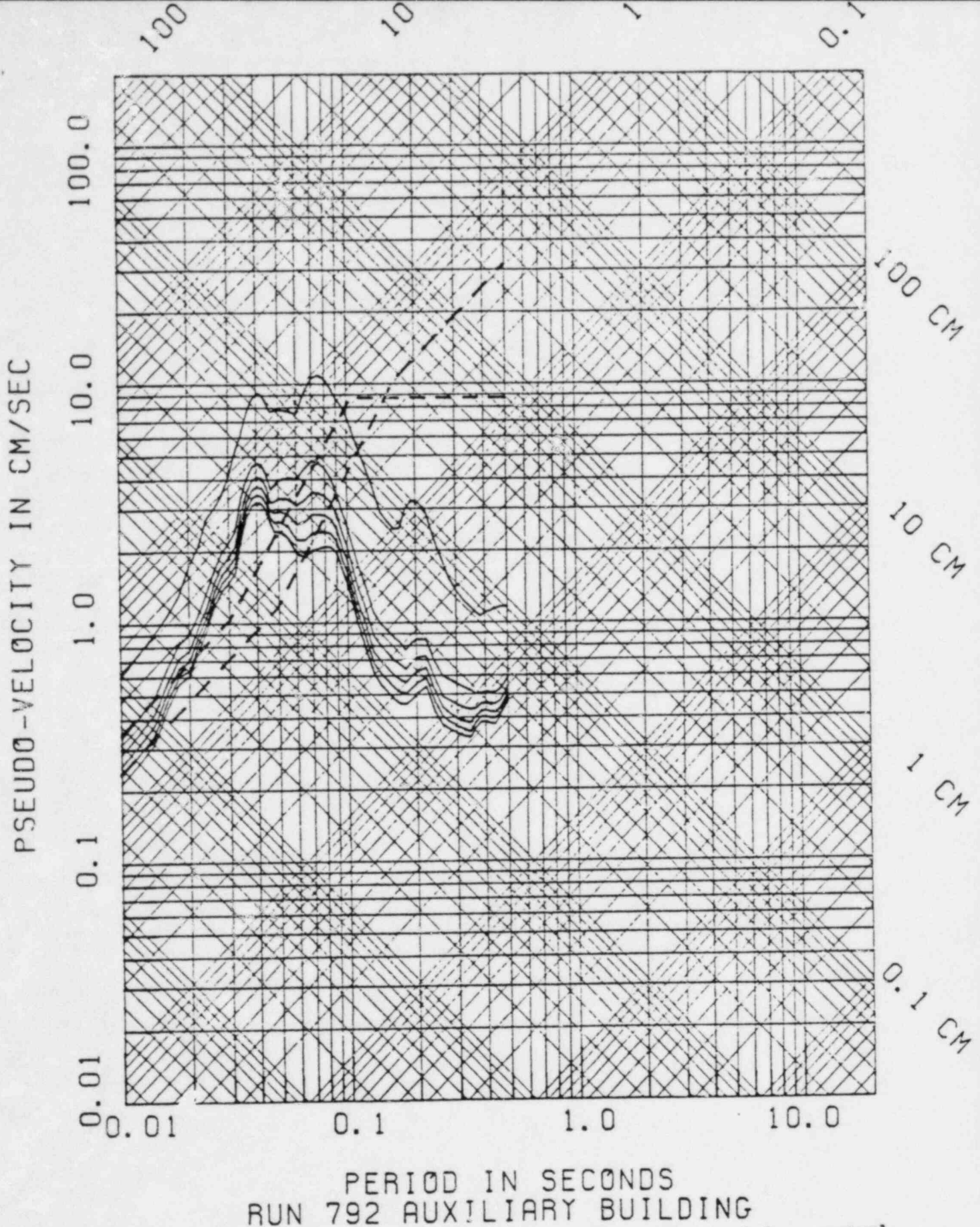

Figure 3A.5 Auxiliary Building envelope response spectra calculated for spectral modulus ratios of percentiles 50, 60, 70, 80, and 90: statistics encompass source and path effects. Top trace is the envelope response spectrum criterion, and dashed lines are the SSE and M_L 4.5 RIS spectra.

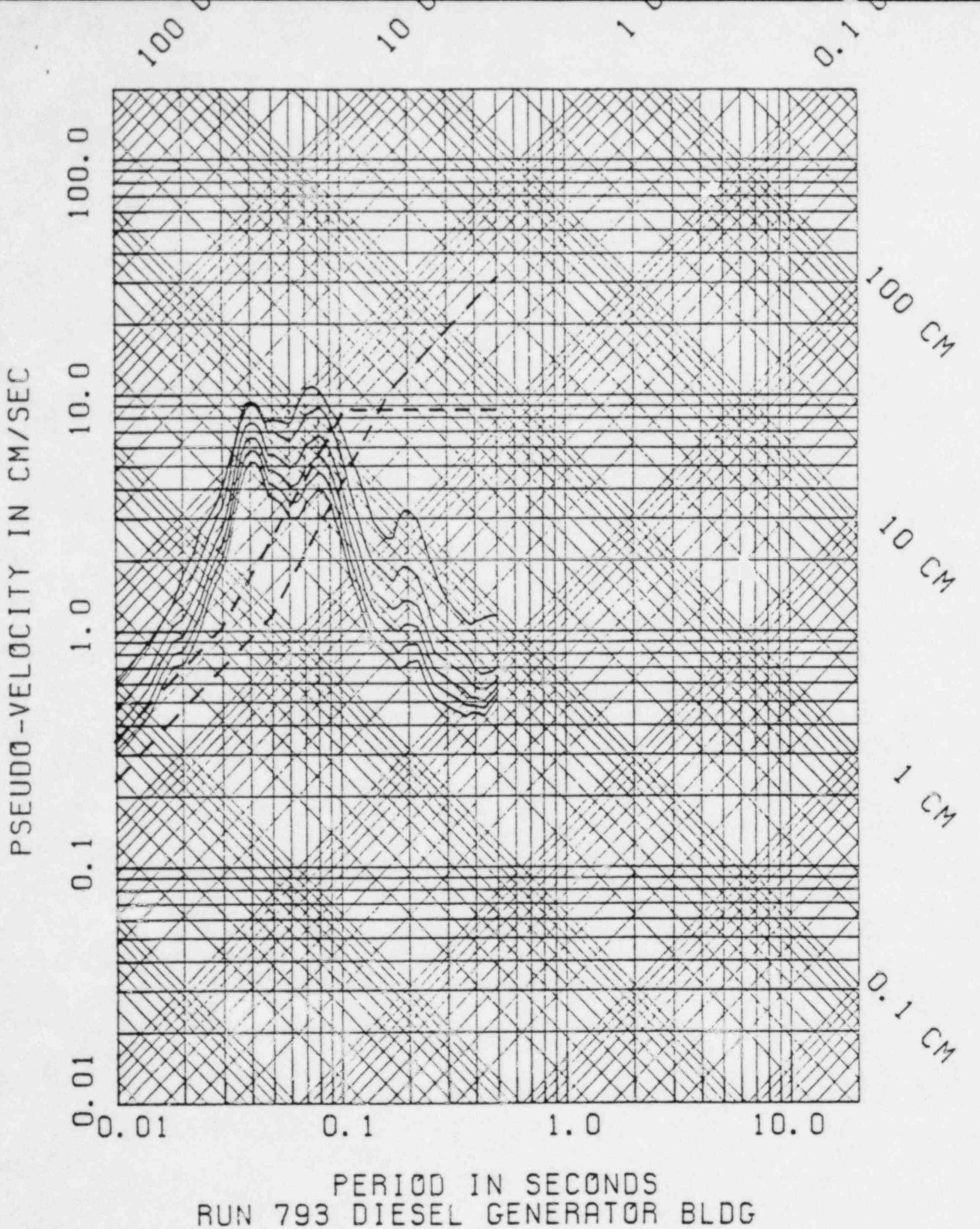

Figure 3A.6 Diesel Generator Building envelope response spectra calculated for spectral modulus ratios of percentiles 50, 60, 70, 80, and 90: statistics encompass source and path effects. Top trace is the envelope response spectrum criterion, and dashed lines are the SSE and M_L 4.5 RIS spectra.

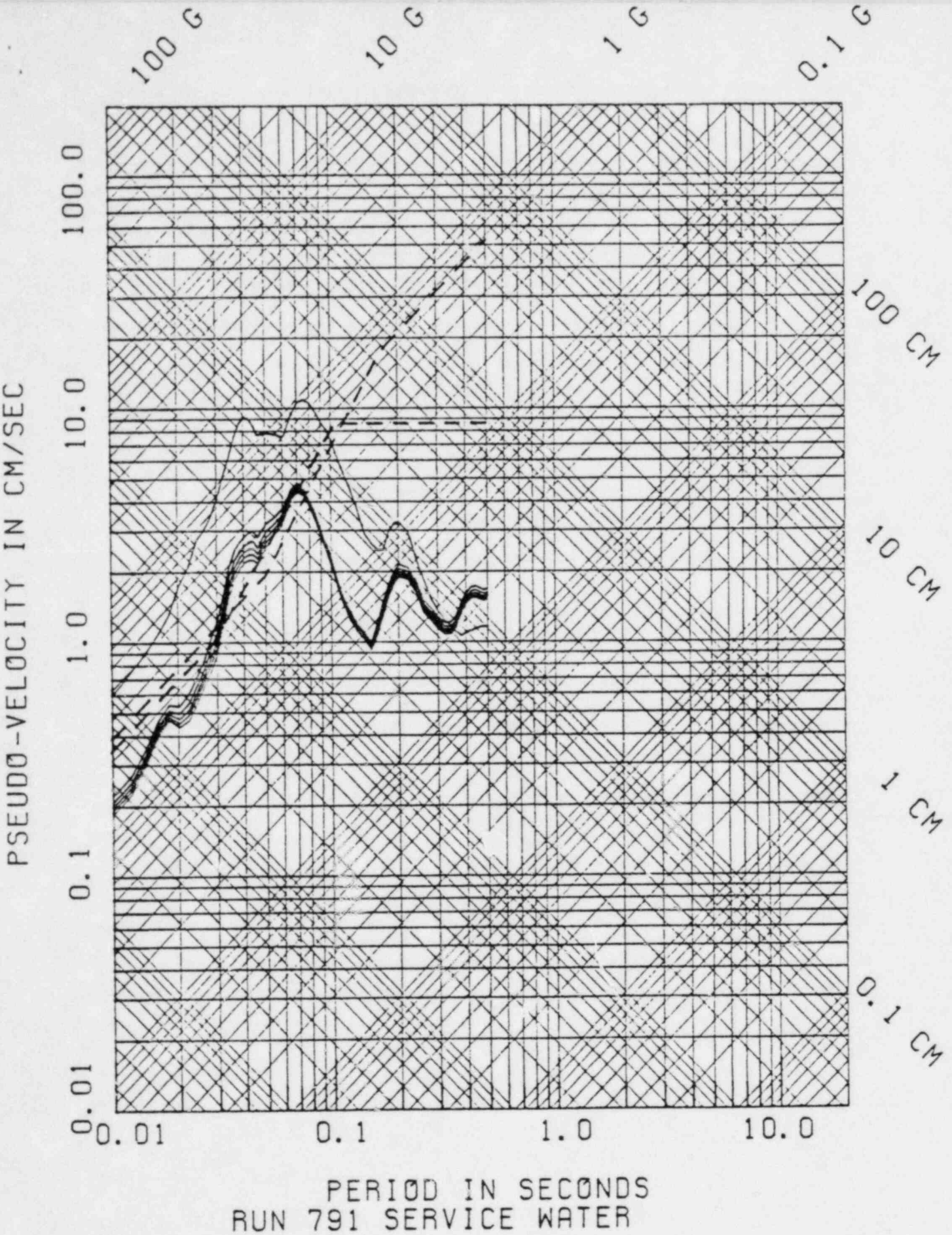

Figure 3A.7 Service Water Pumphouse envelope response spectra calculated for spectral modulus ratios of percentiles 50, 60, 70, 80, and 90: statistics encompass source and path effects. Top trace is the envelope response spectrum criterion, and dashed lines are the SSE and M_L 4.5 RIS spectra.

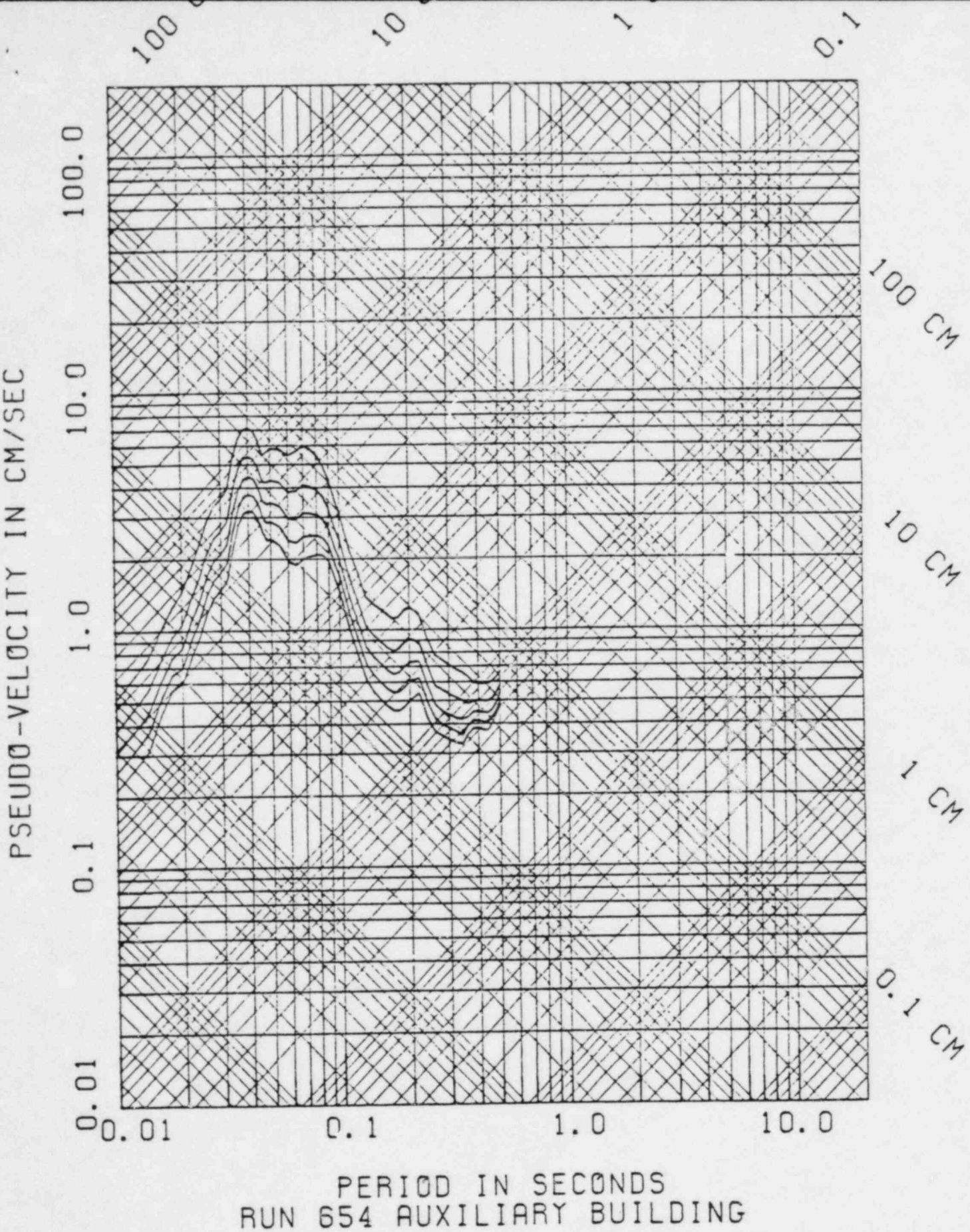

Figure 3A.8 Auxiliary Building envelope response spectra calculated for spectral modulus ratios of percentiles 50, 60, 70, 80, and 90: statistics encompass source, path, and site effects. The statistics are inappropriate because the criterion from the USGS accelerograph data is applied without regard to free-field site differences.

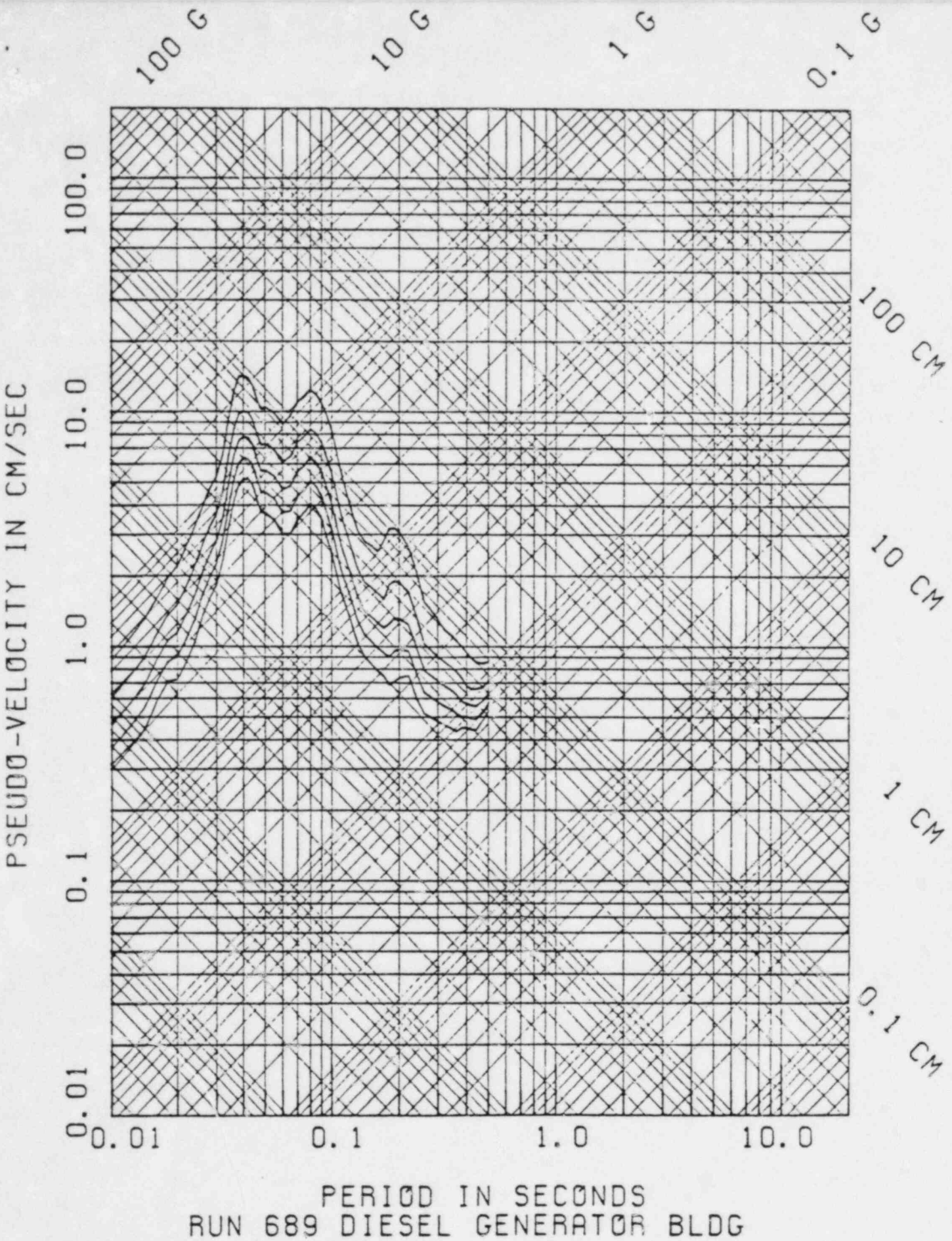

Figure 3A.9 Diesel Generator Building envelope response spectra calculated for spectral modulus ratios of percentiles 50, 60, 70, 80, and 90: statistics encompass source, path, and site effects. The statistics are inappropriate because the criterion from the USGS accelerograph data is applied without regard to free-field site differences.

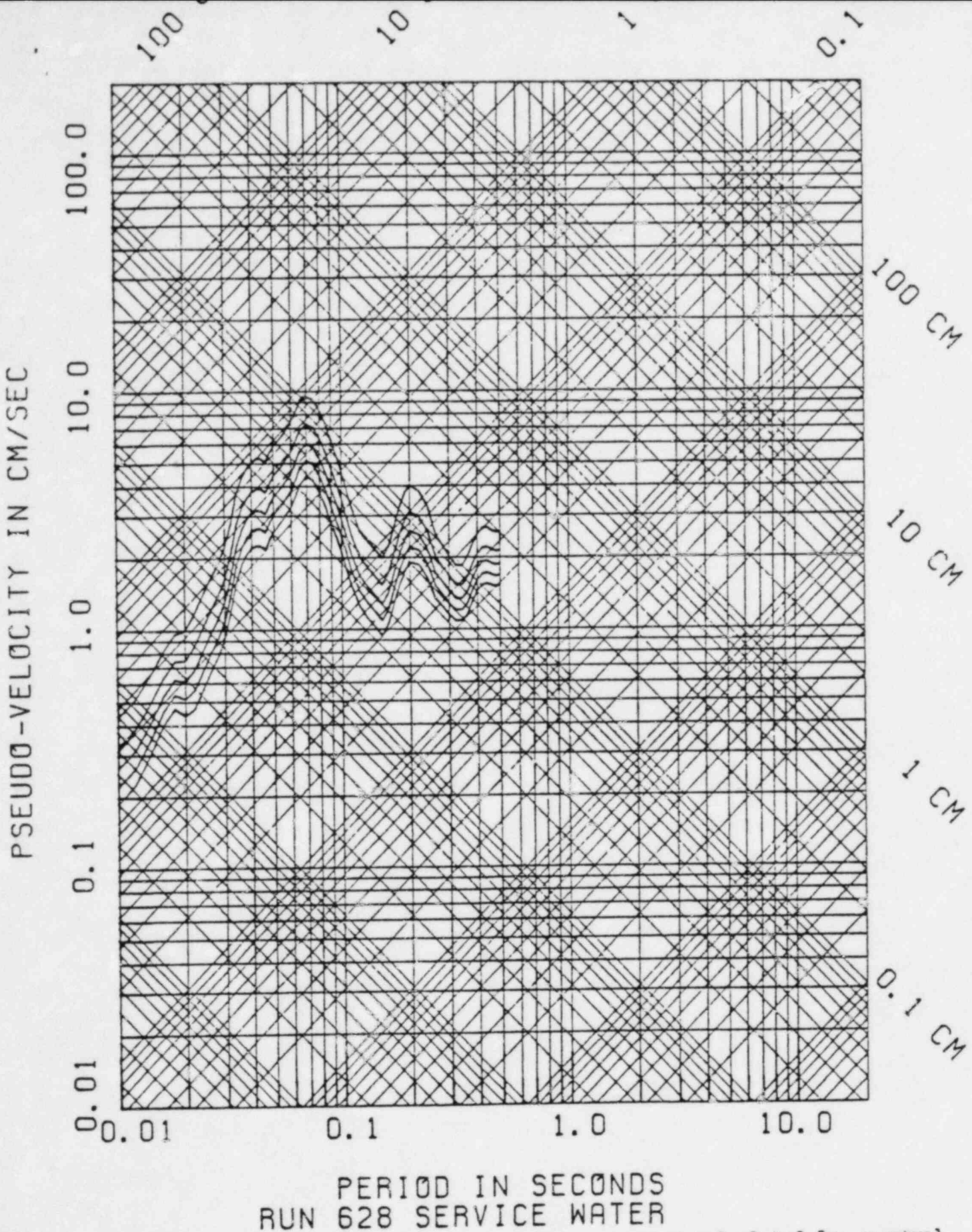

Figure 3A.10 Service Water Pumphouse envelope response spectra calculated for spectral modulus ratios of percentiles 50, 60, 70, 80, and 90: statistics encompass source, path, and site effects. The statistics are inappropriate because the criterion from the USGS accelerograph data is applied without regard to free-field site differences.

Question 4. Explain clearly the relevance to your conclusions of the assertion on page 10 of the Addendum to Appendix B that "most . . . dispersion is due to effects unrelated to the actual foundation/free-field phenomena under investigation."

The relative response of foundation and free field fo a sequence of shots is more reproducible than is indicated by the overall ' spersion of the foundation/free-field spectral modulus ratios shown in F ures IX.D.1, 2, and 3. The fact that most of the overall dispersion is d to the scatter of free-field spectral amplitudes is evident when Fig s IX.D.1, 2, and 3 are compared with Figures VI.C.16, 20, and 28. the latter, the standard deviations reflect only the source and effects. While the standard deviations differ substantially for wo cases, the means are almost the same. Note also that vari the spectra due to random interference effects unrelated to a foundation/free-field phenomena inflate the dispersion.

The implication of these observations is that the dispersion depends on the problem addressed. If the problem is to assess the dispersion of the relative response of a foundation and an unspecified free-field site chosen at random, then the overall dispersion shown in Figures IX.D.1, 2, and 3 is relevant. However, this is not relevant if the problem is to assess for a sequence of events the reproducibility of relative response of a specific site in the field, for example when ratios of foundation to accelerograph pad spectral amplitudes are computed directly, as in Figures VI.C.45 and VI.C.46.

Question 5. Given that uncertainties exist in the use of explosion tests to determine foundation response to earthquake motion, justify the use of mean foundation/free-field spectral ratios, rather than some more conservative measure.

To characterize foundation motions corresponding to the instrument pad "envelope spectrum" obtained from records at Monticello Reservoir, foundation/free-field spectral ratios greater than those recommended by the Licensee should not be adopted. This follows from several considerations.

First, "the envelope spectrum of the response spectra from data that have been recorded at Monticello . . . is a very conservative description of ground motion . . . . Since the ground motion used in deriving the envelope was recorded on a surface soil deposit on the dam abutment, it should be considered as a representation of motion at the surface." (Staff Updated Supplemental Testimony on Seismicity, page 44.) The assessment of the envelope as very conservative is supported by even more data through mid 1983 showing that seismicity at Monticello Reservoir has continued to decline since the above statement was written in December of 1981. Because of the conservatism used in deriving the surface ground motion envelope, it would be unduly conservative to use spectral ratios greater than mean values to derive foundation motions. This would amount to stacking conservatism upon conservatism.

A second reason for not using foundation/free-field ratios greater than the mean values is that the values recommended by the Licensee were derived using conservative experimental and analytical techniques. Instruments were placed at the periphery of buildings, so that any experimental torsion induced in the buildings would be recorded as horizontal translation. It is conservative to assume that motions recorded in this manner apply to all equipment in the structure, even that at the geometrical center of the foundation. Also, the "zero-phase shift" assumption used in deriving foundation motions is conservative relative to the use of observed phase shift, as discussed in the

response to Question 2. Further, for frequencies below 40 Hz, computed response spectra using the "zero-phase shift" filter are very close to those obtained using the unrealistically conservative "impulse filter," as discussed in the response to Question 2A. Therefore, the Licensee's recommendations are conservative.

To the best of the Licensee's knowledge, there are no inherent unconservative biases or assumptions made in the design, conduct, or data analysis of this field experiment, which would reduce the effects of the conservatisms stated. The Licensee's reduced envelope spectra for the Auxiliary Building, Diesel Generator Building, and Service Water Pumphouse are conservative and justified.

Finally, as discussed in the response to Question 1, the explosion tests are appropriate to determine foundation response to earthquake motion. All observational evidence indicates that the explosion test results accurately represent the relative response of foundation and free-field sites to be expected for shallow RIS events. Therefore, the introduction of additional conservatism is not warranted.

Question 6. Weren't the dam abutment data from Test 1, October 1981, obtained on the USGS pad? This being the case, shouldn't Figure VI.C.45 of Appendix B, rather than Figure VI.C.47, be compared to Figure VI.C.48? Justify or modify the estimated reduction factors in light of your answer.

The dam abutment seismograph data for the October 1981 tests were not obtained on the USGS accelerograph pad. The seismometers were installed in the free field in saprolite approximately 50 feet south of the pad. Both Figures VI.C.47 and VI.C.48 show Auxiliary Building foundation/free-field spectral modulus ratios, for Tests 4 and 1 respectively.